**UNIVERSIDADE DE LISBOA**

**Faculdade de Medicina de Lisboa**

# Uncovering the UIS4 protein interacting network and its role during the malaria liver stage infection

**Viriato M'Bana**

**Orientadora: Professora Maria Manuel Dias da Mota**

**Coorientadora: Doutora Ksenija Slavic**

**Tese especialmente elaborada para obtenção do grau de Doutor em Ciências Biomédicas, especialidade Microbiologia e Parasitologia**

**2020**

**UNIVERSIDADE DE LISBOA**

**Faculdade de Medicina de Lisboa**


Uncovering the UIS4 protein interacting network and its role during the malaria liver stage of infection

**Viriato M'Bana**

Orientadora: Professora Doutora Maria Manuel Dias da Mota
Coorientadora: Doutora Ksenija Slavic

Tese especialmente elaborada para obtenção do grau de Doutor em Ciências Biomédicas, especialidade Microbiologia e Parasitologia

Júri:

**Presidente:**

- Doutor José Augusto Gamito Melo Cristino, Professor Catedrático e Presidente do Concelho Científico da Faculdade de Medicina da Universidade de Lisboa

**Vogais**:

- Doutor Rogério Amino, Especialista de reconhecido Mérito e competência, investigador do Institut Pasteur (Paris);
- Doutor António Alfredo Jacinto, Professor Catedrático da Faculdade de Ciências Médicas da Universidade Nova de Lisboa;
- Doutora Maria Manuel Dias da Mota, Professora Associada Convidada da Faculdade de Medicina da Universidade de Lisboa (Orientadora);
- Doutor Edgar Rodrigues Almeida Gomes, Professor associado Convidado da Faculdade de Medicina da Universidade de Lisboa;
- Doutor Rui Miguel Prudêncio da Cunha Pignatelli, Professor Auxiliar Convidado da Faculdade de Medicina da Universidade de Lisboa.

**Instituições Financiadoras e âmbito:**
Fundação para a Ciências e a Tecnologias **(FCT)** que através do projeto (SFRH/BD/113750/2015)

**2020**

A impressão desta tese foi aprovada pelo Conselho Científico da Faculdade de Medicina da Universidade de Lisboa em reunião de 17 de setembro de 2019.

As opiniões expressas nesta publicação são da exclusiva responsabilidade do seu autor.

## Preface

This work is elaborated to obtention of PhD degree, and it is divided into four chapters.

The first chapter relay on literature revision. In this chapter, I wrote about the history of malaria, since its discovery, the theories that surrounded the diseases, as well as the etiologic agent of the disease and biogeography of the two main *Plasmodium* species infecting humans, and the challenge that could negatively impact malaria eradication.

The second chapter focuses on uncovering the role of PbUIS4 at the parasitophorous vacuole membrane, and is preceded by the description of the objective/main goal of the work.

The third chapter is dedicated to the identification of the putative new proteins at the host-parasite interface, using an innovative approach based on proximity dependent biotin identification-BioID.

The discussion followed by the perspective and conclusions is the last chapter of this work.

**Acknowledgements**

**Programa Pós-graduação Ciência para Desenvolvimento (PGCD)** Thank you for believing in me and gave me the opportunity to be a part of this program.

**Maria Manuel Mota,** my acceptance to be part of this laboratory, as well your enthusiasm was and still be one of my main energy sources. Thank you.

**Ksenija Slavic,** my first acknowledgement to you. With you, I start my first baby step in science. Although all the difficulties in the way how we communicate, you were able to help me to grow in science as well personally**.**

**Sonali Setua,** the significant part of this work is based on the Western Blot and immunoprecipitations, techniques that I learned with you. Thank you.

**Vanessa Alexandra Zuzarte Luis**, you have been always there, for any moment that I need. Since Cape Verde, I saw your support and help. Thank you.

**Sofia Marques,** your support and advice were always helpful over these years, which help me to grow personally. Thank you.

**Ana Parreira,** thank you for the sporozoites which without them, the execution of this work would be impossible.

**Irina Franco.** Thank for the teaching and help with the actin polymerisation assay**.**

To my colleagues: **Aparajita Lahree, João Tiago Mello Vieira, Sara de Jesus Santos Baptista, Debanjan Mukherjee.** For all of you, my acknowledgements for your opinions critics and suggestions that contribute**.**

**Francisco Enguita,** Thank you for the production and purification of the recombinant protein.

**Fundação para a Ciência e a Tecnologia.** Thank you for the funding under the project (SFRH/BD/113750/2015)

**Agradecimentos**

**Ao Programa Pós-graduação Ciência para Desenvolvimento (PGCD)**, uma das pedras basilares do desenvolvimento de uma sociedade passa pelo desenvolvimento da ciência. Assim sendo expresso o meu reconhecimento pela iniciativa de criar um programa que visa esse objetivo nos PALOP.

**À Professora Doutora Maria Manuel Mota** Permita-me expressar a minha mais elevada gratidão e admiração. Agradeço pela oportunidade de fazer parte deste extraordinário laboratório que me permitiu concretizar um dos meus maiores sonhos.

**À Drª. Ksenija Slavic** aceite os meus mais elevados agradecimentos, pela forma sábia com que me transmitia os seus conhecimentos e orientação.

**À Drª. Sonali Setua**, foi contigo que aprendi/dei os meus primeiros passos a fazer os Western Blot e as imuno-precipitações, técnicas que me permitiram obter os resultados fulcrais deste trabalho.

**À Drª. Vanessa Alexandra Zuzarte Luís**, agradeço pelo apoio que me tem concedido sempre que recorro a ti sem deixar de lado as ideias e opiniões críticas que me ajudaram na realização deste trabalho.

**À Drª. Sofia Marques**, que pode até não o perceber, no entanto, a forma como te preocupas connosco fez/faz de ti uma figura que ultrapassa uma lab manager, mas sim uma irmã mais velha. Meus agradecimentos pelo apoio, concelhos e sobretudo a forma como te preocupas comigo.

**À Ana Filipa Caetano Parreira,** nunca é demais recordar de que sem o teu trabalho e conhecimentos não seria possível a realização deste trabalho. Muito obrigado pelo fornecimento de mosquitos/parasitas.

**À Drª. Irina Franco**, agradeço pelo apoio na realização dos ensaios da polimerização de actina.

**À Drª. Elina Real**, aceite o meu obrigado pelo apoio e ideias nos desenhos de experiências.

**Ao Drª. Ângelo Chora,** muito obrigado pelas ideias e opiniões que contribuíram para melhorar este trabalho.

**À Drª Inês Bento**, agradeço pelas sugestões das experiências assim como a correção da tese. Muito obrigado.

**Aos meus colegas estudantes de Doutoramento, Aparajita Lahree, João Tiago Mello Vieira, Sara de Jesus Santos Baptista, Debanjan Mukherjee.** Aceitem os meus agradecimentos pelas ajudas/discussão e ideias que contribuíram para o desenvolvimento deste trabalho.

**Ao Leonardo Rocha, Miguel dos Santos e Inês Marreiros,** agradeço pela ajuda e disponibilidade de me ajudarem sempre que precisava. Muito obrigado.

**À Fundação para a Ciências e a Tecnologias (FCT)** que através do projeto (SFRH/BD/113750/2015) financiou a minha bolsa de doutoramento.

**À Cintia Patricia Horta Ramos** As palavras parecem às vezes desprovidas de sentido, tornando difícil encontrar a expressão que traduz o mais profundo reconhecimento por ti. O teu apoio ao longo destes anos, tem contribuído positivamente para a realização deste trabalho.

**À Fundação Calouste Gulbenkian.** Talvez o meu vocabulário não seja assim tão grandioso como é o nome da Fundação, de modos que nele (vocabulário) não existe palavras suficientes e significativas que traduzem o meu agradecimento com o devido reconhecimento. Mas do pouco que consigo. Agradeço pelo financiamento através do projeto iMM/BI/16-2018 que me permitiu obter uma extensão de 5 meses de bolsa. Período esse que foi fundamental para a realização de experiências fulcrais para este trabalho.

**Abbreviations**

| | |
|---|---|
| ATP | Adenosine triphosphate |
| BSA | Bovine serum albumin |
| DMEM | Dulbecco's Modified Eagle Medium |
| DTT | Dithiothreitol |
| EDTA | Ethylenediaminetetraacetic acid |
| EEF | Exo-Erythrocytes Forms |
| EGTA | Ethylene glycol-bis (β-aminoethyl ether)-N, N, N’, N'-tetra acetic acid |
| GFP | Green Fluorescence Protein |
| G-actin | Globular actin |
| HA | Hemagglutinin |
| hDHFR | human Dihydrofolate Reductase |
| HEK | Human Embryonic Kidney |
| h.p.i | hour post infection |
| HRP | Horseradish peroxidase |
| IFA | Immunofluorescence Assay |
| IPTG | Isopropyl β-D-1-thiogalactopyranoside |
| KO | Knock Out |
| LB | Luria-Bertani |
| LC-MS | Nano-liquid chromatography-tandem mass spectrometry |
| MALDI-TOF | Matrix-assisted laser desorption ionisation-time of flight |
| MS | Mass spectrometry |
| MW | Molecular Weigh |
| nM | Nano Mole |
| O. D | Optical density |
| PBS | Phosphate Buffered Saline |
| PMSF | Phenylmethylsulfonyl fluoride |
| PV | Parasitophorous vacuole |

| | |
|---|---|
| PVM | Parasitophorous vacuole membrane |
| RNA | Ribonucleic Acid |
| RPMI | Roswell Park Memorial Institute |
| RT-PCR | Real-time polymerase chain reaction |
| SDS-PAGE | Sodium dodecyl sulfate-polyacrylamide gel electrophoresis |
| SDM | Site-Directed Mutagenesis |
| TEMED | Tetramethylethylenediamine |
| TCL | Total Cell Lysis |
| UIS | Upregulated in Infective Sporozoites |
| UTR | Untranslated Region |
| WT | Wild-type |

**Table of contents** **pag.**

**List of figures** **pag.**

**List of Tables** **pag.**



**Proteomic analysis**

**Abstract**

Malaria, which is caused by Plasmodium parasites, is one of the most prevalent infectious diseases worldwide, with an annual death rate around 435,000, accounting for more than half of all deaths by a vector-borne disease, despite innumerous efforts to eliminate it. The infection initiates when the liver form of the parasite, called sporozoites, are injected into the host skin through a bite by the female Anopheles mosquito. Hepatocyte infection by Plasmodium sporozoites is the first natural step towards the establishment of malaria disease. Inside hepatocytes, the parasite lives in a specialized compartment enveloped by a membrane called parasitophorous vacuole membrane (PVM). The PVM represents the interface between the parasite and the host cell, and most likely plays different roles that may range from protection and signalling to waste elimination. Nevertheless, little is known about the molecular players and interactions occurring at this interface.

A subset of proteins encoded by the "Upregulated in Infective Sporozoites" (UIS) genes have been identified, and it has been shown that some of them are exported to the PVM. One such protein is UIS4, which has been shown to be essential for parasite survival. For instances, sporozoites of the rodent malaria parasites species, Plasmodium berghei (P. berghei) and Plasmodium yoelii (P. yoelii) lacking UIS4 can invade liver cells and begin to grow. However, they do not efficiently develop and replicate.

Despite its important role for malaria parasites during the liver phase of the disease, the biological function of UIS4 remains to be elucidated.

The aims of this work were twofold:

Aim 1. To study the biological function of the UIS4 in the liver stage on the PVM, by revealing its interaction partners.

Aim 2. To search for new host or parasite proteins localized on the PVM during the liver stage of infection.

Our working hypothesis to fulfil the first aim is that UIS4 protects the parasite and that this role is achieved through a network of interacting proteins. Although UIS4-KO parasites have been previously generated in the NK65 parasite line, they did not infect the

mosquito efficiently. Two new UIS4-KO parasites in WT and GFP-expressing P. berghei ANKA lines were created.

To generate these knock-out parasite lines, the P. berghei ANKA UIS4 open reading frame (ORF) was replaced by the hDHFR gene (human Dihydrofolate Reductase) using a double cross-over recombination strategy. The modified parasite line has resistance to pyrimethamine.

The UIS4-KO parasite lines were genotyped to ensure that the transfection constructs integrated into the correct locus. The absence of UIS4 expression in mutant parasites was confirmed by RT-PCR (for RNA expression), immunofluorescence and Western Blot (WB), for protein expression. Assessment of parasite load agreed with previously published studies, both in vivo and in vitro.

To identify the UIS4 interacting partners, immunoprecipitation using an antibody against UIS4 followed by mass spectrometry and WB of infected cells with UIS4-KO and wild-type parasites was performed. Independent experiments identified actin as a major UIS4 interacting partner. Moreover, a similar immunoprecipitation experiment was carried out on mammalian cells transfected with a plasmid expressing the soluble domain of UIS4. Again, actin was immunoprecipitated with UIS4. Notably, in vitro assays of actin polymerization revealed that UIS4 promotes actin polymerization.

In order to find new PVM proteins, an approach based on proximity-dependent biotin labelling, named BioID, was designed. To that end, a parasite line expressing a UIS4-BirA* fusion protein, PbUIS4-BirA*-HA, was generated by transfecting P. berghei ANKA parasites, via a single cross-over recombination, with a plasmid containing approximately 800bp of the UIS4 gene sequence in frame with the BirA*-coding sequence, followed by pyrimethamine treatment and clonal selection. The transgenic parasites were characterized to ensure the correct size of the fusion protein by WB and localization to the PVM by microscopy. Most importantly, the data show that PbUIS4-BirA*-HA parasites behave as wild-type parasites throughout the entire parasite life cycle, and that the biotin supplementation leads to specific biotinylation of proteins on the PVM.

Such immunoprecipitation approach followed by mass spectrometry analysis revealed several novel parasite and host proteins as potential PVM-resident candidates.

Altogether, this study revealed: a) a previously unknown interaction between a critical parasite protein essential for the success of the liver stage of infection and host actin, and b) it also identified new parasite and host proteins that may play a critical role in the interface between Plasmodium parasites and its first obligatory host cell on the PVM.

**Resumo**

Apesar do grande esforço para eliminar a malária, esta doença causada por parasitas *Plasmodium*, continua a ser uma das doenças infeciosas mais prevalentes em todo o mundo, com cerca de meio milhão de mortes anualmente. O aumento da resistência aos antimaláricos em cena aumenta a necessidade de descobrir novos fatores críticos para a infeção e que, em última instância, possam ser usados como alvo para a profilaxia ou tratamento da malária.

A infeção é iniciada quando os esporozoítos são injetados na pele do hospedeiro durante uma refeição de sangue feita pelo mosquito *Anopheles*. A infeção de hepatócitos por esporozoítos de *Plasmodium* é o primeiro passo natural e obrigatório para o estabelecimento de uma infeção por malária. Nos hepatócitos, o parasita reside dentro de um compartimento especializado envolto por uma membrana chamada membrana do vacúolo parasitário (ou PVM, do inglês parasitophorous vacuole membrane). Embora o PVM represente a interface entre o parasita e a célula hospedeira, possivelmente desempenhando diferentes papéis, desde a proteção do parasita, sinalização até à eliminação de resíduos, pouco se sabe sobre os fatores moleculares e as interações que ocorrem nesta tão importante interface.

Um conjunto de proteínas codificadas pelos genes "Upregulated in Infective Sporozoites" (UIS) foi identificado, alguns deles mostraram-se exportados para o PVM e essenciais para a sobrevivência do parasita, nomeadamente o UIS4. Esporozoitos dos parasitas de malária infeciosos para roedores, *Plasmodium berghei* (*P. berghei*) e *Plasmodium yoelii* (*P. yoelii*), deficientes para UIS4, são capazes de invadir as células do fígado e começam a crescer, mas não conseguem se desenvolver e replicar eficientemente. Apesar de sua grande

importância para o estabelecimento da infeção hepática, a função biológica da proteína UIS4 continua desconhecida.

Ao todo, dois objetivos foram perseguidos:

• Objetivo 1. Estudar a função biológica do UIS4 na fase hepática da infeção, revelando outras moléculas que interagem com esta proteína.

• Objetivo 2. Encontrar novas proteínas da célula hospedeira ou do parasita expressas no PVM durante a fase hepática da infeção.

O primeiro objetivo tem por base a hipótese de que a UIS4 protege o parasita e esse papel é alcançado através de uma rede de proteínas que interagem com ela. Embora parasitas deficientes em UIS4 tenham sido gerados anteriormente, foram criados dois novos parasitas transgénicos deficientes em UIS4 em linhas de *P. berghei* ANKA wild-type ou que expressam GFP. Os parasitas deficientes em UIS4 gerados anteriormente tinha sido obtidos em *P. berghei* NK65, que mostra baixa infecciosidade no mosquito. Para gerar estas novas linhas de parasitas transgénicos, a ORF de *P. berghei* ANKA UIS4 foi substituída pelo gene hDHFR (Dihydrofolate Reductase humano), que confere resistência à pirimetamina, usando uma estratégia de recombinação cruzada dupla. As novas linhas foram validadas através de genotipagem para garantir que a integração ocorreu no locus correto. A perda de expressão de UIS4 foi confirmada nestas linhas por RT-PCR (para expressão de RNA), bem como por imunofluorescência e Western Blot (WB, para expressão proteica). Uma diminuição da carga parasitária foi observada de acordo com estudos publicados anteriormente, *in vivo* e *in vitro*. Para identificar novas moléculas que interagem com a UIS4, foi realizada uma imunoprecipitação utilizando um anticorpo contra UIS4 seguido de espectrometria de massa e WB em células infetadas com parasitas wild-type (ou parasitas deficientes em UIS4, como controlo). Experiências independentes identificaram actina como uma molécula potencialmente capaz de interagir com a UIS4. Uma experiência de imunoprecipitação semelhante à anterior foi realizada em células transfetadas com um plasmídeo que expressa o domínio solúvel da UIS4. A actina foi novamente imunoprecipitada com a UIS4. Notavelmente, num ensaio *in vitro* de polimerização de

actina usando o domínio solúvel recombinante de UIS4, os resultados revelam que o UIS4 promove polimerização de actina.

Paralelamente, para encontrar novas proteínas da PVM, foi utilizada uma abordagem baseada na marcação de biotina dependente da proximidade, denominada BioID. Para esse fim, uma nova linha de parasitas expressando uma proteína de fusão UIS4-BirA*, PbUIS4-BirA*-HA, foi gerada transfetando parasitas *P. berghei* ANKA com um plasmídeo contendo aproximadamente 800pb da sequência do gene UIS4 juntamente com a sequência de codificação de BirA*, seguida da seleção por pirimetamina e selecção clonal. Os parasitas transgénicos foram caracterizados para garantir o tamanho correto da proteína de fusão (WB) e localização para na PVM (microscopia). Mais importante, os dados mostram que os parasitas PbUIS4-BirA*-HA se comportam como parasitas wild-type ao longo de todo o ciclo de vida do parasita, que a suplementação com biotina leva a biotinilação específica na PVM e que usando estreptavidina, PbUIS4-BirA*-HA é imunoprecipitado com a biotina em células infectadas com parasitas expressando BirA*. Esta abordagem de imunoprecipitação seguida por análise por espectrometria de massa revelou várias novas proteínas do parasita bem como da célula hospedeira como potenciais candidatos a serem proteínas residentes na PVM.

Em sumário, os dados apresentados nesta tese revelam não só uma nova interação com uma proteína do parasita que é essencial no estabelecimento da fase hepática da infeção, como expõe o potencial de novas proteínas do parasita e do hospedeiro em fazerem parte da importante interface entre o parasita da malária e a célula hepática.

# CHAPTER I- INTRODUCTION

## I. Introduction

Vector-borne diseases such as malaria, dengue, schistosomiasis, sleeping sickness, leishmaniasis, Chagas disease, yellow fever, and Japanese encephalitis kill around 700,000 people every year worldwide (World Health Organization, 2017). These diseases are caused by microorganisms such as parasites, bacteria, and viruses, and are transmitted by arthropods such as mosquitoes, sand flies, triatomine bugs, black flies, ticks, tsetse flies, and mites (World Malaria Report, 2018). Many of these insects are blood-sucking vectors that ingest the pathogen from the blood of an infected host to then infect a new host.

Malaria, which is caused by *Plasmodium* parasites, is one of the most prevalent infectious diseases worldwide, with an annual death rate around 435,000 (World Health Organization, 2018), accounting for more than half of all deaths by a vector-borne disease, despite innumerous efforts to eliminate it (World Health Organization, 2018). The Sub-Saharan region is the one most affected, accounting for more than 92% of the total annual malaria death toll. The economic burden of malaria is estimated to be US$ 12 billion every year due to health care expenses, absenteeism from work and school, decreased productivity, and missed opportunities for investment and tourism in affected areas.

### I.1. The History of malaria

Malaria is one of the oldest diseases known; it is reported in ancient Chinese documents from around 2700 BC, as well as Mesopotamia in 2000 BC and the ancient Egyptian civilization in 1750 BC. The Greek writer Hippocrates described the disease's main symptoms as intermittent fever and enlarged spleen (Arrow et al., 2004; Sullivan, 2006; Cox, 2010; Mordecai et al., 2013).

The word malaria was coined by Italian writers as *mal are*, meaning "bad air," in the early 19$^{th}$ century. They believed that marsh gas was the cause of the disease. A better understanding of malaria came in 1880 when Charles Louis Alphonse Laveran, a French physician working in Algeria, proposed that malaria was caused by a parasite he named *Oscillaria malariae*. In 1884, Ettore Marchiafava and Angelo Celli renamed the parasite *Plasmodium* (Laveran, 1922). However, the malaria vector was still unknown at the time.

In 1897, Ronald Ross, a British physician who collaborated with Scottish medical doctor Patrick Manson, was working in Africa when he proposed that a mosquito was responsible for transmitting *Plasmodium* to people (N. J. White, 2014). The century since 1917 has been an era of searching for malaria treatment, a search that continues today. Initially, the malaria *Plasmodium* was used for treating neurosyphilis by inducing malaria fever in patients (O'Leary, 1928; Whitrow, 1990). The injection of *Plasmodium*-infected blood in neurosyphilis patients was widely practiced for years until the discovery of penicillin, and Julius Wagner-Jauregg, the pioneer of this procedure, was awarded the Nobel Prize for medicine and physiology in 1927. Nowadays the procedure is no longer used.

## I.2. Biogeography of Malaria

At the beginning of the 20$^{th}$ century, malaria occurred everywhere except in Greenland (Gates and Chambers, 2015). However, due to the massive global fight against the disease, mainly by controlling the vector with Dichlorodiphenyltrichloroethane (DDT), together with other residual insecticides, malaria was eradicated from most parts of the world (Sadasivaiah et al., 2007), as illustrated in Figure 1.

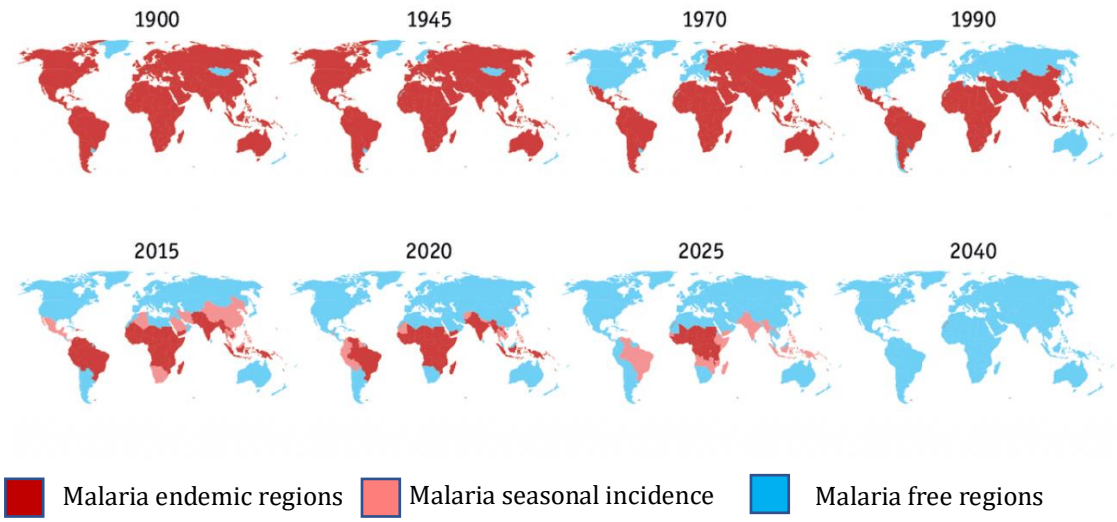


Figure 1. **Global Malaria distribution through time and prediction until 2040.** Adapted from: economist/ Gate foundation

After this massive campaign, the disease has been continuously eliminated from many countries, although at a slow rate, as the figure shows. According to predictions made by the Bill and Melinda Gates Foundation, malaria will be eradicated by 2040 (Gates and Chambers, 2015).

Nowadays malaria is found throughout the tropical and subtropical regions. This includes Central and South America, Sub-Saharan African countries, Southeast Asia, and the Pacific Islands (World Health Organization, 2017). Besides the high incidence in endemic areas, malaria may also occasionally occur naturally in regions where the disease has been eliminated, due to different reasons but mainly changes in rainy season and migration (Martens and Hall, 2000). Reports from 2016 show that malaria is still endemic in 91 countries (World Health Organization, 2017), as shown in Figure 2. Although the report indicates that the malaria burden in Asia is underestimated, 92% of the deaths due to malaria seem to occur in Africa, affecting mainly children under five years of age (World Health Organization, 2017; Hay et al., 2010). Indeed, of the five countries accounting for half of the global incidence of malaria, four are African countries: Nigeria (25%), The Democratic Republic of the Congo (11%), Mozambique (5%), and Uganda (4%); the fifth is India (4%) (World Health Organization, 2018).

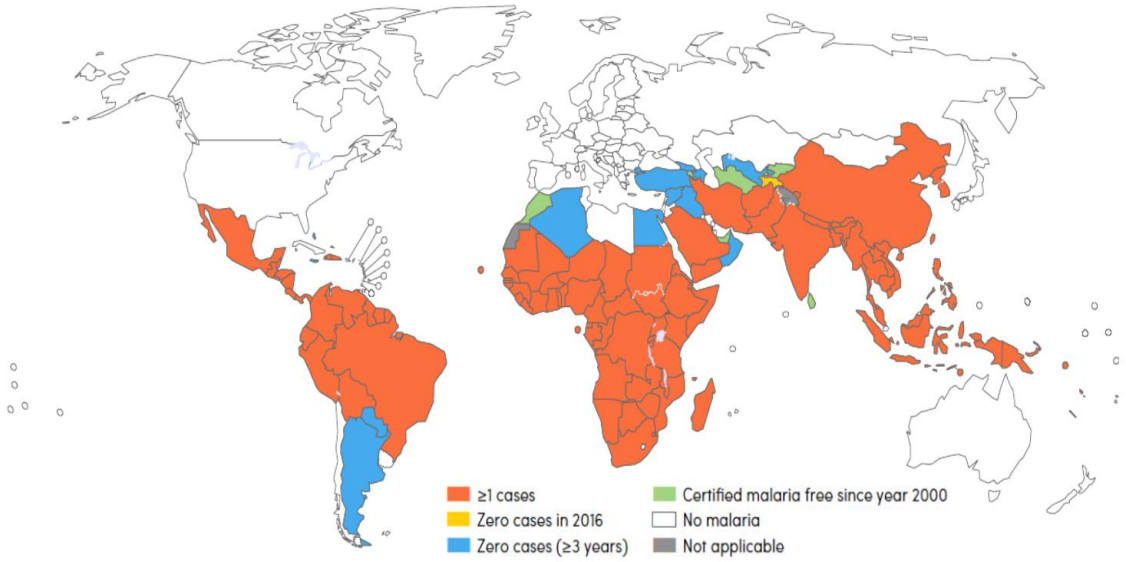


Figure 2.**Global malaria distribution map in 2016.** World Health Organization 2017

## I.3. Challenges of malaria eradication

The prospect of malaria eradication gained momentum twice in history. With the discovery of chloroquine, a drug used to treat malaria, and the powerful insecticide DDT, the hopes were high that malaria could be eradicated.

In 1955, the World Health Organization (WHO) developed the malaria elimination program. The initial results were encouraging and the eradication of malaria in 15 countries led some to believe that malaria could be wiped out in a few decades. However, the Garki Project (Garki Project) concluded that short-term malaria eradication would not be a reality in Africa, considering the tools available at the time. Indeed, malaria rebounded strongly until new malaria eradication programs were adopted. Nonetheless, the goal of a "malaria-free world" has never been abandoned.

The period from 2000 to 2014 marks the second momentum for malaria eradication, with the scale-up of new strategies such as insecticide-treated bed nets and artemisinin-combination therapy, leading to a significant drop in malaria burden (40%), marking a new turning point in malaria elimination.

This initial success revitalized hope in malaria elimination programs. However, it seems that the new programs are still not fully successful. The decrease in malaria rates during the period seems to have reached a stagnation point. In its 2018 malaria report, the WHO reveals that no significant reduction in malaria incidence was observed during the 2015–2017 period. In the three last years, the number of people at risk has remained unchanged at 59 cases/1,000 (World Malaria Report, 2018).

Apart from the issues mentioned above, malaria elimination is facing a new challenge of a different nature. At the present time, it is widely accepted that climate changes could or will have an impact on human infectious diseases (Wu et al., 2016; Tanser et al., 2003). It is known that malaria transmission requires specific environmental conditions, mainly the right temperature and humidity levels that favor the spread of the vector. Thus, climate change has the potential to compromise malaria elimination projects by leading to longer disease-transmission seasons. Climate change may also create new environmental

conditions for the mosquito vector, which may be able to adapt to living in regions not possible before, which then could lead to new sites of malaria transmission.

However, this might not be the only challenge for malaria eradication programs. According to WHO, *Plasmodium* drug resistance, as well as vector resistance to insecticides, is increasing. The resistance to pyrethroids used in insecticide-treated bed nets increased by 10% from 2010 to 2016 (World Health Organization, 2017). Moreover, according to a 2017 WHO report, the increasing incidence of *P. falciparum* carrying histidine-rich protein 2 (HRP2) gene deletions imposes a considerable problem for *Plasmodium falciparum* (*P. falciparum*) infection diagnosis. The deletion of HRP 2 leads to false-negative results, due to the inability of HRP2-based Rapid Diagnostic Test to detect *P. falciparum* (Kozycki et al., 2017; World Health Organization, 2017).

## I.4. Etiologic Agent of Malaria

*Plasmodium,* the causal agent of malaria, belongs to the Apicomplexan *phylum*. Besides *Plasmodium*, this *phylum* comprises a number of protozoans that infect different hosts, ranging from humans to cockroaches (Morrissette and Sibley, 2002). The Apicomplexan *phylum* includes other pathogens such as *Toxoplasma gondii*, which causes a life-threatening disease in immunocompromised individuals; *Eimeria* spp. and *Theileria* spp., which cause animal parasitic infections, and *Neospora* and *Cryptosporidium*, the etiologic agents of severe diarrhea (Morrissette and Sibley, 2002). All these agents are obligate intracellular parasites that have a chloroplast-like structure named Apicoplast and that in most cases replicate inside the parasitophorous vacuole, a specialized compartment (Moore et al., 2008; Dluzewski et al., 1992; Lingelbach and Joiner, 1998). *Plasmodium* species contain a nuclear genome with 14 chromosomes and a circular extra chromosome in the Apicoplast plus the mitochondrial genome (Antinori et al., 2012).

Although they are haploid species for the greater part of their life, apicomplexans undergo a complex life cycle and differentiate into various specialized forms, which make them adapted to invade and infect different hosts as well as different cell types in the same host. *Plasmodium* invasive forms, known as "*zoites,"* are polarized cells characterized by an

elongated shape with an apical region/end containing organelles such as rhoptries and micronemes, that have the necessary biological equipment for parasite motility, adhesion, and invasion, and for producing the parasitophorous vacuole in the host (Carruthers et al., 1999; Nichols et al., 1983). Even though they lack cilia and flagella, apicomplexan *zoites* are motile, reaching up to 10μm/s in speed, moving in a substrate-dependent manner named gliding (Ménard, 2001). This motility is divided into three different categories: circular gliding, a circular movement made in counterclockwise circles; upright twirling gliding, the opposite of circular gliding; and helical gliding, which is a long-distance movement made horizontally (Wetzel et al., 2003; Håkansson et al., 1999).

There are more than 500 *Plasmodium* species, of which five are infectious to humans, namely *P. falciparum*, *P. vivax*, *P. ovale*, and *P. malariae,* as well as *P. knowlesi* which is a zoonotic species (Antinori et al., 2012), Table 1. Cases of infections caused by unusual *Plasmodium* species are rare (Don E. Eyles, 1960; Chin et al., 1968; Vieira et al., 2001).

## I.5. *Plasmodium* species infecting humans

***Plasmodium falciparum*** (*P. falciparum*) is the deadliest human malaria parasite. In the hepatic stage of infection, *P. falciparum* has the highest replication rate found in all human-infecting *Plasmodium* species, producing up to 30,000 merozoites (the infectious form that invades red blood cells) in five to seven days. In the blood, each replication cycle of the parasite takes two days. Although the parasite preference is for young red blood cells (RBCs), *P. falciparum* can also invade RBCs of all ages. Due to its ability to adhere, which is mediated by erythrocyte membrane protein 1 (PfEMP1), the mature forms of the parasite are rarely found in peripheric blood (Oh et al., 1997). In fact, this is the deadliest feature of *P. falciparum.* Untreated, *P. falciparum* infection may take up to 13 years to be resolved (E. A. Ashley. and N. J. White, 2014).

The *P. falciparum* nuclear genome has 14 chromosomes encoding more than five thousand genes; it is rich in A-T content, which covers 81% of the whole genome (Gardner et al., 2002).

***Plasmodium vivax*** (*P. vivax*), identified six years later than *P. falciparum* (1886), is less deadly if compared to *P. falciparum,* but is the most widely spread human malaria parasite. Typical *P. vivax* symptoms involve tertian benign fever. Both *P. vivax* and *P. ovale* are characterized by their ability to form hypnozoites, which are dormant forms of the parasite that hide in the liver and are responsible for malaria relapses that can strike several months or even years after malaria has been apparently resolved (Mikolajczak et al., 2015). During the intra-erythrocytic stage, *P. vivax* preferentially invades reticulocytes, and both young and mature forms of the parasite are found circulating.

The *P. vivax* genome is the largest among the human-infecting *Plasmodium* spp. ever sequenced, with 26.8 megabases of DNA. Despite carrying a number of genes similar to other *Plasmodium* spp., the *P. vivax* genome has considerably higher G-C content than *P. falciparum* (Carlton et al., 2008; Auburn et al., 2016).

***Plasmodium ovale*** *(P. ovale)* was named for the oval shape that the red blood cell acquires upon infection by this parasite (Stephens, 1914). *P. ovale* usually displays low parasitemia, which is thought to be due to its preference to infect reticulocytes. Nevertheless, it produces the second highest number of liver-stage merozoites. Like *P. vivax*, *P. ovale* also assumes quiescent forms, the hypnozoites, that may lead to the relapse of malaria up to four years after resolving the disease (Collins and Jeffery, 2005; Carlton et al., 2008).

***Plasmodium malariae*** (*P. malariae*) was identified together with *P. vivax*. Among the *Plasmodium* species that infect humans, *P. malariae* is the parasite with the slowest development rate, both in the liver (up to 15 days) and in the blood (72 hours). It causes quartan fever and infects, preferentially, old erythrocytes. Although there are no reports of *P. malariae* hypnozoites, this species can remain up to 40 years in the blood of infected hosts and still cause low parasitemia (Stephens, 1914).

***Plasmodium knowlesi*** is a zoonotic pathogen that crisscrosses between its natural hosts, macaques, and humans. It is the only *Plasmodium* species known to cause quotidian fever in humans (cycling every 24h in blood-stage) (B. Singh et al., 2004). The prepatent period is between 9 and 12 days (Antinori et al., 2012). *Plasmodium knowlesi* was named to honor Dr. Robert Knowles, who successfully infected human volunteers with

macaque blood passage, to show the crisscrossing of this particular species. *P. knowlesi* is found mostly in South-Eastern Asia (Collins, 2012; Sabbatani et al., 2012). However, because *P. malariae* is very similar to *P*. *knowlesi*, the possibility of misdiagnosis cannot be ruled out (Collins, 2012).

**Table 1**. *Plasmodium* parasite infecting human host.

| ***Plasmodium* species** | | | | | |
|---|---|---|---|---|---|
| Characteristics | *Plasmodium Falciparum* | *Plasmodium Vivax* | *Plasmodium Ovale* | *Plasmodium malariae* | *Plasmodium knowlesi* |
| Pre-Erythrocytic phase (in days) | 5-7 | 6- 8 | 9 | 14-16 | 8-9 |
| Erythrocytes cycle (in hours) | 48 | 48 | 50 | 72 | 24 |
| Hypnozoites | No | Yes | Yes | No | No |
| Erythrocytes preference | All ages | Reticulocytes | Reticulocytes | Mature erythrocytes | All ages |
| Number of merozoites per hepatic schizont | 30000 | 10000 | 15000 | 20000 | ND |
| Severe malaria | Yes | Yes | No | No | Yes |
| Recurrences (in Years) | Yes (2 years) | Yes (4 years) | Yes (4 years) | Yes (40 years) | Yes (?) |
| Genome singularity | G-C rich | A-T rich | - | - | - |

## I.6. Symptoms and Malaria diagnosis

The incubation period before symptoms appear can vary from seven to 18 days depending on the *Plasmodium* species. The symptoms are fever above 38°C, headaches, vomiting, and feeling hot and shivery (Malaria, World Health Organization). A prompt malaria diagnosis followed by rapid treatment is the first and most important step to malaria control. In the case of suspected malaria infection, the diagnosis must be confirmed. Besides patient history, microscopy images of Giemsa-stained blood film attesting to the presence of the parasite in a drop of the patient's blood is the standard procedure for malaria diagnosis.

With microscopy, it is possible to identify the species, to quantify the parasitemia, and to evaluate the parasite differentiation status, as well as asexual and sexual forms. However, the use of microscopy requires personnel with expertise, and may produce a false-negative result when parasitemia is low. In the past years, non-microscopic methods have also been developed, such as Rapid Diagnosis Test (RDT) based on the detection of

plasmodial antigens. The test works by detecting aldolase that, together with plasmodial lactate-dehydrogenase (pLDH), is found in all human-infecting *Plasmodium* species.

However, *P. falciparum* and *P. vivax* have a specific lactate-dehydrogenase (PfLDH and PvLDH, respectively; see Table 2) (Moody, 2002). Thus, microscopic confirmation is always mandatory in case of a lactate-dehydrogenase negative result. PCR is the most sensitive diagnostic method; however, it is expensive. As for serology tests, they may produce false-positive results when antibodies of a resolved infection are detected.

**Table** *2. Plasmodium* genus detection by RDT Rapid Diagnosis Test (RDT)

| | *P. falciparum* | *P. ovale* | *P. vivax* | *P. malariae* | *P. knowlesi* |
|---|---|---|---|---|---|
| **Aldolase** | X | X | X | X | X |
| **pLDH** | X | X | X | X | X |
| **PfLDH** | X | | | | |
| **PvLDH** | | | X | | |
| **HRP2** | X | | | | |

## I.7. Distribution of *Plasmodium* species in the world

The deadliest human-infecting species, *P. falciparum*, is mostly restricted to Sub-Saharan Africa where it was responsible for more than 99% of the cases reported in 2016 (World Health Organization, 2017). *P. falciparum* also occurs in regions of India and Papua New Guinea, Figure 3-A. Different than *P. falciparum, P. vivax* predominates in South-East Asia, and in Eastern and South America.

Besides Ethiopia and Madagascar, *P. vivax* is virtually absent in Africa due to human genetic resistance in Africa against this plasmodium species, Figure 3-B. *P. vivax* occurs predominantly in three countries and accounts for more than 80% of the cases reported annually worldwide (India and Pakistan, in Asia, and Ethiopia in Africa). In 2015, 74% of *P. vivax* cases occurred in Indo-Pacific regions, followed by 11% in South America and 10% in the WHO African region. With exception of WHO America regions, where *P. vivax* accounted for 64% of the incidence in 2017, *P. falciparum* remains the *Plasmodium* species with greatest occurrence worldwide with 99.7% in Africa, 66% in South-East

Asian regions, 58% in Eastern Mediterranean regions, and 77% in Western Pacific regions, Figure 3-C (World Health Organization, 2017).

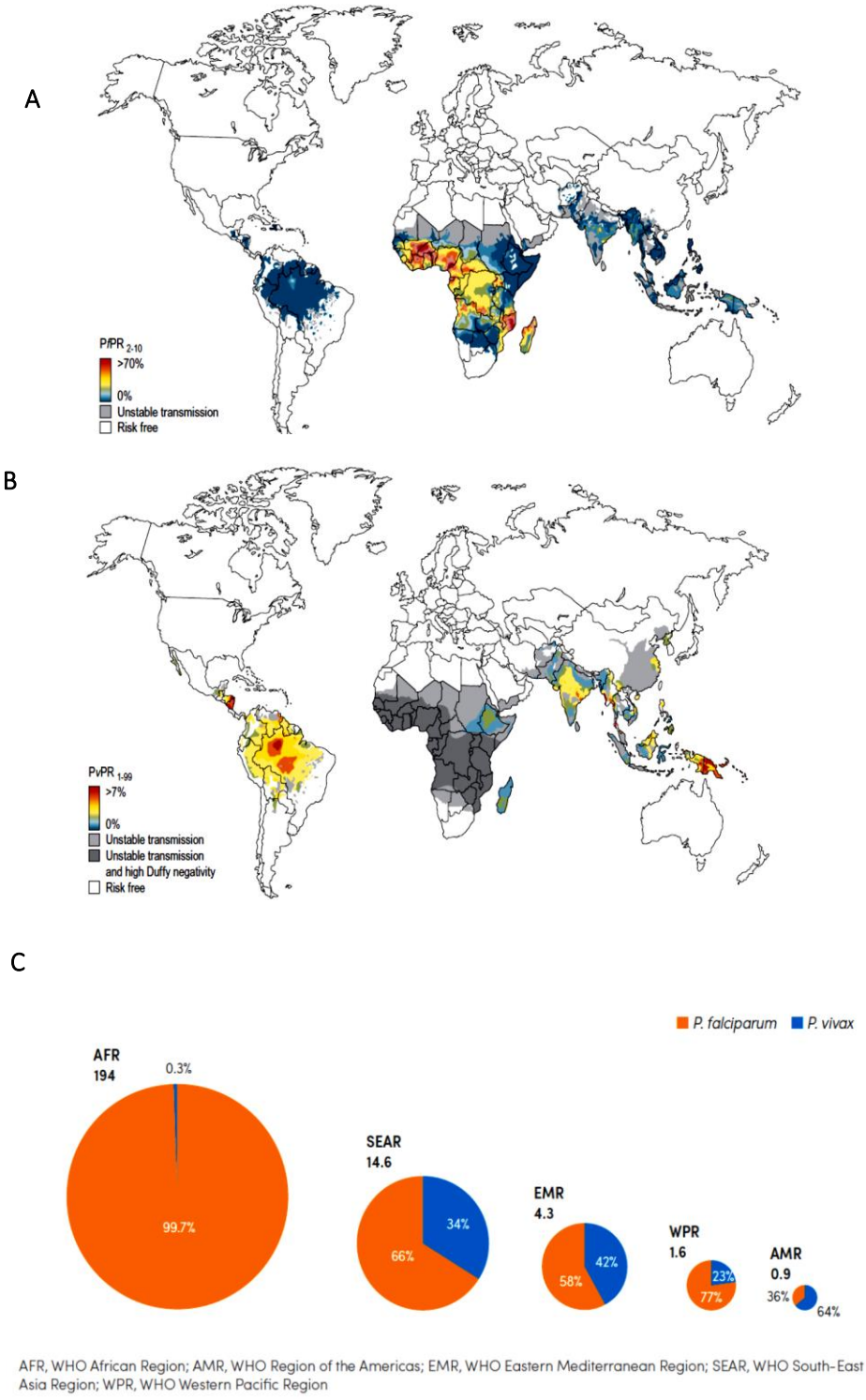


Figure 3. **Global distribution of P. falciparum and P. *vivax* and incidence in 2016**. A) Distribution of *P. falciparum*, B) Global distribution of P. *vivax*, C) Global incidence of P. *falciparum* and *P. vivax*. Adapted: World Health Organization 2017.

## I.8. Environmental and host factors in malaria transmission

Three main factors can impact malaria transmission: temperature, humidity, and altitude. The ideal temperature for malaria transmission is between 16 ºC and 33 ºC (Blanford et al., 2013; Mordecai et al., 2013) while the perfect altitude for malaria occurrence is below 2,000 meters (Drakeley et al., 2005). Relative humidity below 10% is detrimental for *Anopheles gambiae* development (Yamana and Eltahir, 2013), which may explain the increase in mosquito burden, and malaria transmission, observed in endemic regions during the rainy season, when the humidity is higher (N. J. White, 2014).

Mosquito sporozoite development can take three weeks. Therefore, the mosquito's longevity is crucial to ensure the complete sporozoite growth and its successful transmission upon blood feeding.

In the endemic regions, where transmission rates are high, children are the ones most susceptible to malaria, partially due to the immunity adults develop against the parasite throughout life, which accounts for a lower parasitemia. Thus, children represent an important parasite reservoir. Immunity against severe malaria is only seen in children above five years and adult individuals. Nevertheless, sterile immunity has never been observed (Marsh and Kinyanjui, 2006), Figure 4.

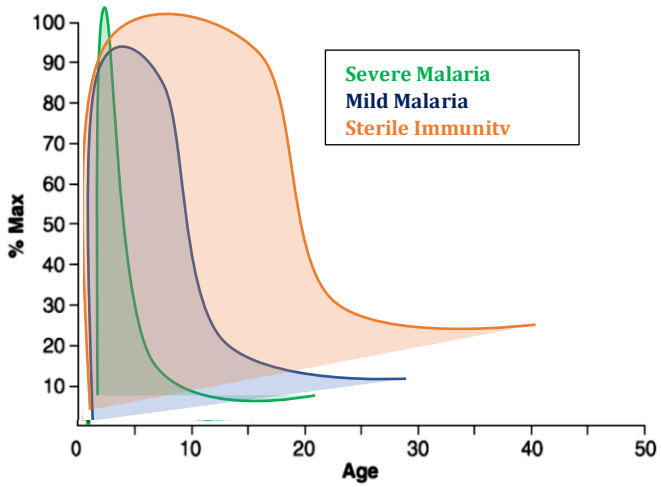


**Figure 4** Dynamics of immunity acquisition against malaria. Adapted from: (Marsh and Kinyanjui, 2006).

It is not common for babies to develop malaria, most likely because of passive transfer of maternal immunity as well as high levels of hemoglobin F in their red blood cells (Amaratunga et al., 2011).

Host genetic factors also play an important role in conferring protection against malaria, particularly the presence of polymorphisms in genes coding for hemoglobin. This is the case of hemoglobin S haemoglobinopathy, which causes sickle cell anemia. The red blood cells with hemoglobin S have an abnormal 'sickle' shape and low oxygen tension (Seakins et at., 1973 ; Taylor et al., 2012; Williams 2012). The mechanisms underlying protection by the sickle trait have been extensively investigated, and current views indicate that the parasite cannot grow or develop inside sickle cells. Besides that, higher rates of parasite clearance and reduced endothelial adhesion also play a role (Bunn, 2013).

Glucose-6-phosphate dehydrogenase (G6PD) deficiency also provides protection against malaria (Louicharoen et al., 2009). However, Mbanefo and colleagues tested this hypothesis in a meta-analysis study, and the data show no correlation between Glucose-6-phosphate dehydrogenase (G6PD) deficiency and the occurrence of severe malaria (Mbanefo et al., 2017). The lack of Duffy antigen on red blood cell surfaces in individuals from the West African countries was also thought to confer resistance to *P. vivax* and *P. malariae* infection (Louicharoen et al., 2009). However, a growing number of studies have reported *P. vivax* infections in Duffy-negative individuals. Therefore, this issue requires further investigation (Dhorda et al., 2011; Culleton et al., 2009; Ryan et al., 2006).

## I.9. *Plasmodium* life cycle

Malaria transmission occurs when an infected female *Anopheles* mosquito bites a vertebrate host. The first step in the infection process is the migration of the infectious liver forms of the parasite, called sporozoites, from the bite site to the liver, crossing a number of obstacles before reaching the bloodstream and then the liver, which occurs through blood flow (Mota et al., 2001).

Although asymptomatic, the liver stage is an obligatory step for the establishment of the disease. Once inside the liver, sporozoites cross several hepatocytes before infecting the final one (Mota et al., 2001).

The role of this migration to the liver for the onset of malaria infection has been the subject of several studies that have generated controversial findings. Mota and colleagues have proposed that migration through the host cells is required for sporozoite activation (Mota et al., 2002). However, another study has shown that parasites lacking the sporozoite microneme Protein Essential for Cell Traversal (SPECT), which therefore do not undergo the cell traversal process, still infect hepatocytes, challenging the hypothesis that migration and cell traversal are essential for establishing infection (Ishino et al., 2004).

Nevertheless, *in vitro P. falciparum* SPECT deficient sporozoites (PfSPECT) fail to establish a normal liver infection in humanized mice (Yang et al., 2017). Thus, the role of traversal for malaria infection onset remains an open question.

From the host cell perspective, Hepatocyte EphA2 receptor was shown to be critical for the establishment of infection. In other words, sporozoites invade hepatocytes showing high expression of the EphA2 receptor (Kaushansky et al., 2016). Once the parasites have entered the hepatocyte, *Plasmodium* undergoes one cycle of replication to produce thousands of blood-infecting forms, the so-called merozoites. Merozoites are released gradually into the bloodstream by budding off from the merosome, a membrane-bound structure named merosome, to then escape the macrophages in the liver. This event is preceded by parasitophorous vacuole membrane (PVM) breakdown and disintegration of the host cell plasma membrane (Burda et al., 2017; Hale et al., 2017). PVM is a specialized vacuolar niche structure surrounded by a membrane required for the parasite to efficiently develop inside a hepatocyte. PVM was reported in 1994 for blood-stage malaria parasites (Heidi G. Elmendorf, 1994).

During *Plasmodium* development inside the hepatocyte, the critical signal of host cell self-death is inhibited through the calcium ($Ca^{2}$+) absorption by merozoites. By keeping the

intracellular $Ca^{2}$+ lower, the parasite inhibits the exposure of phosphatidylserine and thereby interferes with cell apoptosis (Van De Sand et al., 2005).

Merozoites are eventually released from the merosome in the pulmonary microvasculature in a process that can last from 5 to 60 minutes (Baer et al., 2007). Due to their vulnerability, merozoites must invade red blood cells shortly after their release, in order to escape from immune cells (Baer et al., 2007)(Baer et al., 2007).

Multiple molecular players mediate the invasion into the red blood cell, including merozoite proteins found in apical organelles (micronemes and rhoptries), as well as surface erythrocytic proteins. During this process, many receptor-ligand interactions are formed between the parasite and the erythrocyte. The reticulocyte-binding protein homologue 5 (PfRh5), for example, was shown to be a key player in the process of cell invasion by *P. falciparum* (Baum et al., 2009). For *P. vivax* and *P. knowlesi*, this role is attributed to Duffy antigen ($Fy^{a}$ or $Fy^{b}$) (Miller et al., 1976). It has been shown recently that Transferrin receptor1 is critical for the process of reticulocyte invasion (Gruszczyk et al., 2018). The molecular players supporting *P. malariae* and *P. ovale* invasion are still unknown.

Once inside red blood cells, parasites undergo several replication cycles in which each merozoite gives rise to 6–30 new merozoites that are ready to infect new red blood cells. This event occurs every 24 hours for *P. knowlesi*; every 48 hours for *P. falciparu*m, *P. vivax*, and P. *ovale*; and every 72 hours for *P. malariae* (N. J. White, 2014).

The blood stage is the symptomatic stage of malaria infection and is characterized by exponential parasite growth. The typical malaria symptoms are high temperature, feeling hot and shivery, headaches, vomiting, muscle pains, and diarrhea.

While most of the merozoites maintain an asexual replication cycle once inside red blood cells, eventually some differentiate into male and female gametocytes. These are the precursors of the sexual forms of the parasite, which differentiate once inside the mosquito's midgut (Aly et al., 2009).

The sexual development of *Plasmodium* starts with zygote formation after fertilization of the female gamete by a male gamete. The zygote then becomes an ookinete by undergoing a meiotic division. Ookinetes are motile, able to travel across the midgut epithelium before they become oocysts in the beneath-midgut basal lamina. The oocyst develops and undergoes sporogony (sporozoites formation), which takes approximately 14 days, before sporozoites exit the oocyst and invade the mosquito's salivary glands where they stay until injected into the skin of a new host during a blood meal (Aly et al., 2009). See the schematic representation in Figure 5 for *Plasmodium* development in the human host and Figure 6 for the event in the mosquito vector.

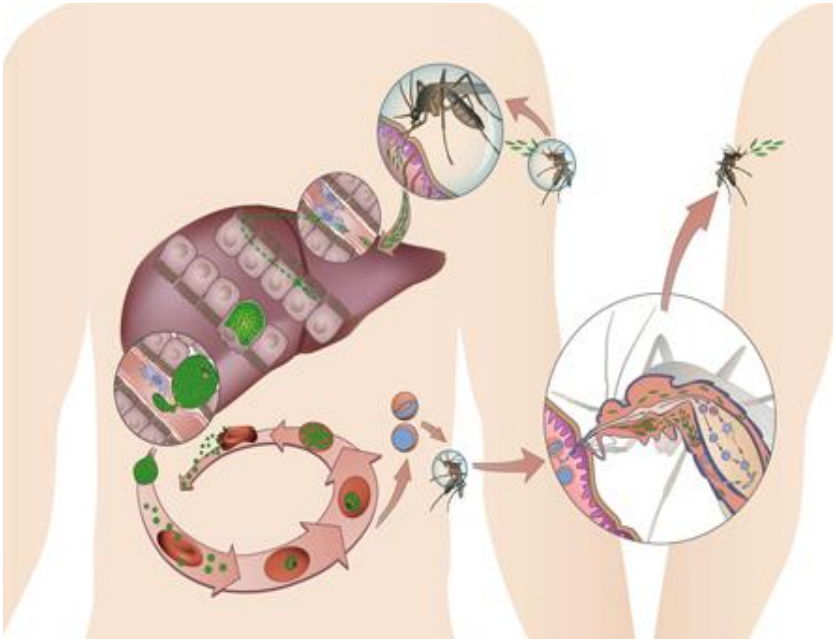

Figure 5. **Schematic representation of *Plasmodium* life cycle in human host**.

The malaria onset begins with the deposition of sporozoites from mosquito salivary gland into the dermis of the host during the blood meal. Sporozoites then travel from dermis to bloodstream and reach to the liver. During their journey to the liver, they traverse several barriers before homing in a final host cell hepatocyte. Sporozoite differentiates into dozens of thousands of new parasites form named merozoites. Merozoites are then released into the bloodstream and infect red blood cells and replicate to generate 10 to 30 daughter merozoites. However, some merozoites differentiate into sexual forms of the parasite maned gametocytes

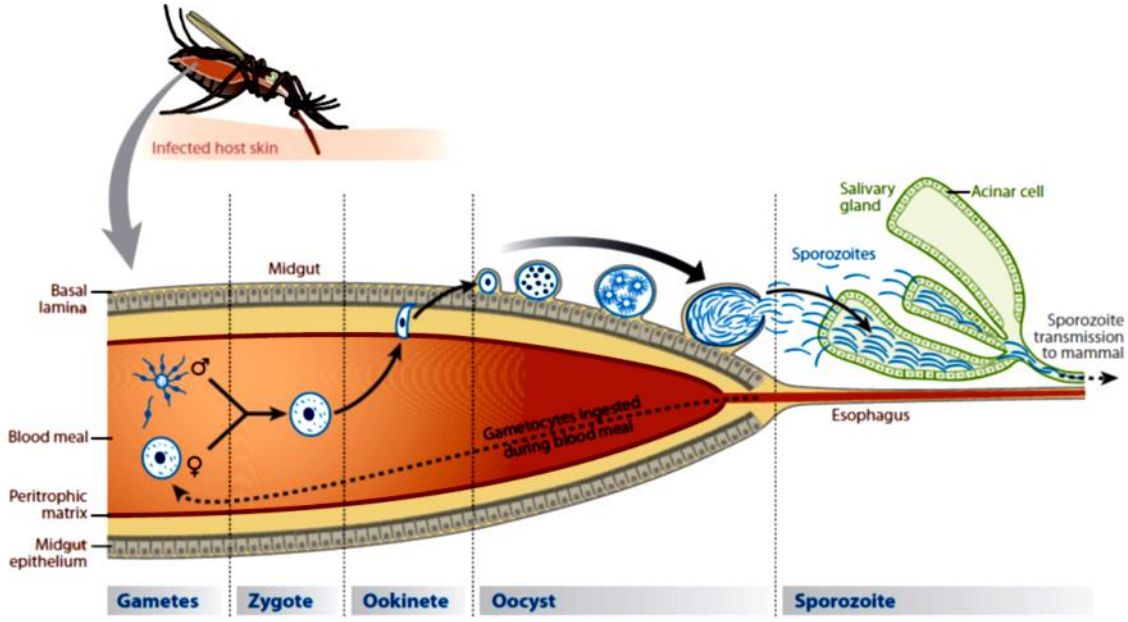


Figure 6. **Fertilization and differentiation of malaria parasites in the mosquito host**.

The ingested gametocytes from a blood meal from an infected individual undergo differentiation into gametes once inside the mosquito and fertilization takes place in the midgut to form zygotes. The zygotes undergo meiosis and form ookinetes. The ookinetes go through the peritrophic matrix of the midgut, enter the apical end of the epithelium, and traverses several epithelial cells before arriving at the basal epithelial surface. Here, they form oocysts which undergo sporogony to develop into thousands of sporozoites, which upon egress from the sporoblast travel in the hemolymph to reach the salivary gland where they´re ready to be transmitted to an individual during a subsequent blood meal. Adapted from (Aly et al., 2009).

## I.10. Development inside hepatocyte

The liver stage is the first natural step towards the establishment of malaria infection. In humans, 5 to 15 days post infection, depending on the *Plasmodium* species (Table 1), a single sporozoite can originate 10,000 to 30,000 first-generation merozoites that exit the liver into the bloodstream, starting a blood-stage infection. As mentioned earlier, to efficiently develop inside a hepatocyte, parasites need to build a specialized vacuolar niche structure surrounded by a membrane, the Parasitophorous Vacuole Membrane (PVM).

## I.10.a. Parasitophorous vacuoles (PV) and the PV membrane (PVM)

From obligate to facultative intracellular parasites, whether Prokaryotes or Eukaryotes, many pathogens have evolved to live inside a vacuolar compartment within the host cell. The membrane surrounding these compartments is derived from the host cell membrane but then is hijacked and remodeled by pathogen-specific proteins and lipids. The strategy of generating a host cell plasma membrane–derived vacuole may be selected because it avoids parasite recognition by the host immune system. As such, these pathogens developed the ability to take over the endomembrane system of the host cell, to prevent or delay the fusion with lysosomes. These pathogen-containing vacuoles are initially composed mainly of host-derived membranes that present molecular features of early endosomes. However, these vacuoles soon are infiltrated by the pathogen's proteins and lipids. As a consequence, the vacuole fusogenicity but also vesicular carriers and other host organelles are altered. The vacuoles differ significantly from pathogen to pathogen with features of late endosomes/lysosomes (*Salmonella*), early endosomes (*Mycobacteria*), or endoplasmic reticulum (*Legionella*), or they may show no particular features (*Chlamydia* and *Toxoplasma*) (reviewed in Kumar and Valdivia, 2009).

## I.10.b. *Plasmodium* PVM: Composition and biological functions

The PVM in *Plasmodium* is formed during the productive invasion and is believed to depend on the contents of the parasite's secretory organelles (Lingelbach and Joiner, 1998).

PVM is a structure with an area of 30-33µm$^2$. It is remarkably dynamic, forming *de novo* every 10–20 seconds (Suss-Toby et al., 1996), and it is passively transported to regions close to the hepatocyte nucleus (de Souza and Attias 2015). The parasite remodels the PVM by exporting its proteins to its surface. It has been recently shown that the PVM formed during the active invasion differs from the transient vacuole created during the sporozoite transmigration (Risco-Castillo et al., 2015) due to the remodeling that occurs throughout the Exo Erythrocyte Form (EEF) development in the former.

While most *Plasmodium* blood-stage exported proteins contain a motif denominated PEXEL (*Plasmodium* Export Element; M. Marti et al., 2004) or VTS (Vacuolar Translocation Signal; C. Lopez-Estraño, 2003), no such domain has been identified in liver-stage exported proteins, which makes it hard to find novel PVM-resident proteins. The development of *Plasmodium* in the liver displays one of the fastest replication rates known in eukaryotic organisms. In a few days, a single sporozoite produces up to 30,000 merozoites. Besides the fact that this growth rate requires an intensive nutrient supply, it also means that the PVM must expand to accommodate the replicants. How exactly this process plays out is still unknown.

PVM acts as the host–*Plasmodium* interface that prevents direct contact between the parasite and the host cell. While PVM provides a defense mechanism for the parasite, it also acts as a site for nutrient acquisition and waste elimination. *Plasmodium* replication inside the liver imposes a massive demand for nutrients, which are provided through the PVM. On the other hand, toxic metabolites produced by the parasite need to be excreted. PVM channels have size exclusion around 855 Dalton but the molecular identity of these channels remains unknown (Bano et al., 2007). It also remains to be investigated how molecules bigger than 855 Daltons are transported across this membrane.

Although playing a pivotal role in *Plasmodium* development and survival in the hepatocytes, little is known about the molecular interactions established between the parasite and the hepatocyte on the PVM surface. Until now, only a reduced number of proteins have been identified on the PVM (Table 3) and these proteins have been the subject of extensive studies to uncover their role during *Plasmodium* development. Since no homologs for these proteins are known in other organisms, predicting their biological function is complex (Nyboer et al., 2017). PVM proteins are described below and summarized in Table 3.

**CSP** (Circumsporozoite Protein): Initially described as a sporozoite-stage specific antigen, and the major sporozoite surface protein (Hollingdale et al., 1983). In addition to the plasma membrane of the sporozoite, CSP is also found on the EEF's plasma membrane, PVM, and tubulovesicular network (TVN). Besides its role in the exit of sporozoite from the oocysts (Wang et al., 2005), the sporozoite entry into the mosquito salivary gland, and

hepatocyte invasion (Myung,et al., 2004), it has been proposed that CSP plays an essential role during sporozoite development inside the hepatocyte (A. P. Singh et al., 2007). CSP was also found to interfere with host gene expression and translation.

**NF-κB** (nuclear factor kappa B): Is a protein complex that plays a vital role in DNA transcription, involved with different cell stimuli including hepatic acute-phase response, innate/adaptive immunity, and cellular survival (Tian and Brasier, 2003). CS interacts with importin α3, an NF-κB biding partner. By interacting with importin α3, CSP deeply changes the transcriptional program of the host cell because it competes with this complex and inhibits the NF-κB translocation to the host cell nucleus (A. P. Singh et al., 2007).

**EXP1** (exported protein 1): Is a cross-stage PVM protein expressed both in the blood and in the liver, in the liver stage of the disease. EXP1 was identified in 1983 in patients with blood-stage malaria (Hall et al., 1983) and later in the liver (Sanchez et al., 1994). Although a cross-stage protein, EXP1 seems to have distinct functions during different *Plasmodium* developmental stages. In the intrahepatic development, EXP1 has been proposed to be crucial for the establishment of the parasite, by interacting with the host Apolipoprotein H (ApoH) (Sá e Cunha et al., 2017). On the other hand, it was found that blood-stage EXP1 functions as a membrane glutathione S-transferase that degrades the resulting product from heme oxidation, being thus potentially inhibited by artesunate (Lisewski et al., 2014). How EXP1 plays distinct roles according to disease stage is an interesting question to be explored.

**EXP2** (exported protein 2): This is another cross-stage exported protein (Günther et al., 1994). EXP2 is known to be part of the *Plasmodium* translocon of exported proteins, PTEX, responsible for the export of PEXEL motif-containing proteins and PEXEL-negative proteins in the blood stage of infection (De Koning-Ward et al., 2009). EXP2 is highly expressed in the ring stage and is thought to produce pores. This has been proposed because EXP2 is very similar to *Escherichia coli* α-pore-forming toxin (Bullen et al., 2012). The role of EXP2 during the liver stage remains unknown.

**LISP1** (liver-specific protein 1): LISP1 is mostly expressed in the later stages of parasite development in the liver. It is involved with the rupture of the PVM and merozoite exit, and the knockout of LISP1 that leads to merozoite trapping inside the host hepatocyte (Ishino et al., 2009).

**LISP2** (liver-specific protein 2): LISP2 is a protein expressed at mid-late stages of parasite development in the liver. It has been shown that LISP2-deficient parasites are unable to form merozoites (Orito et al., 2013).

**SPELD:** This is the short name of sporozoite surface protein essential for liver stage development. It is expressed in the oocyst, in the sporozoite, and in EEFs. It is a unique gene only found in *Plasmodium* species without any known homologues in other species (Al-Nihmi et al., 2017). It is highly expressed in the plasma membrane of the mature sporozoites; its role at this stage seems to be crucial. *SPELD*-deficient parasites fail to properly initiate the blood stage and have a more extended prepatency period, indicating a role during the malaria liver stage. SPELD-ko sporozoites can generate protective immunity to EEF. Interestingly, downregulation of several Plasmodium genes, including the ones coding for proteins expressed on the PVM, namely UIS4, EXP1, and LISP2, were observed in SPELD-ko parasites (Al-Nihmi et al., 2017). Why the expression of these genes in SPELD-ko parasites is affected remains an open question.

**Fam a-b:** These multigene families of proteins were first described in patients with blood-stage disease, and then later in the liver stage. They were implicated in phospholipid transferring during the liver stage when the parasite requires host-derived phosphatidylcholine (Fougère et al., 2016; Itoe et al., 2014).

**PL**: This is a *Plasmodium berghei* phospholipase implicated in PVM rupture during the liver stage. Parasites lacking PL undergo complete merozoite development. However, they fail to exit the liver (P. C. Burda et al., 2015). There may be functional redundancy between PL and LISP1, as disruption of either one leads to similar phenotypes.

**Py02667:** A member of the Early Transcribed Membrane Protein (ETRAMP) family. Py02667 is expressed during the blood and liver stages. It is likely to have an essential role during *Plasmodium* development in the blood, as its disruption at this stage of disease was not possible most likely because the parasite was not viable, and thus its role is yet to be discovered (Mackellar et al., 2011).

**IBIS1**: Intra-erythrocytic *P. berghei*-Induced Structures (IBIS) protein 1 is part of the intraerythrocytic membranous network and thus it is not in the parasite itself during the blood-stage of the disease. Likewise, it is expressed on the PVM and TVN during the liver stage of the disease. Although no specific phenotype has been associated with disruption of this protein during the mosquito and liver stages of infection, the deletion of this gene results in slow parasite growth in the blood (Ingmundson et al., 2012).

**UIS3:** The expression of UIS3, Upregulated in Infective Sporozoites 3 protein, is limited to the sporozoite and liver stages. Since its discovery, a few studies have tried to unveil the function of this protein (Matuschewski et al., 2002a). Infection with UIS3-deficient parasites was shown to confer protection against subsequent infection with WT parasites (Jobe et al., 2007; Mueller et al., 2005). Although controversial (Favretto et al., 2013), UIS3 was implicated in the interaction with lipid fatty acid binding protein in the liver, suggesting a role in nutrient acquisition (Mikolajczak et al., 2007). However, a recent study challenged this finding. The work of Real and colleagues reported an interaction between UIS3 and the host autophagy machinery, mainly the light chain 3 protein (LC3) (Real et al., 2017). Through this interaction, UIS3 acts as an inhibitor of autophagy and therefore protects the parasite from being eliminated by the host cell (Real et al., 2017).

**UIS4**: Up-regulated in Infective Sporozoites 4 is one of a set of 30 genes that undergo transcriptional changes in the sporozoite stage (Matuschewski et al., 2002a). UIS4 is a protein with 220 amino acids and 25 KDa weight (http://plasmodb.org/plasmo/). It is exclusively transcribed in sporozoites that are ready to infect the host, and its expression was proposed to be controlled by SLARP Sporozoite Liver stage Asparagine-Rich Protein (Silva et al., 2016). Interestingly, UIS4 does not have an orthologue in *P. falciparum,* but it

does in *P. vivax, P. berghei*, and *P. yoelii.* Because it does not carry any conserved domains, predicting its biological function is challenging.

Even though UIS4 is massively transcribed in the sporozoites, at this stage its production is under translational repression. It is only during an active invasion process that the gene is no longer repressed. The premature translation of UIS4 leads to the loss of sporozoite infectivity (Silvie et al., 2014). UIS4 belongs to the family of Early Transcribed Membranes Proteins (ETRAMP) and is abundantly expressed on the PVM. A short lysine-rich stretch preceded by a signal peptide, a transmembrane domain, and a highly negatively charged C-terminal region are characteristics of this family of molecules (Spielmann, et al., 2003). UIS4 is localized not only on the PVM but also in the TVN (Grützke et al., 2014).

UIS4 is one of the most widely used liver-stage PVM markers. Parasites lacking this protein cannot efficiently complete liver-stage infection. In mice infected with UIS4-KO parasites, there is a delay in parasitemia if compared with mice infected with WT parasites (A.-K. Mueller et al., 2005). Injecting a high dose of KO-UIS4 parasites could confer partial protective immunity against subsequent sporozoite injection (Mueller et al., 2005). Suggested as a potential transporter as well as a signaling protein due to its localization, UIS4 has been the subject of many studies that attempted to uncover its biological role. Recently, it was shown that UIS4 is required for the recruitment of the host late endocytic compartment around the PVM, which was proposed to deliver cholesterol to the liver-stage parasites (Petersen et al., 2017).

**Table 3.** *PVM proteins known so far*

| Protein | EXP1 | UIS3 | IBIS | UIS4 | LISP1 | SPELD | LISP2 | Fam-a1/2 | EXP2 | CSP | LISP2 | PY 02667 | PY 03652 | PL |
|---|---|---|---|---|---|---|---|---|---|---|---|---|---|---|
| Exp. Stage | BS, LS | Spz, LS | BS, LS | LS | LS | Spz, LS | LS | BS, LS | BS, LS | Spz, LS | LS | BS, LS | BS, LS | Spz, LS |

BS= blood stage, LS= liver stage, Spz= sporozoite, Exp.=Expression

## I.11. Host factors implicated in *Plasmodium* liver stage development

Malaria has been a major killer of children worldwide for thousands of years. As such, it is one of the most powerful known forces of evolutionary selection in the recent history of

the human genome (Kwiatkowski, 2005). Thus, it is not surprising that the malaria onset depends on an interplay between parasite and host factors.

Indeed, there are growing pieces of evidence and epidemiological confirmations that G6PD deficiency, $\alpha^+$ thalassemia, and hemoglobin C, are protective reactions against malaria mortality (Cappellini and Fiorelli, 2008). These are strategies that would protect the host during the blood stage of infection. Indeed, it has been shown that Reactive Oxygen Species (ROS) induction in hepatocytes leads to a decrease in parasite load during the liver stage of infection. Interestingly, oxidative stress is a hallmark of most disorders associated with the protective genetic traits such as G6PD-deficiency and all the haemoglobinopathies (Cappellini and Fiorelli, 2008; Voskou et al., 2015). Thus, besides being related to malaria protection in the blood stage, G6PD-deficiency also plays a role in reducing the parasite load in the liver. Whether or not the resistance mechanism associated with these disorders, and that acts as a trigger in the liver, is due to ROS-mediated impairment of liver-stage infection, remains to be shown.

Within each infected hepatocyte, the invading parasite originates tens of thousands of new erythrocyte-infectious parasite forms that are then released into the bloodstream. *In vivo*, partial development of *Plasmodium* parasites has been shown to occur in a population of sporozoites that either enter the lymph circulation or stay in the dermis (Amino et al., 2006). However, once in the vertebrate host, the hepatocyte is the only cell type that can efficiently support the full growth and development of the parasite. Thus, hepatocytes seem to provide a unique cellular environment that allows *Plasmodium* parasites to grow and replicate significantly.

Recently, different hepatocyte molecules that modulate the success of liver-stage infection have been identified (Kaushansky et al., 2016; Meireles et al., 2016; Itoe et al., 2014; Rodrigues et al., 2008; Yalaoui et al., 2008).

The high rate of proliferation that *Plasmodium* undergoes during the liver stage demands, for example, a massive lipid supply to support the biogenesis of new membranes and PVM maintenance. In fact, during the liver stage of infection, malaria parasites impose dramatic metabolic changes in the host cell, which alters the expression of genes coding for lipid

metabolism proteins (Itoe et al., 2014). Phosphatidylcholine (PC) plays a critical role in parasite survival and integrity of PVM in the liver, as shown previously. The inhibition of PC neogenesis affects not only parasite survival but also the protein composition of the PVM (Itoe et al., 2014).

Interestingly, it has been recently shown that a short-term high-fat diet regime of the host impacts parasite development in the liver (Zuzarte-Luís et al., 2017). This is because high-fat metabolism that takes place in mitochondria (probably for energy production) results in the production of reactive-oxygen-species, which dramatically affect parasite development, even though a significant impact on hepatocyte viability is not seen.

Polyamines have an essential role in *Plasmodium* growth. Their synthesis has been shown to play a crucial role in parasite development in the blood and liver (Meireles et al., 2017). The inhibition of arginase, a well-known enzyme implicated in polyamine synthesis, results in a failed development of *Plasmodium* in the liver or blood.

In addition to these macronutrients, the parasite also requires essential micronutrients for its development in the liver and blood, such as iron, zinc, and calcium. Parasites have evolved strategies to scavenge these micronutrients from their hosts.

Iron is an essential nutrient needed for almost all living organisms including *Plasmodium*. Its acquisition by *Plasmodium* is vital for complete parasite development inside host cells. Reduced iron availability in hepatocytes led to a significant and dose-dependent inhibition of *Plasmodium* replication, whereas iron supplementation dramatically increased parasite development both *in vitro* and *in vivo* (Portugal et al., 2011; Clark et al., 2014).

Calcium ($Ca^{2+}$) is also involved in many biological processes and has been implicated in the development of the first generation of merozoites (Sturm et al., 2006). Indeed, the release of calcium from the infected cell is taken up by merozoites thereby inhibiting the switch of phosphatidylserine to the outer leaflet of the host plasma membrane, a hallmark of the apoptosis process.

The co-evolution of the host and the pathogen is driven by constant opposite forces of resistance and adaptation, ultimately leading to the development of strategies for better

survival of the pathogen as well as tactics for pathogen elimination by the host (Kumar and Valdivia, 2009). Autophagy, a host cell-autonomous defense mechanism that threatens intracellular pathogens, is a clear example, among others, of host response that may modulate parasite adaptation strategies (Casadevall, 2008; Kumar and Valdivia 2009; Kayath et al., 2010).

## I.12. Host cytoskeleton manipulation by intracellular pathogens

Manipulations of the host cell's cytoskeleton are commonly performed by intracellular pathogens to allow their entering into, replication in, or exit from the host cell. Actin is one of the cytoskeleton components widely manipulated by intracellular pathogens. In the case of intracellular bacteria, entering the host cell is achieved through different mechanisms described below.

The *Zipper*-based mechanism occurs through the interaction established between the pathogen with a specific signaling receptor on the host cell, stimulating actin rearrangement and consequently pathogen endocytosis.

Unlike zipper, the *trigger* mechanism does not require direct interaction between the pathogen and the host cell (Colonne et al., 2016). The internalization of a pathogen occurs by injection of an effector that promotes actin rearrangement inside the host cell, using a specific secretion system (Muschiol et al., 2006). Some bacteria enter the cell by using their phagocytic capability (for more details see Figure 7).

Once inside the host cell, to avoid elimination, the intracellular pathogen must choose to either ride, hide, or fight. Most of the intracellular pathogens living inside a vacuole circumvent their killing by hiding or fighting, and sometimes this involves actin.

*Rickettsia,* for example, promotes actin comet tail formation, by which it moves in the cell (Colonne et al., 2016).

Apicomplexan parasites also manipulate the host cell cytoskeleton upon infection, although the mechanisms involved in this process seems to be distinct from those observed in bacteria.

*Cryptosporidium* lives intracellularly in the cytoplasm, creating a plate-like junction by manipulating the host cell F-actin that separates the parasite from the host cell cytoplasm (Elliott and Clark, 2000). With this structure, the parasite mimics the host's adherents and focal junctions, which are the typical host cell structures that connect filamentous actin to the membrane.

Being an intracellular pathogen, *Toxoplasma gondii* manipulates host cell cytoskeleton during invasion by promoting the actin polymerization at the host–parasite contact site (Gonzalez et al., 2009). The parasite activates the Arp2/3 complex (actin-nucleating factor, defined below) to induce actin polymerization and to stabilize the moving junction allowing the parasite to enter the cell.

*Trypanosoma cruzi* hijacks the sphingomyelinase-mediated plasma membrane repair pathway to enter the host cell (Fernandes et al., 2011). By opening the host cell membrane, *Trypanosoma cruzi* triggers the calcium (Ca+) influx and lysosome exocytosis. The acid sphingomyelinase released from the lysosomes converts sphingomyelin into ceramide. Next, ceramide induces the membrane invagination and finally the parasite endocytosis.

Being obligate intracellular pathogens that spend most of their life cycle inside a vacuole, malaria parasites are not an exception when it comes to manipulating the host cell cytoskeleton. To be able to enter and exit the host cell, *Plasmodium* interferes with the host cell actin.

The involvement of the host actin with parasite infection is described further in this document.

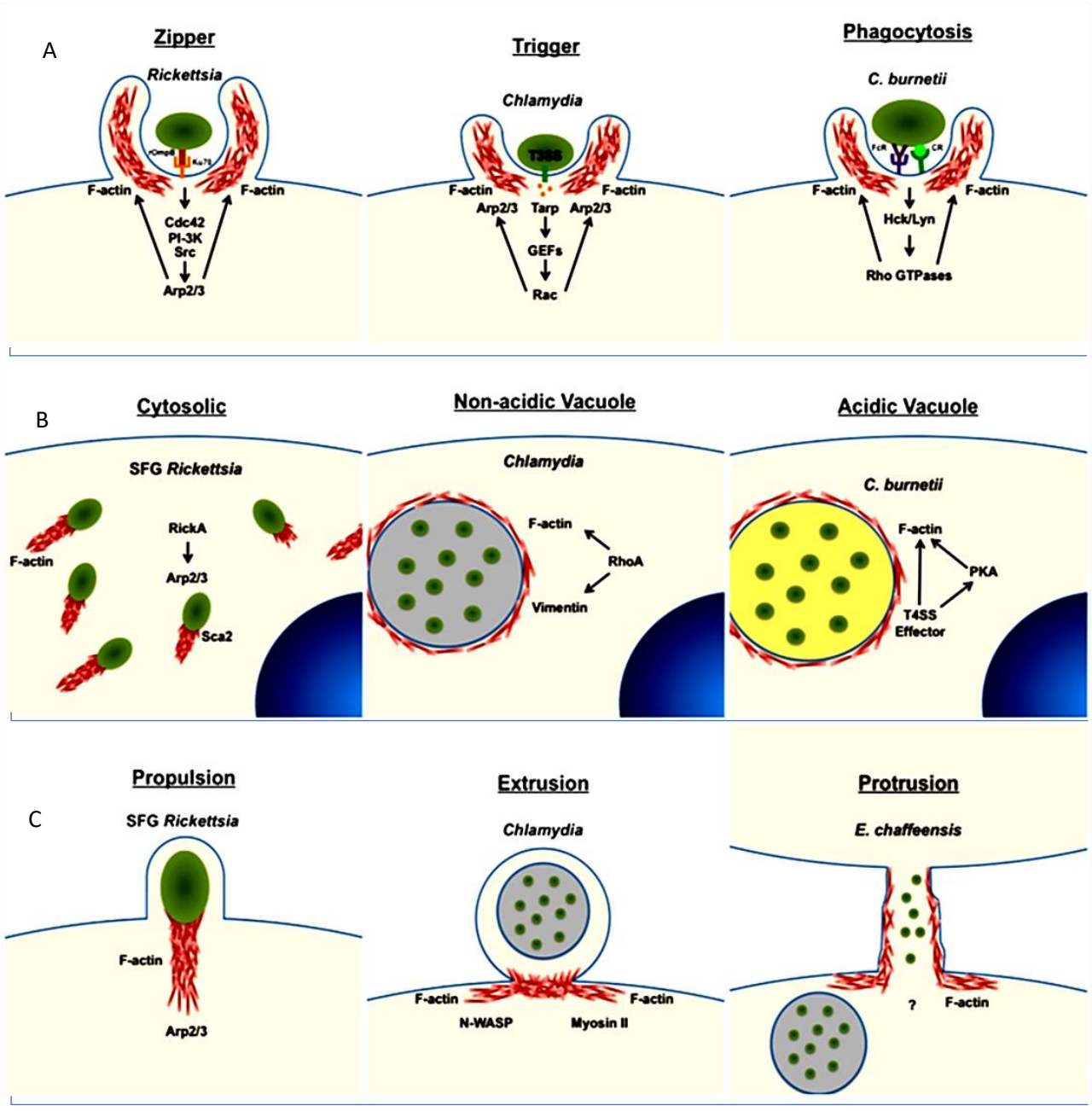


Figure 7. A**ctin manipulation by intracellular pathogens**. Intracellular bacteria actively manipulate the host actin cytoskeleton to facilitate invasion, intracellular replication, and dissemination. (A) Host cell entry: In non-phagocytic cells, bacteria use a zipper or trigger mechanism to facilitate infection. Phagocytic cells engulf bacterial pathogens by phagocytosis. (B) Intracellular life: Some cytosolic bacteria form actin tails to facilitate mobility within the cell. Pathogens that reside within membrane-bound vacuoles manipulate the cytoskeleton to facilitate vacuole formation and stability. (C) Host cell escape: One group of bacteria use actin-based motility to exit infected cells and move into non-infected cells. Some host membrane-bound pathogen-containing vacuoles are pinched off by extrusion, a process that requires actin remodeling. Other intracellular bacteria actively remodel actin at the host cell surface to form membrane protrusions, connecting infected and uninfected neighboring cells. Bacteria are then transported through protrusions into neighboring cells to start a new infection cycle. Adapted from Colonne et al. (2016).

## I.13. Actin: the molecular features and functions

Actin is one of the most abundant proteins in eukaryotic cells, representing on average 5 to 20% of total cell protein content. It is the major skeletal protein found in most cells (Drazic et al., 2018). Actin is highly conserved, having been found from yeasts to humans, and it plays crucial roles that vary from cell mobility to intracellular trafficking. Actin is found in two main forms: monomeric actin, which is named G-actin, and filamentous actin, which is designed as F-actin (Dominguez and Holmes, 2011).

G-actin has three main isoforms: α-actin, which is found in cardiac and smooth muscles, and β-actin and γ-actin that are expressed mostly in muscle and non-muscle cells. The difference between these isoforms is accentuated at the N-terminus (Perrin and Ervasti, 2010), shown in Figure 8.

Filamentous actin is the result of G-actin polymerization. This process depends on different players (nucleotide, actin-binding proteins (ABP), and small molecules). Actin polymerization starts with an aggregate of three G-actin monomers (nucleation), and the filament then grows by addition of subsequent monomers, with all monomers oriented in the same direction. Thus F-actin is polarized, with a plus (+) end and a minus (–) end.

However, the polymerization process is reversible, and monomer addition occurs faster at the (+) end than the (–) end, while the latter is also more prone to depolymerization. This steady-state of actin dynamics is named actin treadmilling. ATP is a crucial player in this process by facilitating the nucleation process and filament growth (Wegner and Isenbergt, 1983). Indeed, G-actin-ATP is the monomer added to elongate the actin filaments. *In vivo* studies have shown that besides ATP, ABP and small molecules play a crucial role in actin assembly and disassembly (Wegner and Isenbergt, 1983).

Like monomeric actin, filamentous actin could also be assembled. Generally, two structure types are generated: actin bundles and actin networks. Actin bundles are divided in two distinct categories and functions. The first type has actin filaments aligned in parallel, which is where the structure that supports the plasma membrane protrusions, such as microvilli, is found. The second type designated contractile bundle is the contractile ring structure found during cytokinesis (Cooper GM, 2000).

Actin turnover inside the cell is governed by different ABPs. Cofilin, for example, is a crucial player in actin filament disassembly. It binds to actin filament and thereby enhances depolymerization. By linking to ADP-actin, cofilin works as a monomer that blocks actin from being integrated into a filament, which then impairs actin nucleation as well as filament elongation (Dominguez and Holmes, 2011).

As for profilin, it is an ABP that plays the opposite role. Profilin acts by catalyzing the exchange of ADP-actin into ATP-actin monomers. This exchange allows monomers to dissociate from cofilin; once free and available they promote actin incorporation into a filament (Dominguez and Holmes, 2011).

Actin-related protein 2/3 (Arp2/3) complex is a central and potent actin monomer nucleator in most eukaryote cells (Goley and Welch, 2006). It promotes nucleation by working as a platform site where nucleation initiates. These and other actin-binding proteins are regulated by different cell stimuli, as well as by their adaptor molecules. For more actin-binding proteins see Table 4.

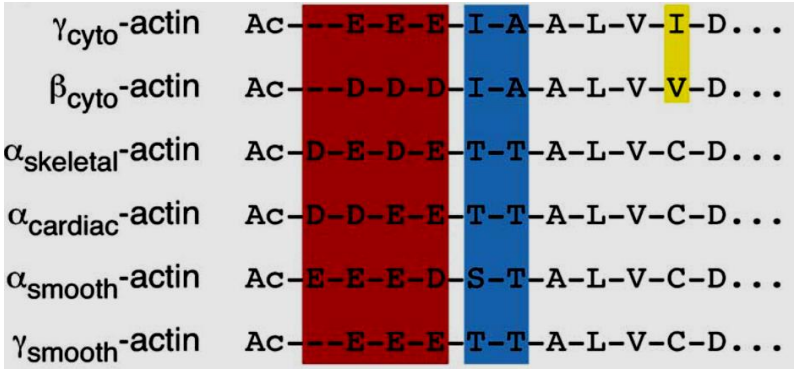


Figure 8. **Globular actin isoforms.** Globular actin isoform. Alignment of the N-terminal ends of the six mammalian actin isoforms. In red is the stretch with the most variability in and between muscle and cytoplasmic isoforms. Blue residues vary between cytoplasmic and muscle isoforms. In yellow are residues that vary between $\beta_{cyto}$-actin and $\gamma_{cyto}$-actin. Substitution of Isoleucine in gamma isoform by Valine in beta isoforms. **Adapted from: (Perrin and Ervasti, 2010)**

Table 4. The Role of Actin-Binding Proteins in Actin Regulation

| **Actin-binding Protein** | **Actin Regulation** |
|---|---|
| α-actinin 2 | Bundling |
| Arp2/3 complex | Branching, nucleation |
| CaMKIIβ | Bundling |
| α-N-catenin | Bundling |
| Cofilin | Depolymerisation, severing |
| Cortactin | Nucleation-promoting factor |
| Drebrin | Anti-bundling |
| EPS8 | Caps barbed ends to stabilise F-actin |
| Formin (mDia2) | Nucleation |
| Gelsolin | Anti-bundling, capping, severing |
| N-WASP | Nucleation-promoting factor |
| Neurabin I | Bundling |
| Neurabin II/Spinophilin | Bundling |
| Profilin II | Polymerisation |
| Synaptopodin | Bundling |
| WAVE 1 | Nucleation-promoting factor |

Adapted from: (Lin and Webb, 2010).

In apicomplexan parasites, actin is found mostly in monomeric form (Dobrowolski et al., 1997). In *Toxoplasma gondii*, for example, G-actin represents 98% of total actin, a ratio that is highly conserved among apicomplexans, see Figure 9. Amino acid sequences from *T. gondii* actin share 93% similarity with *P. falciparum* and 88% with *Cryptosporidium* (Dobrowolski et al., 1997). Unlike *T. gondii*, which has only one gene coding for actin (ACT1), *P. falciparum* has two, namely Pf-actin-I (Wesseling et al., 1988-a) and pf-actin-II (Wesseling et al., 1988-b). These two genes share 79% sequence similarity in amino acids (Wesseling and Smits, 1988). However, unlike Pf-actin-II, which is mostly transcribed at the sexual parasite stage, Pf-actin-I is present throughout the entire life cycle (Wesseling et al., 1989; Das et al., 2017).


*Figure 9.* Sequence comparison between human non-muscle actin amino acids 237–251 and apicomplexan actin I orthologues over the amino acids 239–253 . Adapted from: (Angrisano et al., 2012).

Despite displaying actin-dependent motility, *Plasmodium* parasites were believed not to have filamentous actin because it was not visible with a microscope under physiological conditions (Skillman et al., 2011; Wetzel et al., 2003). Nevertheless, treatment with depolymerizing agents like Cytochalasin D or with filamentous stabilizer agent jasplakinolide inhibits *P. knowlesi* merozoite motility, suggesting a role for F-actin in *Plasmodium* motility (Gonzalez et al., 2009). Indeed, F-actin was visualized in gametocyte cytoskeleton using super-resolution microscopy years later (Hliscs et al., 2015). Biochemical *in vitro* assays show the presence of unusually short F-actin filaments. Besides being short, these filaments are characterized by instability and short persistence (Schüler et al., 2005). This plasmodial actin property was hypothesized to be due to the low existing affinity among *Plasmodium* actin molecules , and the high rate of ATP hydrolysis (Herwig Schu et al., 2005).

One of actin's main features is its ability to switch between unpolarized and polarized structures in a highly dynamic way, a process regulated by ABP and small molecules. Nevertheless, in *Plasmodium*, relatively few regulatory molecules are known to be present and classic regulators such as Arp2/3 complex and the nucleation-promoting factors, such as WASP, are missing. The *Plasmodium* genome encodes Arp1 and Arp 4 homologues (Gordon et al., 2005). Arp1 gene is expressed throughout the parasite life cycle and if deleted the organism is not viable (Siden-Kiamos et al., 2010). The *Plasmodium* genome also encodes an actin-polymerizing protein that is a homologue of profilin. *Plasmodium's* profilin differs from its orthologues and contains a characteristic mini-domain specific to apicomplexan parasites (Kursula et al., 2008). This gene is crucial for blood stages of malaria parasites as well for sporozoite motility, as shown previously in *P. berghei* (Kursula et al., 2008; Moreau et al., 2017).

Actin is one of the parasite main components of the motility machinery, called the glideosome. The glideosome is located between the inner membrane complex and the plasma membrane. Besides actin (F-actin), the glideosome is composed of myosin A (MYOA) and glideosome assembling proteins (GAP), Figure 10 (Frénal et al., 2017). *Plasmodium* motility results from the back translocation of adhesin powered by myosin motor proteins along the filamentous actin.

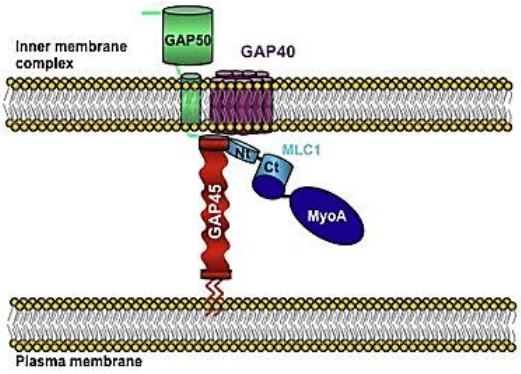


Figure 10. Glideosome machinery: Glideosome", the molecular machinery of gliding motility. Abbreviations: GAP45 and GAP50, gliding associated protein 45 KDa and 50 KDa; MyoA, myosin A; MLC, Myosin light chain or Myosin tail-interacting protein.

In apicomplexans, the actin turnover process (mainly depolymerization) is ensured by two ADF proteins, *ADF1* and *ADF2*.

Although constitutively expressed, *ADF1* seems to play an important role limited to the blood stage/asexual stage. It differs from the conventional ADF by lacking the consensus residues to bind F-actin. Thus, *ADF1* does not bind to F-actin but it does interact with G-actin (Herwig Schu et al., 2005).

*ADF2* shares great homology with the conventional ADF. The *ADF2*-deficient parasite still has motility and undergoes normal development into ookinete; however, both the ookinete-to-oocyst and sporozoite-to-EEF transformations were significantly altered (Doi et al., 2010).

In summary, actin reorganization is critical for the cell to display a variety of cell functions, including trafficking and cell motility. In *Plasmodium*, actin regulation is mostly undertaken by non-classical players

## I.14. Host actin implication in *Plasmodium* infection

### I.14.a. Host actin manipulation during *Plasmodium* entering

The invasion of the host cell by *Plasmodium* parasites, mainly the *zoites* forms, is a rapid process that takes less than one minute and is preceded by the generation of a moving junction (Gonzalez et al., 2009). For some time, the host actin was considered a passive player during *Plasmodium* cell invasion but it is now clear that actin is actively involved in the process. Indeed, *Plasmodium* invasion requires not only the involvement of the parasite cytoskeleton but also the hots' filamentous actin. The implication of the host actin was shown through treatments with jasplakinolide and Cytochalasin, and negatively affected the invasion of the host cell by *Plasmodium* (Gonzalez et al., 2009). Also, the host Arp2/3 complex, the main actin nucleating factor, has been shown to colocalize with the moving junction and to be functionally involved in the invasion process Nevertheless, further studies are required to understand the details of the regulation signaling of this system, since the inhibition of nucleation-promoting factor, WASP, failed to inhibit the Arp2/3 complex (Gonzalez et al., 2009).

### I.14.b. Contribution of host actin for intracellular *Plasmodium* development

One of the hallmarks of *P. falciparum* blood-stage infection is that it affects the cytoadherence of the infected red cells that adhere to the endothelium, thus avoiding parasite elimination. Electron-dense protrusions, referred to as knobs, are on the surface of the infected red blood cell (RBC) and act as attachment site. The main knob component is the knob-associate histidine-rich protein (KAHRP), located in the cytoplasm of the infected RBC where it forms the complex with the host cell's F-actin and spectrin (Deitsch and Wellems, 1996; Oh et al., 2000; Pei et al., 2007).

Besides KAHRP, *P. falciparum* erythrocyte membrane protein 1 (PfEMP1), a family of cytoadherence receptors located on the knob, is exported to the surface of RBC where it also binds to F-actin and spectrin. Thus, the parasite takes advantages of the host cell's cytoskeleton components to generate the structure that blocks its clearance. The β-actin of the host hepatocyte was shown to undergo a dramatic reorganization because of

*Plasmodium berghei* EEF, which seems to correlate with the parasite release (Gomes-Santos et al., 2012).

### I.14.c. Host actin in *Plasmodium* egress

The exit of *Plasmodium* parasites from either the hepatocytes or the RBCs is an essential step for infection to take place. The breakdown of the host cytoskeleton has been involved in the last step of *Plasmodium* development in the liver (Burda et al., 2017). Before leaving the cell, merozoites collapse the host cell plasma membrane, producing the merosome, where merozoites are safely packed, and are released from the liver into the blood (Burda et al., 2017).

Likewise, in the liver stage, the red blood cells undergo dramatic cytoskeleton changes before merozoite egress. Adducin, a component of the plasma membrane cytoskeleton, has been shown to vanish from the host cell plasma membrane, while many cytoskeleton proteins, mainly spectrin, ankyrin, and actin, are degraded by proteolytic enzymes (Millholland et al., 2011). Thus, the host cell's cytoskeleton and actin are manipulated by the *Plasmodium* parasite throughout the entire course of infection, from invasion, to development, to exit.

**OBJECTIVES**

## OBJECTIVES

Although discovered more than 65 years ago, the liver stage of malaria is still not fully understood. Even though the liver stage is asymptomatic, it represents a target for antimalarial drugs, as well as for the development of malaria vaccine. For the parasite to successfully establish inside the hepatocytes it must do so using the PVM, which acts as a host–parasite interface.

Once inside the host cell, *Plasmodium* shifts a range of proteins to the PVM surface. Some of these proteins have been characterized; however, the role of many remains to be elucidated. This includes UIS4, which belongs to a subset of *Plasmodium* proteins encoded by the "Upregulated in Infective Sporozoites" (UIS) genes, which are exported to the PVM and are essential for parasite survival. *Plasmodium berghei (P. berghei)* and *Plasmodium yoelii (P. yoelii*) sporozoites lacking UIS4 can invade liver cells and begin to develop, but parasites disappear during the infection. Although UIS4 is crucial for the establishment of malaria parasites in the liver, its biological function remains unknown.

Given that PVM is at the host–parasite interface, it is possible that proteins on the PVM surface are there to benefit the parasite. Moreover, there is scarce information on the molecular composition of the PVM and thus new players in the *Plasmodium*–hepatocyte interaction may be identified.

Thus, the goals of this work were to unveil the biological function of the PbUIS4 during the liver stage of infection, as well as to reveal new PVM-resident proteins by investigating the proteins in the vicinity of PbUIS4, which may reveal novel proteins of the parasitophorous vacuole membrane in the liver stage of malaria infection.

# CHAPTER II- FINDING PbUIS4 INTERACTING PARTNERS

## II. Finding PbUIS4 interacting partners

UIS4 is a member of a subset of proteins encoded by the "Upregulated in Infective Sporozoites" (UIS) genes, which encode 31 proteins (Matuschewski et al., 2002b). UIS4 is one of the main markers for parasite PVM, and it is essential for a successful development of *Plasmodium berghei (P. berghei)* and *Plasmodium yoelii (P. yoelii)* during the malaria liver stage (Kumar, et al., 2009). Without UIS4, *P. berghei* and *P. yoelii* parasites are still able to invade the hepatocytes but their development is incomplete.

Despite the importance of UIS4 for the development of malaria parasites in the liver, little is known about the biological role of this protein. Recently, a study has shown that UIS4 is involved in lysosome accumulation at the PVM periphery in infection caused by *P. berghei* (Petersen et al., 2017). Although it still unknown what leads to lysosome accumulation in the areas surrounding the PVM, it has been proposed that the lack of cholesterol release from this vesicular compartment in UIS4 deficient parasites may partially explain the incomplete parasite development.

UIS4 is a protein with unusual structure and amino acid sequence and is not similar to any other protein outside the *Plasmodium* genus. It has a disorganized and flexible domain at the C-terminal region, which possibly acquires a specific structure when binding to other molecules. It is difficult to predict the role of UIS4 during liver-stage malarial infection because the protein does not share structure or amino acid sequence homology with any known protein. To fully understand the role of a given protein, in many cases it is necessary to uncover and characterize its interaction network. In that context, this study aimed to reveal the potential interacting partners of UIS4 using an immunoprecipitation method.

### II.1.a. Generation of UIS4-deficient parasite

Although *UIS4*-deficient parasites have been previously generated in *P. berghei* NK65 in parasite line, (A.-K. Mueller et al., 2005). Therefore, to carry out immunoprecipitation experiments proposed here, a new *UIS4*-deficient transgenic parasite was generated using *P. berghei ANKA*, here called PbUIS4-KO. PbUIS4-KO was made by replacing the open

reading frame (ORF) of PbUIS4 coding sequence for the gene coding for human Dihydrofolate Reductase (DHFR), using a double cross-over recombination strategy. Transfected parasites were selected through their resistance to pyrimethamine (Figure 11-A). The PbUIS4-KO parasite was genotyped to ensure that the transfection construct integrates into the correct locus, Figure 11-B.

As expected, the wild-type clone (line 1) does not show any integration band. Three different transfected clones (lines 2, 3, 4) were obtained. Line 2 shows the transfected parasite, which could be considered a mix population of transfected and wild-type parasites, due to the amplification of wild-type and integration locus. In line 4 (clone 4) no band for the transfected parasite is shown (wild-type locus detection and no integration locus). Line 3 (clone 3) is the pure transgenic parasite, having the integration locus amplified, and no wild-type locus detected. This clone was used to perform the experiment.

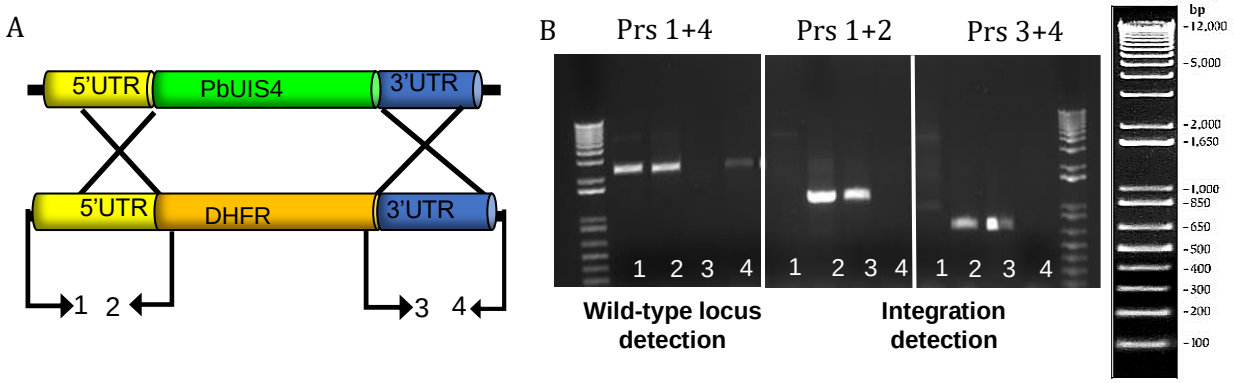


Figure 11. **PbUIS4-KO parasite generation**. A) Double crossover strategy for the generation of *Plasmodium berghei* ANKA PbUIS4-KO. ORF for PbUIS4 was replaced by hDHFR (human Dihydrofolate Reductase) using double cross-over recombination strategy. 1kb fragment from PbUIS4 5´UTR and 0.6kb from 3'UTR were amplified from P *berghei* ANKA DNA and cloned to flank hDHFR gene in the transfection construct. B) Genotyping of transfected parasites by PCR. Primers 1 and 4 amplify the wild-type locus, with ≈3000kb. Primers 1 and 2 detect the integration and amplify a fragment around 1500bp, Primers 3 and 4 detect the integration at the 3' end and amplify a fragment around 700bp. Prs= primers. Ladder= 1Kb ladder from Invitrogen.

## II.1.b. Validation of UIS4-deficient parasite

The expression of UIS4 was examined in transgenic parasites at the sporozoite stage and throughout their development in the liver. Using RT-PCR and immunofluorescence assay (IFA) we were not able to detect the expression of UIS4 in transgenic parasites (Figure 12-A, in sporozoite stage and EEF stage, Figure12-B). Furthermore, Western Blot (WB) analysis was performed in the sporozoite stage (Figure 12-C and on EEF stage, Figure 12-D). All tests comparing PbUIS4-KO to the wild-type parental line indicated that our transgenic parasite was not expressing UIS4, and the results are in agreement with others previously published (A.-K. Mueller et al., 2005).

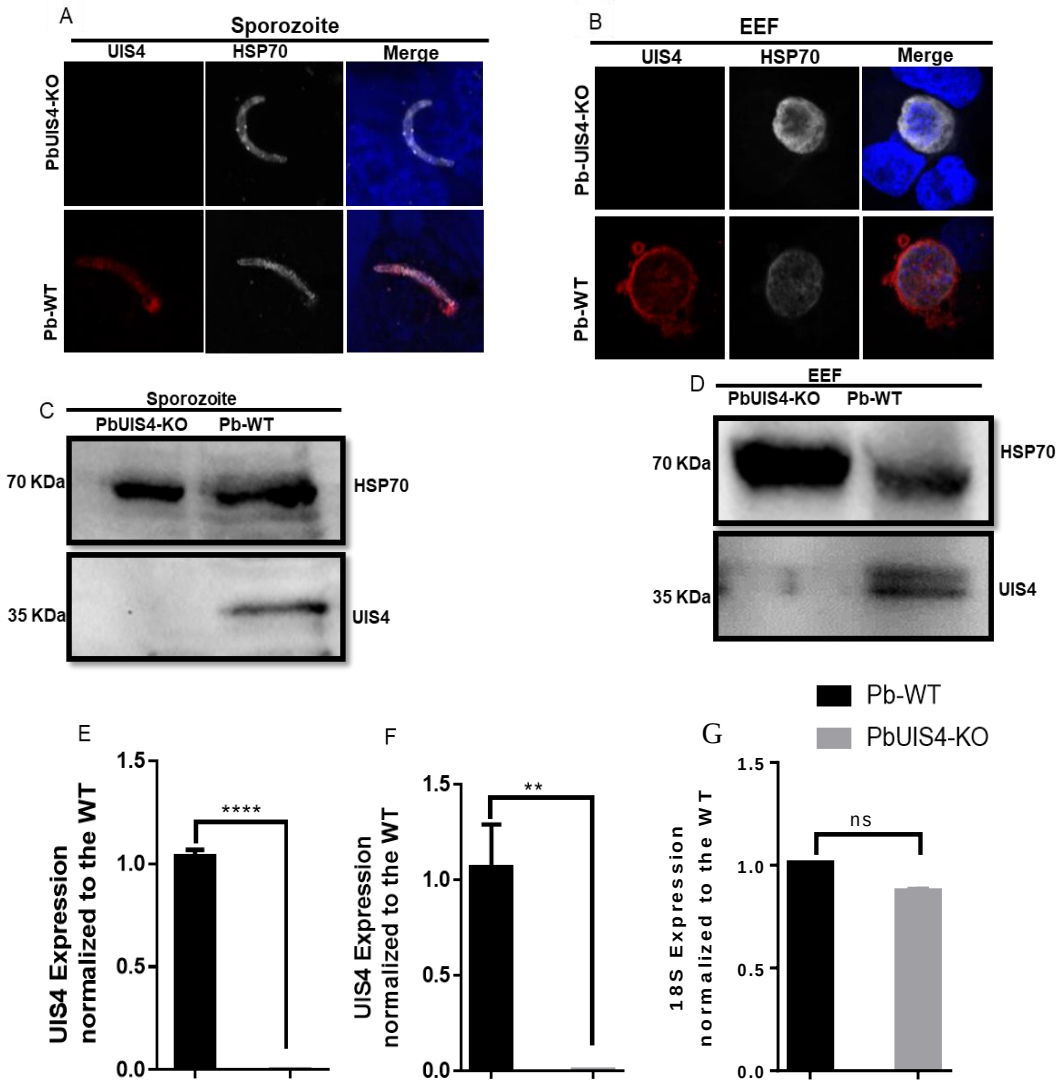


Figure 12. **PbUIS4-KO do not express UIS4 either in sporozoites or during the liver stage infection** The hepatoma cell line was infected with PbUIS4-KO or with Pb-WT parasites, followed by fixation and staining at 2 h.p.i (A) and 48 h.p.i (B). C) Sporozoites dissected from infected mosquito with PbUIS4-KO or Pb-WT were pelleted and lysed with Laemmli buffer followed by separation on SDS-PAGE and probing with anti-UIS4 and HPS70 antibodies. D) Hepatoma cell line was infected with Pb-UIS4-KO and wild-type parasites. Cells were lysed at 48hpi, subjected to SDS-PAGE separation and probed with anti-UIS4 and anti-HPS70 antibodies. E) UIS4 expression quantified by RT-PCR. RNA from PbUIS4-KO or wild-type sporozoite (E) or Huh7 infected cell (F) was extracted following by cDNA synthesis and RT-PCR reaction. G) Expression of housekeeping gene (18S).

The development of PbUIS4-KO parasites was assessed by measuring liver load *in vivo* and *in vitro*, by RT-PCR (Figure 13). PbUIS4-KO-infected C57Bl/6J mice had a reduction of around 95±4% parasite liver load if compared to Pb-WT-infected mice ($p<0.0001$, Figure 13-A). *In vitro*, the parasite load of PbUIS4-KO in Huh7 and HepG2 hepatoma cell lines was compared to that of Pb-WT. In both cell lines, at the analyzed time point, 45h.p.i, PbUIS4-KO produced approximately 20% of the Pb-WT parasite load ($p=0.0054$ and $p=0.02$ for Huh7 and HepG2 cells, respectively, Figures 13-B and 13-C).

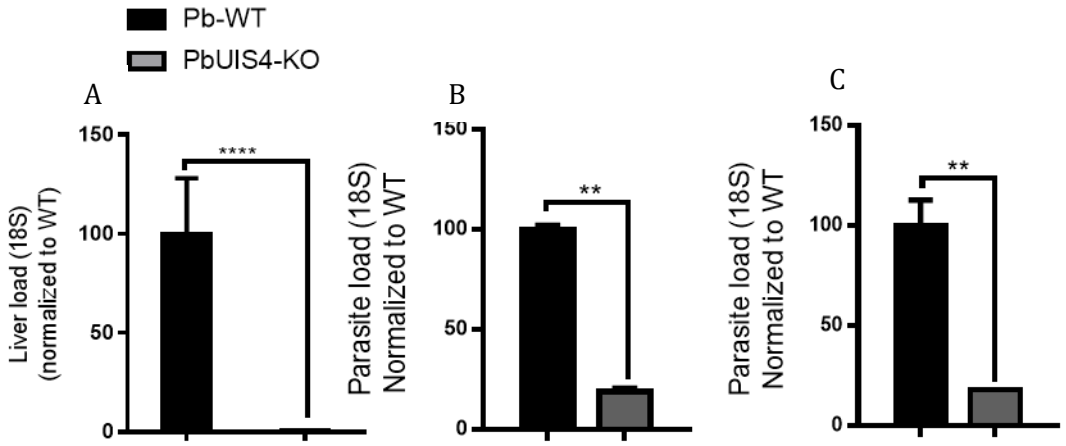


Figure 13. ***Plasmodium*** **liver-stage infection is reduced in PbUIS4-KO**. A) Liver load in C57BL/6J mice injected with Pb-WT or PbUIS4-KO sporozoites at 45 h.p.i., n (mice)=5 per condition. B) Parasite load in HepG2 hepatoma cells infected with Pb-WT or PbUIS4-KO sporozoites at 45hpi, n (mice) =3. C) Parasite load in Huh7 hepatoma cells infected with Pb-WT or PbUIS4-KO sporozoites at 45 h.p.i, n (mice) =3.

The parasitemia of C57Bl/6j mice infected with PbUIS4-KO or the Pb-WT parental line was monitored. While one mouse infected with Pb-WT become positive after 3 d.p.i, and four more mice were positive after 5 d.p.i, one mouse injected with UIS4-KO parasite showed detectable parasitemia at 7 d.p.i and three more at 11 d.p.i. Two of the mice infected with UIS4-KO did not show parasites in the blood. At 30 days p.i., parasitemia-negative mice were sacrificed (Figure 14).

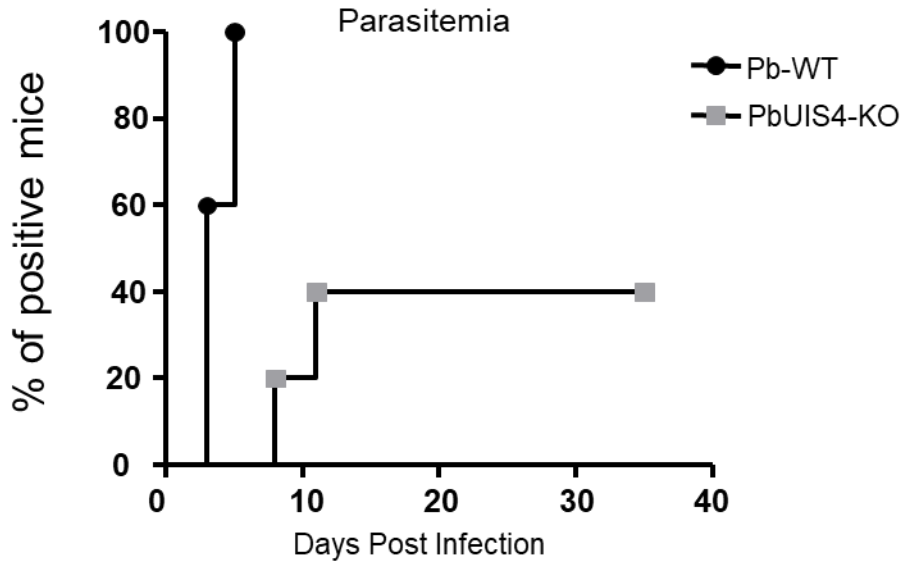


Figure 14. **PbUIS4-KO show delayed blood stage patency. .** 5 C57BL/6J mice injected with 50.000 Pb-WT or PbUIS4-KO sporozoites by intravenous injection. Parasitemia was monitored by blood smear from 2 to 30 days post infection. N (mice) 5 per condition. N(experiment)=1

Furthermore, the survival kinetic of PbUIS4-KO parasite was evaluated from 24 h.p.i to 52 h.p.i. (Figure 15-A). The results show that at an early time point there is no difference between WT and UIS4-deficient parasite. But at 36 h.p.i onward, survival of PbUIS4-KO is compromised and at a later time point (55 h.p.i) only a few PbUIS4-KO parasites are found. Interestingly, the size of PbUIS4-KO is significantly smaller (Figure 15-B, and Figure 15-C).

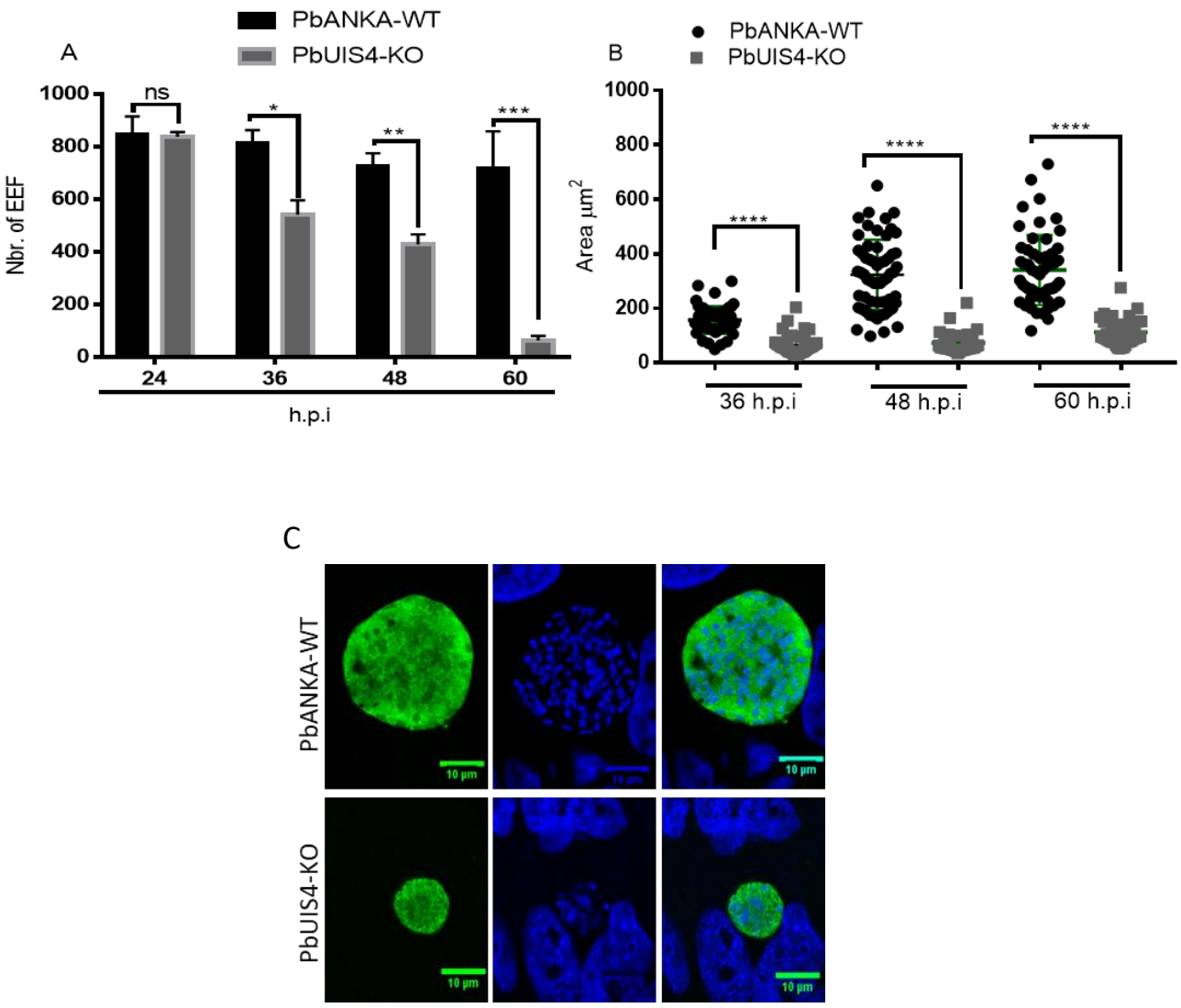


Figure 15. **PbUIS4-KO development.** Huh7 hepatoma cell line was infected with PbUIS4-KO or with Pb-WT parasites, followed by fixation at the corresponding time point and staining of HSP70 and DNA. A) Counting of EEF was done using Confocal Laser Scanning Microscope (LSM 710) Zeiss. Each time point is the mean of three coverslips. EEF= Exo-Erythrocytes Forms. B) Quantification of parasite size. C) Representative image of parasite development at 60 h.p.i

## II.2. PbUIS4 interacts with host actin

We next investigated potential partners interacting with UIS4. To this end, immunoprecipitation was done using an antibody against UIS4 and lysates from HepG2 cells infected with either PbUIS4-KO or Pb-WT parasites at 24 h.p.i, given that at this time point there were still an equivalent number of PbUIS4-KO EEF to Pb-WT alive (Figure 15-A). Lysate proteins were separated on SDS PAGE, and silver staining was performed to verify the purity of the immunoprecipitated samples and to examine if there was any difference between the two immunoprecipitated extracts, as observed in Figure 16.

Indeed, the sample obtained by UIS4-immunoprecipitation from cells infected with Pb-WT parasites had more proteins than the extract derived from PbUIS4-KO-infected cells (Figure 16). Three different bands were particularly prominent in the WT sample. These bands were excised from the gel for mass spectrometry analysis. Bands of the same size in the PbUIS4-KO were also extracted.

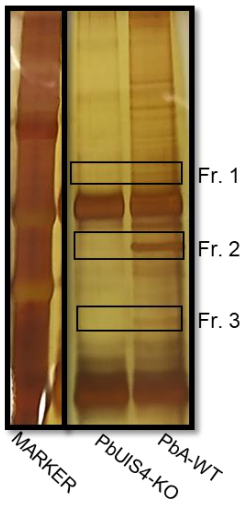


Figure 16. **Silver Stain of SDS-PAGE Lysates of PbUIS4-KO and PbANKA-WT.** Infected cells were incubated overnight with α UIS4 antibody, followed by Protein G incubation and subsequent elution. After separation on SDS PAGE and silver staining, the bands in the squares were excised for analysis.

The mass spectrometry data were acquired using positive reflector MS and MS/MS modes using a 4800plus MALDI-TOF/TOF (ABSciex) mass spectrometer and then analyzed using 4000 Series Explorer Software v.3.5.3 (Applied Biosystems). The 25 most intense precursor ions in the MS spectra were selected for MS/MS analysis.

The search for similar sequences was performed against the SwissProt protein database with no taxonomic restriction and the restriction search for *Homo sapiens* and *Plasmodium.* Protein identification was only accepted when significant protein homology scores were obtained ($p<0.05$, scores higher than 70) and at least one peptide was fragmented with a significant individual ion score ($p<0.05$). The identified proteins were validated using different criteria. First, we disregarded the common mass spectrometry contaminants (Keratin); the hits score was used as the elimination criterium. Second, all the proteins found in both extracts were considered as nonspecific binders and were excluded. Proteins with more than 20K Daltons or less than their migration mass on the SDS PAGE gel were not taken into account (Supplementary Table). Table 5 lists the three proteins selected from both searches and after all matching was done.

**Table 5**. Mass spectrometry result from PbANKA-WT fraction 2

| **Accession** | Mass | Score |
|---|---|---|
| **ACTG_HUMAN** | 41766 | 755 |
| **ACTB_HUMAN** | 41710 | 744 |
| **ACTBL_HUMAN** | 41976 | 286 |

One protein was identified in the sample excised from PbUIS4-KO fraction 2 (SEMG1_human with score 23) but it was not a significant hit (a score below 70). On the other hand, actin proteins were found significantly enriched in the sample excised from the cell lysate infected with the WT parasites.

An additional immunoprecipitation was performed followed by immunoblot analysis to validate the mass spectrometry result. Actin was immunoprecipitated with the UIS4 antibody (Figure 17). This finding corroborates the result obtained by mass spectrometry.

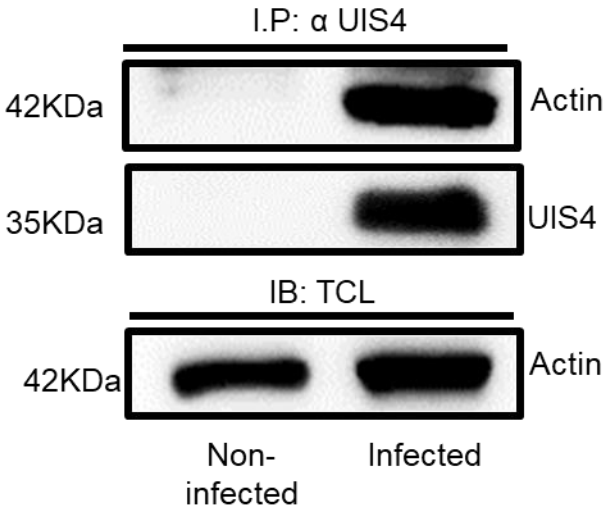


Figure 17. **Western Blot**. Extract from Pb-WT infected and non- infected cells were incubated with α UIS4 antibody overnight at $4^0$C followed by Protein G incubation and subsequent elution. After separation on SDS PAGE, samples were probed with anti-actin and anti-UIS4 antibodies. I.B= immune Blot, TLC= total cell lysed.

Next, immunofluorescence analysis was performed to examine the localization of monomeric and filamentous actin to UIS4 in hepatoma cells infected with WT *P. berghei*. While no apparent colocalization was observed for UIS4 and the monomeric actin form (Figure 18-A), colocalization with phalloidin staining was detected, suggesting that UIS4 may indeed be interacting with the actin filamentous form, *in situ* (Figure 18-B).

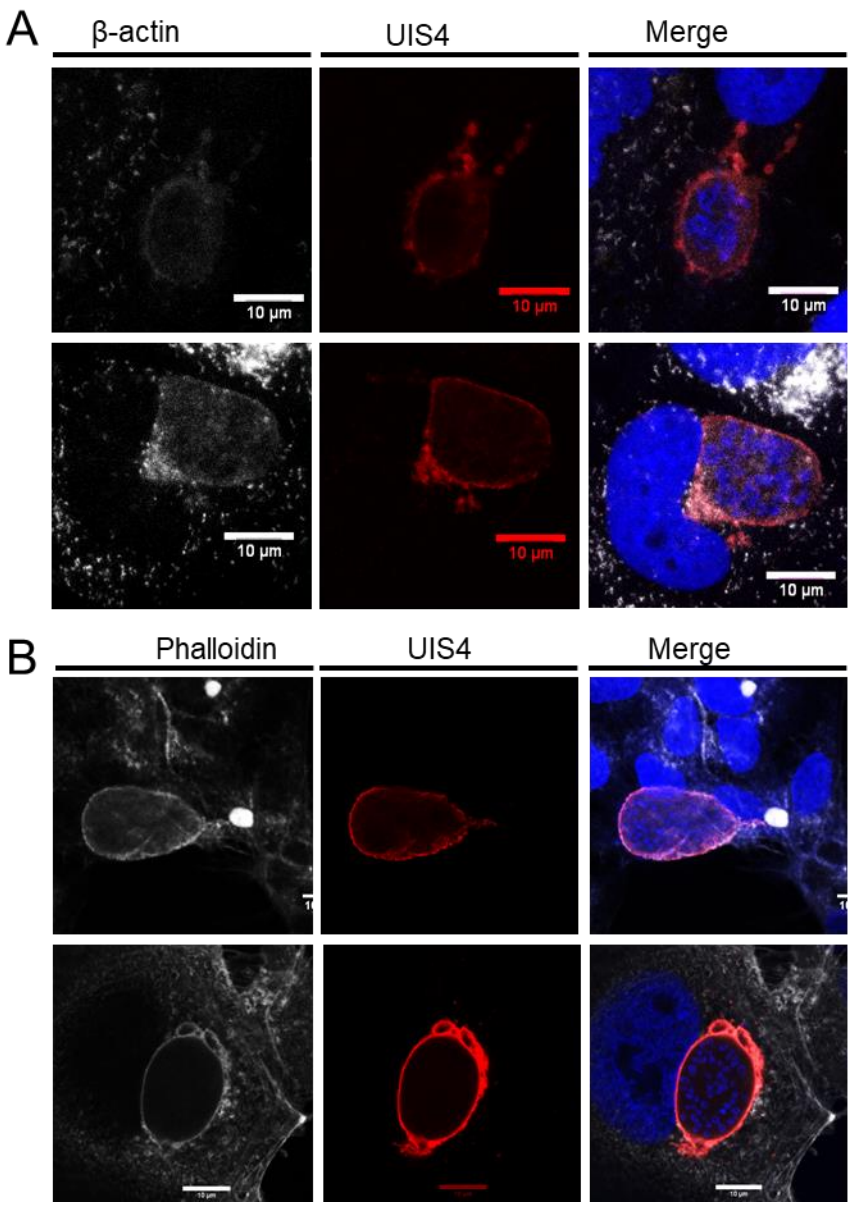


Figure 18. **PbUIS4 colocalization with F-actin and β-actin**. Pb-WT sporozoites were used to infect Huh 7 cells. A: Following 48 h.p.i, cells were fixed and stained with UIS4 antibody and β-actin (fluorophore 647) or (B) stained with UIS4 (fluorophore 568) and phalloidin (fluorophore 6479). Scale bar 10µm.

## II.3. PbUIS4 soluble domain is responsible for the actin interaction

PbUIS4 contains a cytosolic domain and one transmembrane domain that is implanted on the PVM, and a soluble domain that faces the host cell cytosol. Thus, PbUIS4 is able to interact with PVM actin, as well as with the host cell's actin. To investigate this issue, an immunoprecipitation was carried out using human embryonic kidney cells (HEK 293) transfected with a plasmid expressing PbUIS4 soluble domain (amino acids 121 to 220) fused to an HA tag. As a control for nonspecific actin binding, cells transfected with the soluble domain of PbUIS3, also a protein of the PVM, were used. We also performed immunoprecipitation from non-transfected cells. As suspected, the results showed that actin interacts with the soluble domain of UIS4 in transfected cells, but not with UIS3 (Figure 19).

It is important to note that the Myc-tag antibody was used because no antibody against UIS3 exists. On the other hand, the immunoprecipitation of actin from cells transfected with UIS4-HA cannot be considered as a nonspecific binding to HA tag since *in vivo* experiments showed that the cell-line infected with the WT parasite does not express any HA-tag fusion with UIS4.

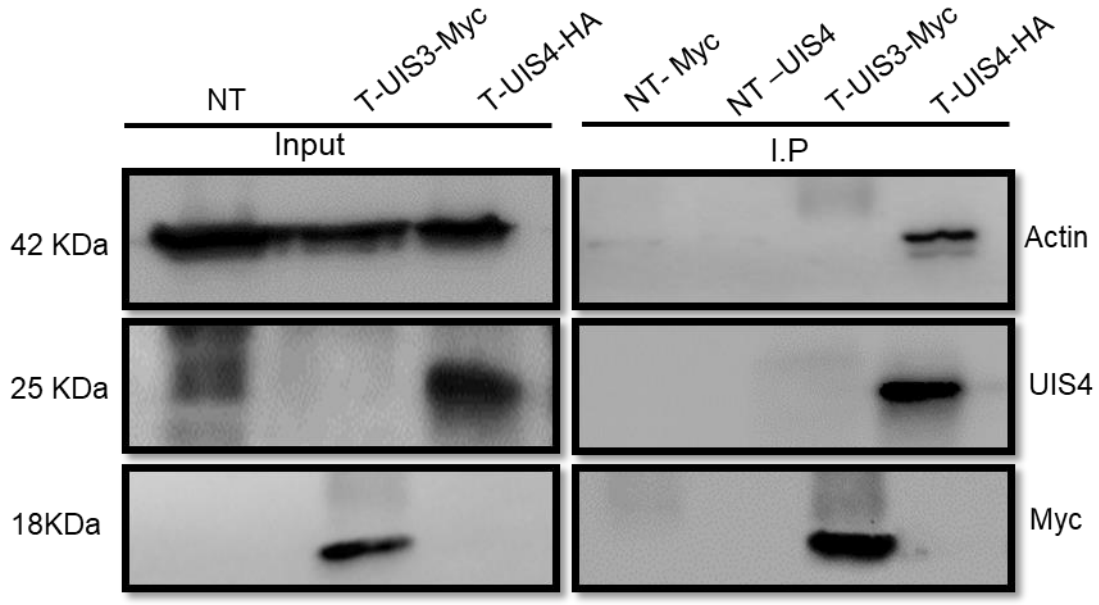


Figure 19. **UIS4 soluble domain interacts with actin.** HEK-293 T cells were transfected with plasmids expressing UIS4 soluble domain (UIS4-HA) or UIS3-Myc. A total of 5 µg of each plasmid were used to transfect the cells. After transfection, cells were incubated for 48h before cell lysis and immunoprecipitation was done using anti-UIS4 and anti-Myc antibodies (I.P). I.P from the transfected cells and controls were separated on a 15% SDS-PAGE before being transferred to nitrocellulose membrane, and probed with anti-actin, anti-UIS4, and anti-Myc antibodies. NT= Non-Transfected; T=Transfected; NT-Myc = Non-Transfected immunoprecipitation with anti—Myc antibody, NT-UIS4 = Non-Transfected immunoprecipitation with anti—UIS4 antibody

## II.4. PbUIS4 promotes actin Nucleation *in vitro*

The finding that PbUIS4 interacts with the host actin raises several questions regarding the effect of this interaction on actin dynamics and consequently on parasite survival. Actin exists in two main forms: monomeric actin, named globular actin or G-actin, and filamentous actin or F-actin (Dominguez and Holmes, 2011). The latter is generated from G-actin. The monomeric actin may be sequestered by PbUIS4, inhibiting or promoting actin polymerization. Alternatively, actin could be in its filamentous form (F-actin), which could lead to actin depolymerization or F-actin stabilization. Importantly, highly dynamic

actin reorganization events occurring during development of *P. berghei* parasites inside human hepatoma cell line had been reported (Gomes-Santos et al., 2012). Thus, this study aimed to investigate whether PbUIS4 affects actin dynamics. To that end, an actin polymerization assay was carried out, using the recombinant PbUIS4 soluble domain, rUIS4 (Figure 20).

In ideal conditions, recombinant actin monomers spontaneously polymerize into filamentous actin. The canonical and widely used actin polymerization biochemical assay applies two types of monomeric actin: non-fluorescent G-actin and monomeric actin labeled with a fluorophore, designated pyrene actin. Pyrene iodoacetamide labels cysteine at position 374 in fluorescent actin monomers increases 20-fold upon incorporation into actin filament (Cooper et al., 1983). Thus, in this assay, the pyrene-actin fluorescence is monitored over time using a spectrofluorometer.

Different rUIS4 concentrations of rUIS4 were tested to evaluate their effect on actin polymerization, *in vitro*. Surprisingly, actin nucleation was promoted at the low rUIS4 concentration tested (nM), whereas at high levels this effect was no longer observed (Figure 21), which may be explained by dimerization of PbUIS4 at these concentrations. Alternatively, it may be due to the limitation of monomer assembly caused by steric inhibition.

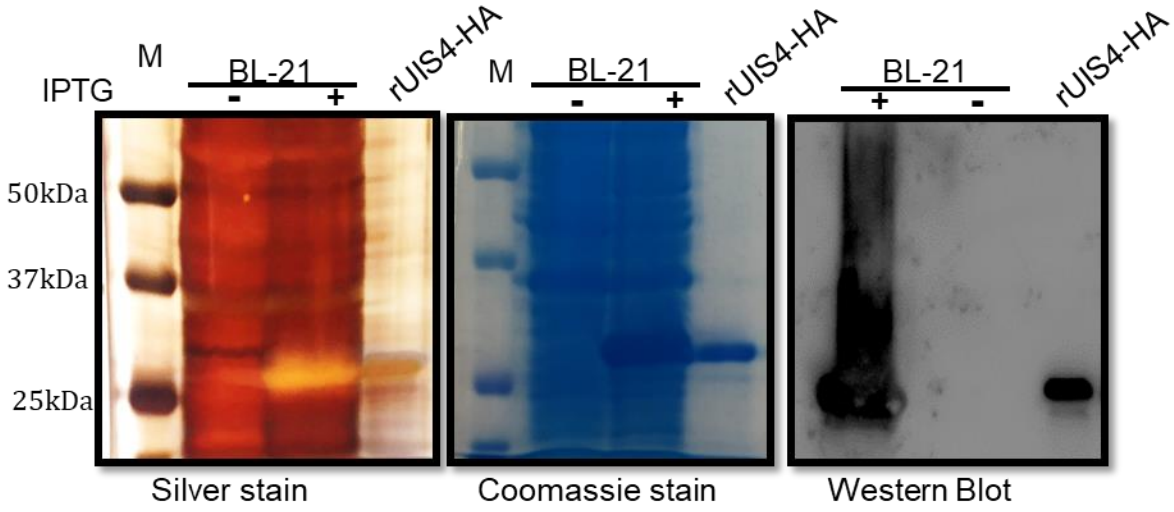


Figure 20. **Generation and validation of recombinant soluble domain of UIS4** Pellets of BL-21 competent *E. coli* cells transformed with rUIS4 expressing plasmid, supplemented or not with IPTG were lysed in SDS sample buffer before separation on SDS PAGE, together with purified rUIS4. Gels were stained with Silver or Coomassie dye or were used for protein transfer to a nitrocellulose membrane followed probing with anti-UIS4 antibody. M= molecular weight marker, Ladder= precision plus from Bio Rad

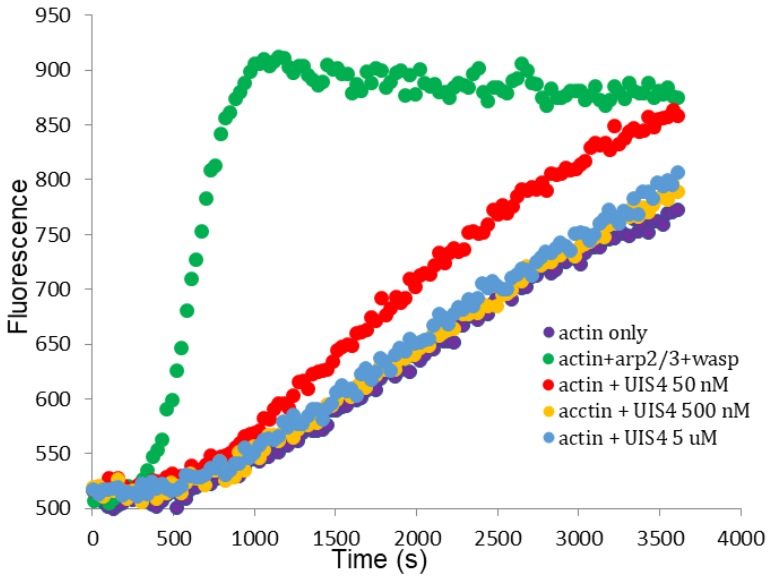


Figure 21. **PbUIS4 promotes actin Nucleation. Pyrene actin polymerization assay**. In this pyrene actin polymerization assay, actin monomers were converted into Mg-actin for 2 minutes on flat-bottom black solid plates at room temperature, followed by rUIS4 addition at different concentration. Arp2/3 and WASP was used at 10nM and 400nM respectively. The fluorescence intensity was read every 30 seconds for 1h. Each read is the mean of four different reads.

**In summary**

The new PbUIS4-KO parasite lines generated in *P. berghei ANKA* and in *P. berghei* GFP background both display the same phenotype as that of the UIS4-KO parasite previously generated. Although a drastic reduction in parasite liver load is observed *in vivo*, around 0.5% of defective parasites were able to survive and were responsible for infection. The data presented show that UIS4 interacts with the host actin. This interaction seems to occur via the UIS4 soluble domain, which has an impact on actin polymerization dynamics.

Further experiments are required to assess the biologic relevance of UIS4–actin interaction *in situ*, in a *Plasmodium*-infected hepatocyte. Experiments that rely on live images of host actin polymerization during *P. berghei* development inside the hepatoma cells are currently being performed.

## II.5. Materials and Methods

**PbUIS4-KO plasmid**

### Generation of PbANKA-UIS4-KO transgenic parasite line

To generate the PbUIS4 knockout (PbUIS4-KO), transgenic parasites in *Plasmodium berghei* ANKA *(P. berghei* ANKA*)* ORF of PbUIS4 was replaced by the gene coding for hDHFR (human Dihydrofolate Reductase) using double cross-over recombination strategy. The following primers: 5'UTR GGTACCTGGATTCATTTTTTGATGCATGC'-3 forward and 5'-GGGCCCTTTATTCAGACGTAATAATTATGTGC 3' reverse were used to amplify 1Kb upstream of the ORF and 5'-AAGATATCATAATTCATTATGAGTAGTGTAATTCAG'-3 forward, 5'-GCGGCCGCAAGTTTGCATATACGGCTGCTTCC '3UTR reverse for producing a fragment 0.6Kb downstream of the ORF. DHFR-resistance cassette provides the resistance of transfected parasites to pyrimethamine.

*P. berghei* transfection was performed using a standard protocol (Janse et al., 2006). Briefly, mice were infected with wild-type *P. berghei* ANKA parasites and the infected blood with approximately 1-3% parasitemia was incubated overnight in culture to produce schizonts for transfection. Mature schizonts were collected on the Nycodenz gradient and then transfected using Amaxa electroporation system. After schizonts transfection, the solution (containing transfected merozoites) was injected into a tail vein of an anesthetized mouse. The transformed parasites were selected by injecting mice with 100 µg of pyrimethamine 30 hours after infection.

DNA was extracted from positive mice and genotyped using the following primers: 5'-CTGCGATTTTTCTTATATTTACTATTAA-3'external forward primer 5'CATGTTATGCATACAACATATGTAAA-3' external reverse primer, 5'-CAATGATTCATAAATAGTTGGACTTG-3' DHFR forward primer and 5'-GATGTGTTATGTGATTAATTCATACAC-3'DHFR reverse primer.

The cloning of transgenic parasites was done by injecting 1 to 2 of transgenic parasites per mouse, through serial dilution to obtain a genetically homogenous transgenic parasite line.

**PCR and Genotyping PCR**

All the PCR were performed in a Bio-Rad machine using the following conditions:

Initial denaturation at 95ºC for 3 min was preceded by denaturation at 92ºC for 30sec, followed by annealing at 56ºC for 45sec, extension at 68ºC for 2 min. Denaturation steps were repeated 34 times. The final extension was done at 68ºC for 12 min.

**Phenotype Validation of the transgenic parasites**

The transgenic parasite line was validated through genotyping to ensure that the transfection construct was integrated into the correct locus, using the following set of primers: 5'-CTTTCAGCACATAATTATTACGTCTG-3' (genotyping forward primer)

5'-CATAAAACAATTTGTTCTCTTTCTGAATTAC-3' (genotyping reverse primer), to amplify the wild-type locus.

The primers, 5'-CAATGATTCATAAATAGTTGGACTTG-3' forward and

5'-GATGTGTTATGTGATTAATTCATACAC-3' reverse were used to detect the resistance cassette (Dihydrofolate Reductase).

The lack of UIS4 expression was confirmed in transgenic parasites by RT-PCR, immunofluorescence, and Western Blot. Establishment of the infection by UIS4-deficient parasites was assessed *in vivo* using C57Bl/6J mice injected intravenously with 50,000 UIS4-deficient or wild-type parental lines. Parasitemia was monitored from two days post infection (d.p.i) until day 25 d.p.i by blood smear stained with Giemsa staining. *In vitro,* the parasite development was carried out through time course from 24 to 60 h.p.i, using Huh7 hepatoma cell line and. All the validations were performed according to the wild-type parasite P*. berghei* ANKA.

**Sporozoites purification**

To produce sporozoites, the Anopheles *stephensi* mosquito was infected by blood feeding on mice infected whit either the wild-type or transgenic parasites. Infected mosquitoes

were dissected after 21-35-days post-infection. The sporozoites were collected from the salivary glands of dissected mosquitoes.

**Hepatoma cell line infection**

To establish liver-stage infection *in vitro*, a confluent Huh 7 hepatoma cell line cultured in RMPI 1640 complete medium, was infected by direct exposure to the sporozoites collected from the salivary glands of the infected mosquitoes. Cells were centrifuged for 5 min at 3000 rpm following incubation at 37ºC with 5% $CO_2$. The culture medium was replaced after 2 hours post infection with fresh medium containing fungizone 0.03%.

**Immunofluorescence Assay**

Cells were seeded on coverslips overnight before infection. At the desired time point, cells were fixed with 4% of paraformaldehyde in PBS (Nzytech MB04602, Ref: sc281698) for 15min and permeabilized with a solution containing 2% BSA (Nzytech MB04602) and 0.2% saponin in PBS for 30 min and were washed three times for 10 min. Coverslips were incubated with primary antibody diluted in an appropriate volume of the permeabilizing solution used above or in PBS containing 0.1% Triton X and 2% BSA for 2h, followed by washing for three times for 10 minutes each and incubated with secondary antibody for 1h. After three washes, coverslips were mounted with Fluoromount-G (Invitrogen Ref: 00-4958-02) and stored in the dark overnight to be used in the Immunofluorescence analysis.

**cDNA synthesis and Real Time-PCR**

Following RNA extraction by Trizol (Purezol RNA extraction reagent, Bio-Rad, ref: 732-6890), cDNA was synthesized using a cDNA synthesis kit from Nzytech Bio-Rad machine (Bio-Rad Thermal Cycler T100) with the following conditions: 200-500µg of RNA were used for synthesis reaction as follows: 25ºC for 10min, 50ºC for 50min and 85ºC for 5min. Real-Time PCR was performed using the 7500 Applied Bioscience Fast with SYBGR kit (Bio Rad #172-5124).

**Immunoprecipitation**

Twenty-four hours post-infection, (h.p.i) the plate with 4 million HepG2 hepatoma cells lines infected with 4 million PbANKA-WT or PbANKA-UIS4-KO was washed three times with PBS 1X, followed by 5 minutes of incubation with trypsin at 37ºC. Trypsin was inactivated by adding complete medium. The cells were harvested next.

Cells were centrifuged at 1200 rpm at 4ºC for 5 minutes and washed two times with PBS1X. The pellet was transferred to a canonical 1.5ml Eppendorf tube with 1ml of PBS1X, spun for 5 min at 5000rpm and the supernatant was removed. The cell was lysed with 0.5ml of lysis buffer.

**Cell lysis procedures**

A total of around $6x10^6$ cells were lysed with 0.5 ml of lysis buffer, 50mM Tris-HCl pH 7.4, 0.5% NP-40, 250mM NaCl, 5mM EDTA, 50mM NaF. A cocktail of proteases inhibitors (Roche, REF: 05056489001) and phenylmethanesulfonylfluoride fluoride was added to the lysis buffer just before cell lysis. Cells were incubated for 30 minutes on ice and were subsequently centrifuged at 4ºC for 15 minutes at 14000rpm. The supernatant was collected, and the amount of proteins quantified using Pierce™ BCA Protein Assay Kit (Thermo Scientific).

**Pre-clearing and I.P procedures**

The pre-clearing was performed by incubating the supernatant from the previous step (here called lysate) with the protein G beads (Dynabeads Protein G, Thermo Fisher life technologies, ref: 10004D). A total of 50ul corresponding to 1.5mg of beads was pipetted into a 1.5ml Eppendorf tube, placed on a magnetic rack for 30 seconds and the liquid was removed. Beads were washed once by placing the Eppendorf containing beads and wash buffer on a magnetic rack for 30 seconds; the wash buffer was removed and the lysate added. The lysate was incubated with 50µL (1.5mg) of the beads previously washed, for 1 hour at 4ºC with rotation. The Eppendorf tube containing lysate and beads was placed on the magnetic rack for 30 seconds, and the supernatant transferred to a new 1.5ml Eppendorf tube. 5µL (10µg) of anti-UIS4 antibody (SICGEN; ref: AB0042-500) was added

to the supernatant from the pre-clearing step and incubated overnight at 4ºC with rotation.

After adding the complex, the sample and the anti-UIS4, 50µL of the beads were added, and mixed by up-and-down pipetting before incubation at 4ºC for 1h with rotation. In the meantime, three Eppendorf tubes were prepared and labelled: a tube for beads, a tube for elution, and for the elute. The tube was removed from the mixer and placed for 30 seconds on the magnetic rack to have the liquid removed. Beads were washed three times with 200µL of wash buffer (PBST 0.02%). Samples were eluted in 30µL of glycine (50mM, pH 2.8), mixed by up-and-down pipetting and placed in the mixer for 5 minutes. In the meantime, 1.5µL of 1M Tris-HCl pH10.02 added to the tube for the elute. After 5 minutes, the tube was placed on the magnetic rack for 2 minutes before transferring the liquid to the elute tube and mixed by pipetting.

**Western blot**

Proteins were separated on a 5% stacking gel (30% Acrylamide, 1M Tris-HCl, 10% SDS, 10% APS, TEMED) and 10% SDS PAGE resolving gel (30% Acrylamide, 1.5M Tris-HCl, 10% SDS, 10% APS, TEMED), and transferred into a Nitrocellulose Membrane. To detect PbUIS4, the membrane was blocked with TBS containing 5% of non-fat milk and 0.2% of Tween 20 during 1hour at room temperature and probed with goat anti-UIS4 1:1000 at 4ºC overnight with rotation, followed by washing three times with PBST 0.2% and then with rabbit anti-goat HRP conjugated 1:10000 (Invitrogen Ref: 81-1620). The actin detection was performed by probing the membrane with rabbit anti-actin 1:1000 (Sigma, ref: A2066) overnight, fowling incubation with goat anti-rabbit HRP conjugated 1:10000.

**Cell transfection with UIS4 soluble domain**

A total of 5 million Human Embryonic Kidney 293T (HEK-293T) cells were seeded on a 10cm cell culture dish for overnight incubation with DMEM but no antibiotics. The transfection was performed with 5µg of plasmid using FUGENE 6 as the transfection reagent in a 3:1 ratio of transfection reagent and DNA. At 48h post-transfection, cells were lysed directly on the plate followed by immunoprecipitation.

**Silver staining**

The silver staining was performed according the protocol from the Thermo Scientific Silver Stain Kit (Prod # 24612), and PROTSIL from Sigma (PROTSIL1-1KT).

After protein separation on a 10% SDS-PAGE, the gel was washed 2 times for 5 minutes in ultrapure water. Fixation was done for 15 minutes in fixative solution (30% ethanol:10% acetic acid). Following the fixation, the gel was washed 10 minutes in 30% ethanol, then 2 times for 5 minutes in ultrapure water. The gel was sensitized for 10 minutes, then washed 2 times for 10 minutes with water. Next, the gel was stained with silver stain solution for 30 minutes. The gel was developed into developer solution after washing for 90 seconds. Development was ended after reaching the desired bands intensity with 5% acetic acid or using stopping solution for 10 minutes.

**Mass Spectrometry Analysis**

The protein bands excised from a 1D-PAGE gel, were distained, reduced, alkylated, and digested with trypsin (Promega, 6.7 ng/µl) overnight at 37 $^{0}$C. The tryptic peptides were actively extracted from the bands, desalted, and concentrated using POROS R2 (Applied Biosystems) and eluted directly onto the MALDI plate using 0.6 µl of 2.5 mg/ml CHCA (alpha-cyano-4-hydroxycinnamic acid, Sigma) in 50 % (v/v) acetonitrile and 5 % (v/v) formic acid.

The data were acquired using a positive reflector MS and MS/MS modes using a 4800plus MALDI-TOF/TOF (ABSciex) mass spectrometer and using 4000 Series Explorer Software v.3.5.3 (Applied Biosystems). External calibration was performed using CalMix5 (Protea). The twenty-five most intense precursor ions from the MS spectra were selected for MS/MS analysis. The raw MS and MS/MS data were analyzed using Protein Pilot Software v. 4.5 (ABSciex) with the Mascot search engine (MOWSE algorithm). The search parameters were as follows: monoisotopic peptide mass values were considered, maximum precursor mass tolerance (MS) of 50 ppm and a maximum fragment mass tolerance (MS/MS) of 0.3 Da. The search was performed against the SwissProt protein database with no taxonomic restriction. A maximum of two missed cleavages was allowed. Carboxyamidomethylation

of cysteines, oxidation of methionine and N-Pyro Glu of the N-terminal Q were set as variable modifications.

**Protein Identification**

Protein identification was only accepted when significant protein homology scores were obtained ($p<0.05$, scores higher than 70) and at least one peptide was fragmented with a significant individual ion score ($p<0.05$).

**Recombinant UIS4-HA protein (rUIS4-HA) production**

The codon-optimized UIS4-HA fragment encoding the soluble domain of UIS4 was cloned into pET28a+ expressing vector in frame with His-Tag, with Kanamycin as the selection marker. *Escherichia coli* BL21 competent cells were transformed with the plasmid mentioned before using a standard transformation protocol, as follows. Briefly, competent cells were thawed on ice. After adding 5 ng of the plasmid, the mixture was placed on ice for 30minuts followed by heat shock at 42°C for 30 seconds and returned on ice for 2 minutes. After adding 1mL of media at room temperature, the tube was placed at 37°C for 60minuts with a vigorous shake (220 rpm). The transformed cells were then spread onto the agarose plates containing the kanamycin antibiotic for overnight (16-18h) incubation at 37ºC. Following the transformation, a bacterial colony was picked and inoculated into the culture in Luria-Bertani (LB) broth culture medium supplemented with Kanamycin and incubated overnight at 37ºC with shaking. Cells were then diluted 1:100 into fresh medium supplemented with the Kanamycin and incubated at 37ºC with agitation. The culture was left to grow until O.D. reached 0.6-1. The protein induction was done by adding 0.3mM of the Isopropyl β-D-1-thiogalactopyranoside (IPTG), followed by incubation for 5 hours.

**Recombinant Protein purification protocol**

Recombinant His-tagged protein was initially purified by metal chelating affinity chromatography using His-Trap Ni-containing columns (GE Healthcare) connected to an AKTA Explorer chromatographic system (GE Healthcare). The His-trap column (1 ml bed

volume) was equilibrated with sodium phosphate buffer pH 6.8 containing 1 M NaCl and 25 mM imidazole before protein injection. His-tagged proteins were eluted by a linear gradient of imidazole from 25–500 mM in the same phosphate buffer.
Fractions containing protein were collected, pooled and, further polished by size exclusion chromatography purification using a Sephadex S-200 column (GE Healthcare) eluted with PBS. Fractions containing protein were analyzed by SDS–PAGE.

**Actin polymerization Assay**

Actin and Pyrene-Actin were prepared following the manufacturer instructions. Briefly, Actin and Pyrene-actin were resuspended in ice-cold dd$H_2O$ aliquoted in 10 µl aliquots, freeze in liquid Nitrogen and stored at -80 ºC).

To depolymerize actin, both actin and Pyrene actin were incubated on ice for 1 h and then centrifuged to pellet to discard the polymerized actin at 100.000 g, 4ºC, 1 h in a Ultracentrifuge (rotor TLA-120 = 54.000 rpm). A total of 90% of the supernatant was kept (~220 µl) at 4ºC and quantified in nanodrop using $\varepsilon=2.66 \times 10^4$ (MW=43 KDa)

rUIS4 was dialyzed overnight at 4ºC with agitation. The polymerization assay was preceded by Mg-actin conversion with the addition of 0.2mM of EDTA, and 50nM of $MgCl_2$ and incubated at room temperature for 2 minutes on a black plate flat bottom microplate before measuring the fluorescence intensity. The fluorescence intensity was measured on the microplate reader (infinite M 200 Tecan), with 30 seconds of intervals. Each read is the mean of four different reads.

**Required solutions for actin polymerization assay** (all with miliQ water)

- **ATP 100 mM** (from Cytoskeleton, #BSA04): resuspend in 1 ml of cold 100 mM Tris pH 7.5. Freeze in liquid $N_2$ and store at/below -20ºC in 50 ul aliquots.
- **Tris·Cl 100 mM pH 8.0:** 1.21 g Tris/100 ml miliQ water – adjust pH with HCl. Filter.
- **Tris·Cl 100 mM pH 7.5:** 1.21 g Tris/100 ml miliQ water – adjust pH with HCl. Filter.
- **EGTA 0.1 M pH 8.0:** 1.9 g EGTA/50 ml miliQ + 4 pellets NaOH -> finish adjusting pH with concentrated NaOH solution. Filter.

- **GENERAL ACTIN BUFFER (G-ACTIN BUFFER)**: Tris·Cl 5 mM pH 8.0, $CaCl_2$ 0.2 mM Prepare without ATP and DTT (always add fresh before assays!)
- **10x KMEI POLYMERIZATION BUFFER**: Imidazole 100 mM, HCl 500 mM, $MgCl_2$ 10 mM, EGTA 10 mM
- **G-Mg BUFFER:** Tris·Cl 5 mM pH 8.0, MgCl2 0.1 mM Prepare without ATP and DTT (always add fresh before assays).
- **10E/1M BUFFER (10x):** EGTA 2 mM, MgCl2 0.5 mM

# CHAPTER III- FINDING NOVEL HOST AND PARASITE PROTEINS PUTATIVELY EXPRESSED AT THE PVM

## III. Finding novel host and parasite proteins putatively expressed at the PVM

Hepatocyte infection is the first step prior to establishment of malaria infection. Being at the host–parasite interface, it is expected that the PVM would have proteins playing critical roles during hepatocyte liver infection (Nyboer et al., 2017). Several proteins have been shown to be crucial for a successful infection to take place on the PVM (Matuschewski et al., 2002a; Real et al. 2017; Mueller et al. 2005; Kumar et al., 2009). These findings led to an increased interest in identifying additional liver-stage PVM proteins in *Plasmodium* species. However, identification of new PVM proteins has proven to be a challenge because no PVM signature sequence has yet been described, and because liver-stage malaria is complex to study due to the poor technical tools available (Nyboer et al., 2017).

Numerous methods have been developed and applied to characterize protein–protein interactions, in many different fields. Classical methods are strongly hypothesis-based or rely on biased screening methods, varying between biochemical (co-immunoprecipitation) and genetics approaches (Yeast-2-hybrid). However, to apply these approaches, a prior knowledge or prediction of potential candidate proteins is necessary.

This study aimed to identify new putative proteins on the PVM. PbUIS4 is one of the highly expressed known proteins found at the host–parasite interface, and the study sought to use this protein as the bait to identify new putative proteins on its vicinity. To that end, proximity-dependent biotin labeling was performed, hereafter referred to as BioID (Roux et al., 2012), and we screened for biotin ligase (BirA) fused with UIS4 on the PVM.

BioID is labeling approach targeting proteins that interact or are very close to each other. It is an unbiased protein screening method for the identification of physiologically relevant *in vivo* proteins (Roux et al., 2012). This approach relies on the use of the promiscuous prokaryotic biotin protein ligase derived from *E. coli*, named BirA, which is fused with a protein of interest. When BirA-fusion protein is expressed in cells, upon addition of biotin, it biotinylates the interacting proteins or those in the vicinity of the target protein. Next, they are selected using streptavidin or avidin. Selected proteins are then identified by mass spectrometry.

In *E. coli*, BirA covalently biotinylates acetyl-CoA-carboxylase, and the biotinylation occurs in two steps as shown in Figure 22.

- Step 1: Generation of the biotinyl-adenylate, catalyzed by BirA in the presence of biotin and ATP. This reactive compound remains attached to the BirA. $Biotin + ATP \rightarrow Bio - 5 - AMP + Ppi$
- Step 2: Biotinyl-adenylate is transferred to apo-carboxylase, which results in the biotinylation of the target protein.

$$Bio - 5 - AMP + Apo - Protein \rightarrow Biotinol - Protein + AMP$$

In *E. coli*, biotin transfer occurs through the recognition of specific binding peptides of the target protein. To act as a promiscuous biotinylating enzyme, BirA was mutated to release biotinyl-adenylate upon its generation (Roux 2013), at the biotin derivate binding site located at the N-terminus (Xu and Beckett, 1996). The promiscuous BirA is hereafter referred to as BirA*.

Biotinoyl-AMP acts as a promiscuous biotinylation reagent, likely due to its instability and reactivity, by binding to any primer amine group at any lysine residue available in the 10nm radius, which results in the biotinylation of interacting and neighboring proteins (Figure 22) (Roux 2013).

Since its conception, BioID has been extensively applied for the identification and characterization of new protein–protein interaction in different living cells. Successful use of this methodology enabled important discoveries in many fields, from cell biology to parasitology and cancer (Firat-Karalar et al., 2014; Kim et al., 2014; Khosh-Naucke et al., 2017).

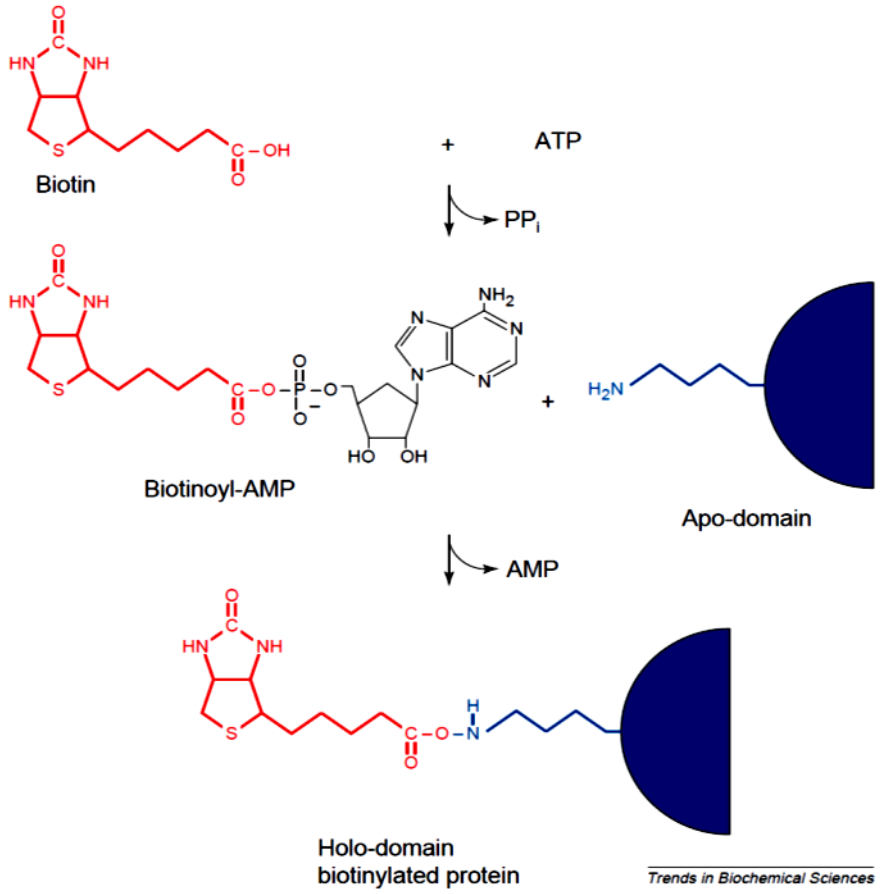


Figure 22. **Biotinylation reaction. Biotinoyl-AMP formation is catalysed by BirA* from biotin and ATP, with PPi release**. Biotinoyl-AMP formation is catalysed by BirA* from biotin and ATP, with PPi release. Biotinoyl-AMP remains attached to BirA* until its transfer to a specific primary amine; the loss of AMP leads to protein biotinylation. PPi = Pyrophosphate *Adapted from:* Trends in Biochemicals Sciences.

BioID is not the only method based on promiscuous labeling of protein–protein interaction or proximity. Other approaches include **BLINC,** *Biotin Labeling Intercellular Contact*; **APEX**, *Proximity Labeling with Ascorbate Peroxidase*; **EMARS,** *Enzyme-mediated Activation of Radical Sources*; and ***SPPLAT*,** *Selective Proteomic Proximity Labeling Assay using Tyramide* (Chen and Perrimon, 2017).

Since biotinylation is a covalent modification, it endures the harsh washing conditions of the process, minimizing the chances of false positive hits. This is one of the main advantage of BioID, if compared to other methods. Nevertheless, BioID also has limitations and

drawbacks: the large size (35KD) of the BirA* enzyme may compromise the function of the target protein due to improper protein folding or shifting in case of the exported proteins. These limitations have been recently resolved by the improvement of the BioID method and development of a new version called BioID2 (D. I. Kim et al., 2016).

In BioID2, BirA* was replaced by the biotin ligase from *Aquifex aeolicus.* This enzyme has the advantage of being smaller than the former (25KD). Moreover, BioID2 seems to be more efficient and requires less biotin than BioID; nevertheless, both versions reach saturation at the same time.

On the other hand, biotinylation itself could impair the post-translational modification of the labeled protein (Chen and Perrimon, 2017). The extent of biotinyl-5'-AMP diffusion is estimated to attain the 10–20nm range, meaning that biotinylation can occur far away from the fusion protein, which could give rise to the identification of false positive hits.

Thus, it is important to emphasize that the approach here described using biotinylation points to proteins that are in the vicinity of a target protein but are not necessarily interacting with it. It is therefore of utmost importance that the results obtained through BioID be validated by other methods, such as IFA and Western Blot.

Using this protocol, the candidate proteins identified by mass spectrometry (Figure 23) analysis were further validated using bioinformatic tools.

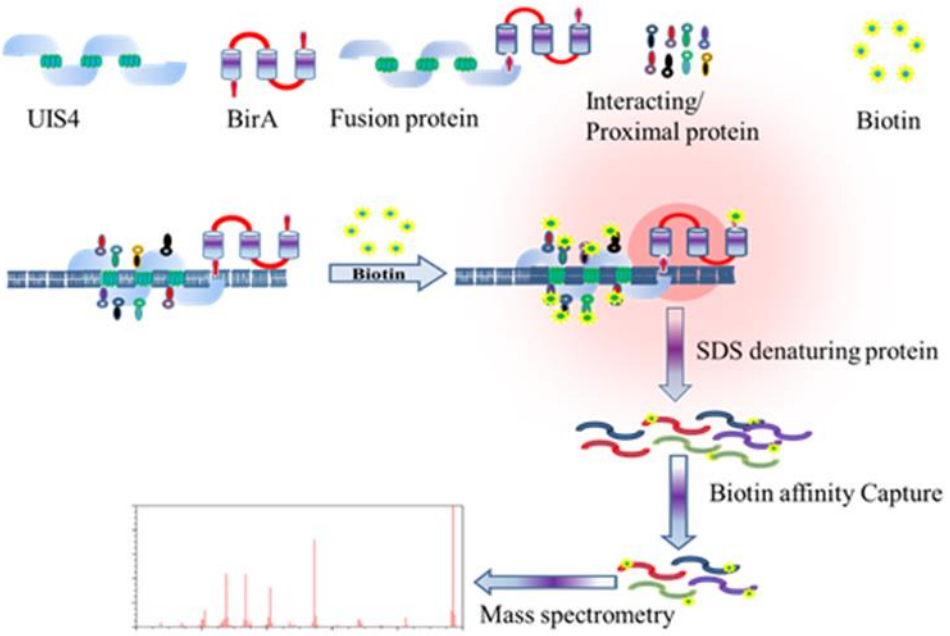


Figure 23. **Schematic representation of expression of promiscuous biotin–ligase fused to a protein at the PVM**, leading to the biotinylation of proteins vicinal to that fusion protein. After stringent cell lysis and protein denaturation, biotinylated proteins are affinity-based purified. The candidate proteins can be identified by mass spectrometry

## III.2. Expressing BirA* at the *Plasmodium berghei* PVM

To target BirA* on the *P. berghei* PVM, approximately 800bp of *P. berghei* ANKA UIS4 ORF sequence was cloned into the transfection plasmid in frame with the BirA*-HA, the hemagglutinin (HA) coding sequence, which is referred to hereafter as PbUIS4-BirA*-HA. Upon transfection of *P. berghei* ANKA parasite, integration into the UIS4 locus occurs via single cross-over recombination and leads to expression of the fusion protein in transgenic parasites. The transgenic parasites were selected through pyrimethamine pressure, and a clonal parasite population was obtained through limiting dilution. The HA tag serves as a marker for localizing the BirA* on the PVM (Figure 24).

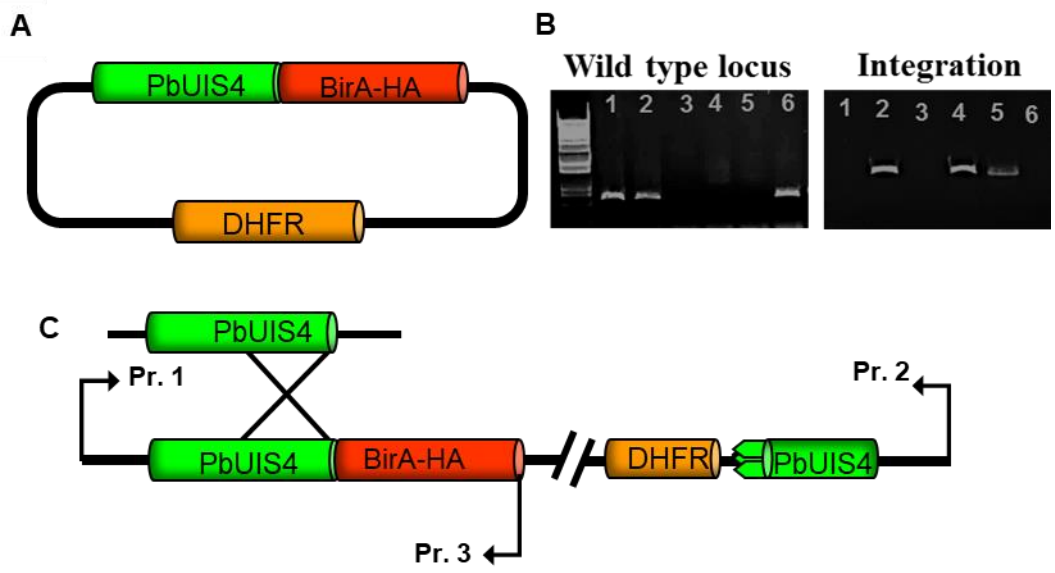


Figure 24. **Generation of the transgenic P. berghei parasite line expressing PbUIS4-BirA*-HA.** A) Final plasmid vector for PbUIS4-BirA*-HA-expressing parasite. B) Agarose gel of the genotyping PCR of the transgenic parasites following the cloning by limiting dilution. C) Genotyping strategy of PbUIS4-BirA*-HA-expressing parasite: Primers Pr.1 +Pr.2 were used to detect the wild-type locus located at the 5' and 3' UTRs, respectively. The combination of primers Pr.1+Pr.3 was used to detect the integration locus. Clones 1 and 6 are the wild-type parental clone and show the wild-type UIS4 locus and no integration of the transfection construct. Clone 2 shows a mixed parasite population with and without integration of the transfection construct. Clones 4 and 5 contain only the integration of the transfection construct and thus no wild-type UIS4 locus. Clone 3 did not amplify and thus was not considered further.

## III.3. Phenotypic validation of PbUIS4-BirA*-HA transgenic parasite line

PbUIS4-BirA*-HA parasite (clone 4) was investigated by Western blot to ensure that the fusion protein is of the correct size, and further by immunofluorescence assay (IFA) to ensure it is localized on the PVM (Figure 25-A and Figure 25-B).

Also, transgenic parasites were phenotypically investigated using IFA to assess their growth (Figure 25-C) and their sizes were compared to that of wild-type parasites, to

investigate whether the PbUIS4-BirA*-HA fusion protein could be compromising the parasite development *in vitro* (Figure 26-A).

To investigate whether PbUIS4-BirA*-HA parasites can establish a normal life cycle, C57BL/6 mice were infected intravenously with sporozoites expressing UIS4-BirA*-HA, collected from the salivary glands of infected mosquitoes at 21–35 d.p.i. The infected mice were monitored for the onset of parasitemia. As expected, parasites were detected 3–4 d.p.i. in the blood of all mice, as shown in Figure 26-B. This finding indicates that PbUIS4-BirA*-HA parasites undergo normal development throughout their life cycle.

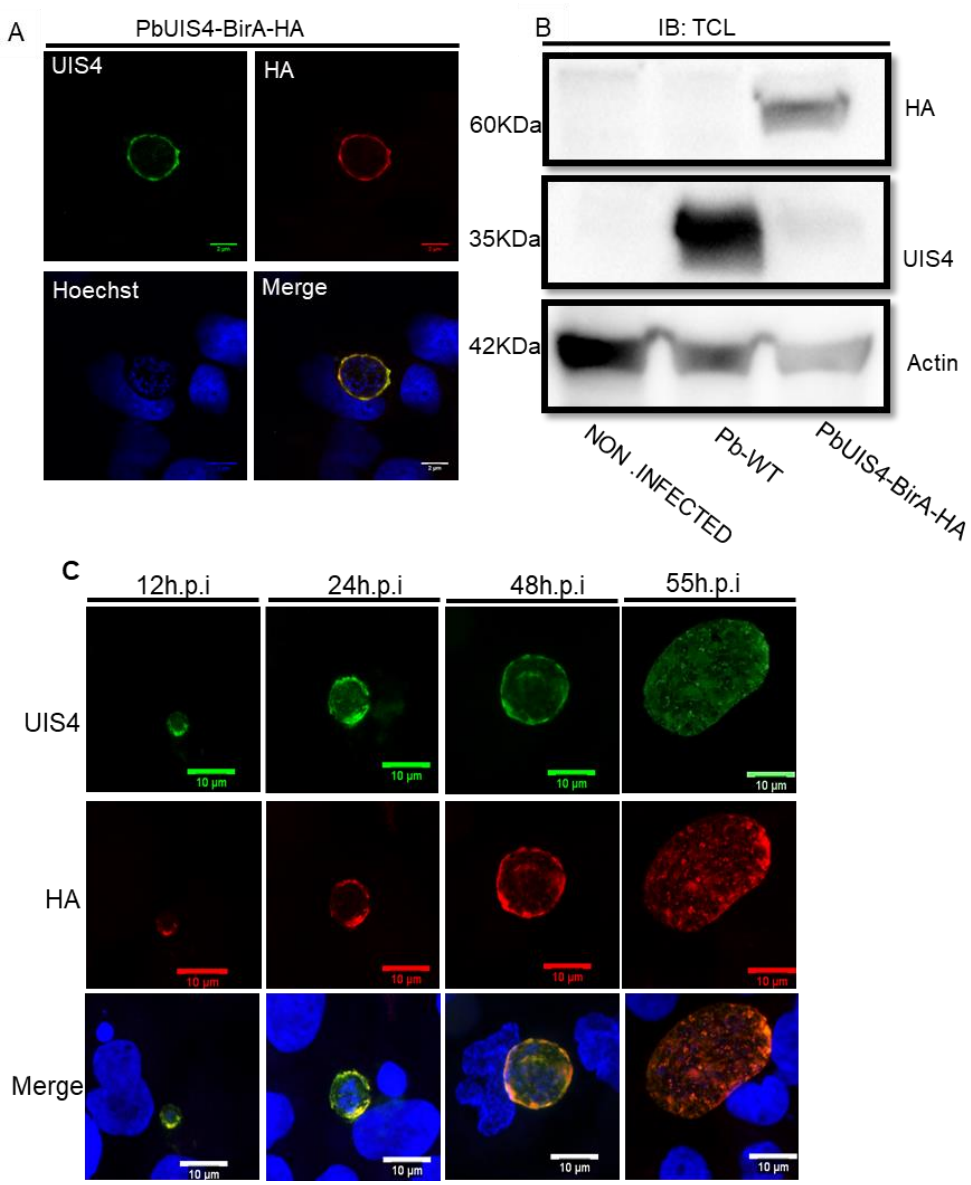


Figure 25. **Characterization of PbUIS4-BirA*-HA transgenic parasite. A) UIS4-BirA*-HA expression at the PVM**. Huh 7 hepatoma cell line cultured on coverslips and infected with PbUIS4-BirA*-HA. At 48h.p. i, cells were fixed and stained. B) Western blot. Huh7 cell infected with PbUIS4-BirA*-HA, wild-type parental line and a not infected cell (needs to change in the figure to not infected). At 24h.p. i, cells were lysed. Proteins separated on SDS-PAGE were transferred to a nitrocellulose membrane, followed by blocking with 5% milk. The membrane was then probed with anti-UIS4, anti-HA antibodies. C) Huh 7 hepatoma cell line cultured overnight prior to infection with Pb-UIS4-BirA*-HA ant wild-type parental line. Infected cells were fixed and stained at different time points (12-55h.p. i) and stained with anti-UIS4, anti-HA and Hoechst.

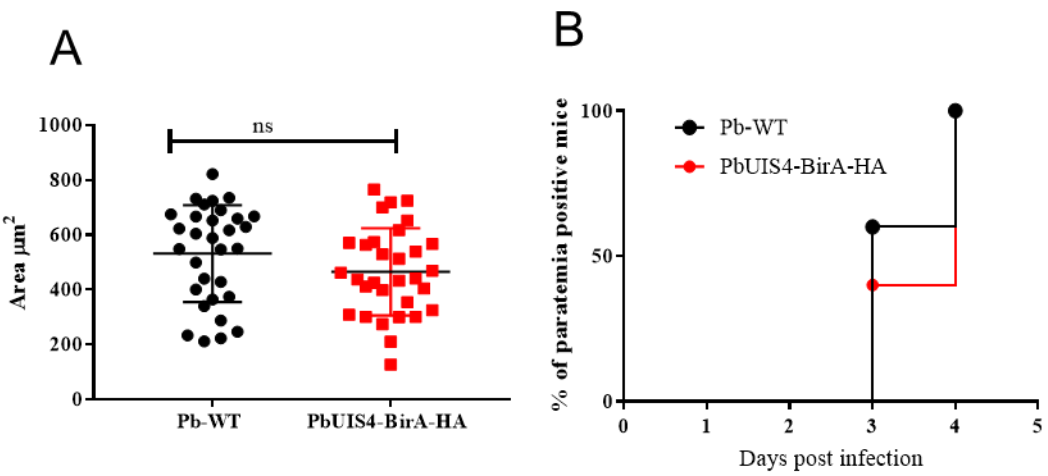


Figure 26. **Characterization of PbUIS4-BirA*-HA transgenic parasite**. A) Size of parasites at 48 h.p.i. Huh7 hepatoma cell line cultured overnight on coverslips prior to infection with PbUIS4-BirA*-HA ant wild-type parental line. Infected cells were fixed and stained at the considered time points. The parasite size was measured using UIS4 stain. B) Prepatency of C57BL/6J mice injected with 5000 Pb-WT sporozoite or PbUIS4-BirA*-HA sporozoites. Parasitaemia was monitored from 2-4 days post-infection by smear and stained with Giemsa.

## III. 3.a. Protein biotin labelling at the PVM

To verify whether PbUIS4-BirA*-HA could biotinylate proteins on the PVM, the Huh7-hepatoma cell line was infected either with PbUIS4-BirA*-HA or with wild-type parental line and supplemented with 50µM biotin. Biotin supplementation was carried out at 2 h.p.i. for the time point fixed at 24 h.p.i, or at 24 h.p.i. for the time point fixed at 48 h.p.i.

IFA results revealed strong accumulation of biotin around the PbUIS4-BirA*-HA parasites, but not in WT parasites. Biotin seemed to colocalize with UIS4, consistent with biotinylation occurring on the PVM (Figure 27).

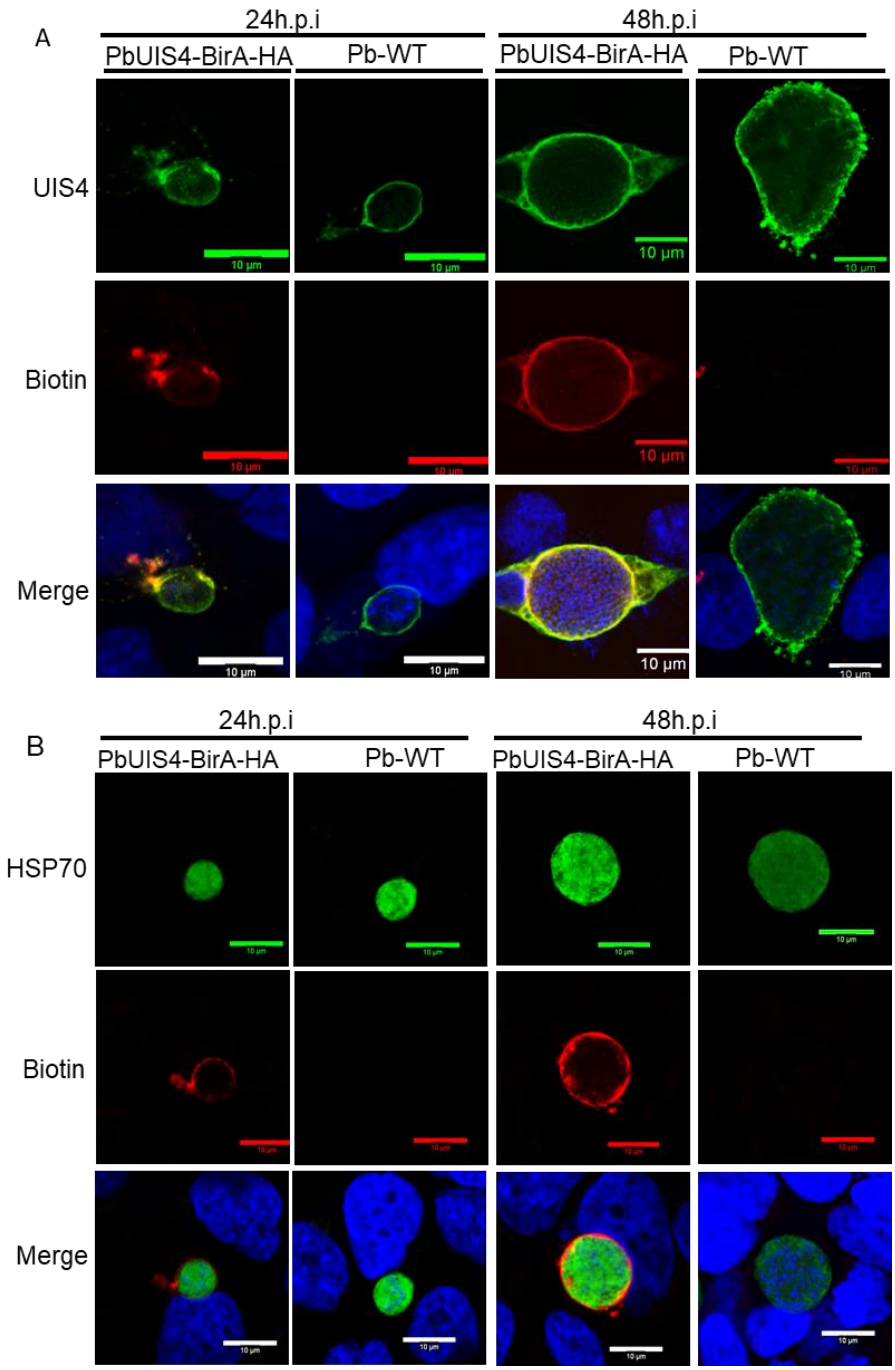


Figure 27. **PbUIS4-BirA*-HA biotinylates proteins at PVM surface**. Huh7 cells were infected with Pb-WT or PbUIS4-BirA*-HA and supplemented with 50uM of biotin at 2h.p.i for fixation at 24h.p.i. or 24h for fixation at 48 h.p.i. A) Infected cells were stained with UIS4 antibody 488, streptavidin 568 and DAPI 405. B) Infected cells were stained with of HPS70 antibody 488, streptavidin 568 and DAPI 405

However, biotin is a vitamin (vitamin B7) and plays a vital role in cell growth and protein synthesis. And recently it has been demonstrated that biotin is critical for *Plasmodium* development (Dellibovi-Ragheb et al., 2018), thus we sought to evaluate whether supplementation with biotin affects the development of the parasite. To that end, PbUIS4-BirA*-HA and WT parasites were grown in medium supplemented or not with biotin for 48h. The quantification (size measurement) shows that although the biotinylation event occurs in the presence of PbUIS4-BirA*-HA expression, it does not affect parasite development at the analyzed time point (Figure 28).

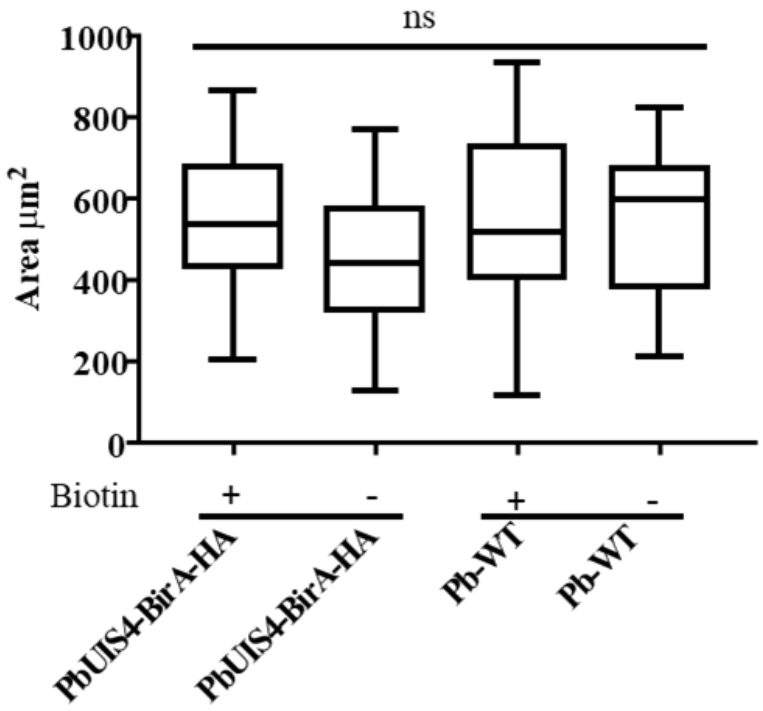


Figure 28. **Biotin supplementation does not influence parasite development**. Huh 7-hepatoma cell line cultured on coverslips were infected with PbUIS4-BirA*-HA or wild-type parental line. At 24 h.p.i, cells were supplemented with or without biotin for 24h, followed by fixation and stained with anti-UIS4, streptavidin and Hoechst. Parasite size was measured using UIS4 staining contour.

## III.3.b. Quantification of biotin positive parasites

Since the goal of this study is to find putative new proteins near PbUIS4, it is necessary to determine if the biotinylation radius is limited to PVM, and how long the process of biotinylation remains active.

For this reason, the timing and extent of biotinylation on the PVM were assessed. For that, a time course with biotin supplementation was performed between 24–55 h.p.i. As previously described, a high biotinylation rate occurred during 24 to 36h post biotin supplementation and was restricted to the PVM. Incubation for more than the period mentioned above leads to biotinylation inside parasite cytosol, as shown in Figure 29-A and Figure 29-B.

It is important to emphasize that for all time points analyzed, biotin was incubated for 22–24h, as shown in Figure 29-C.

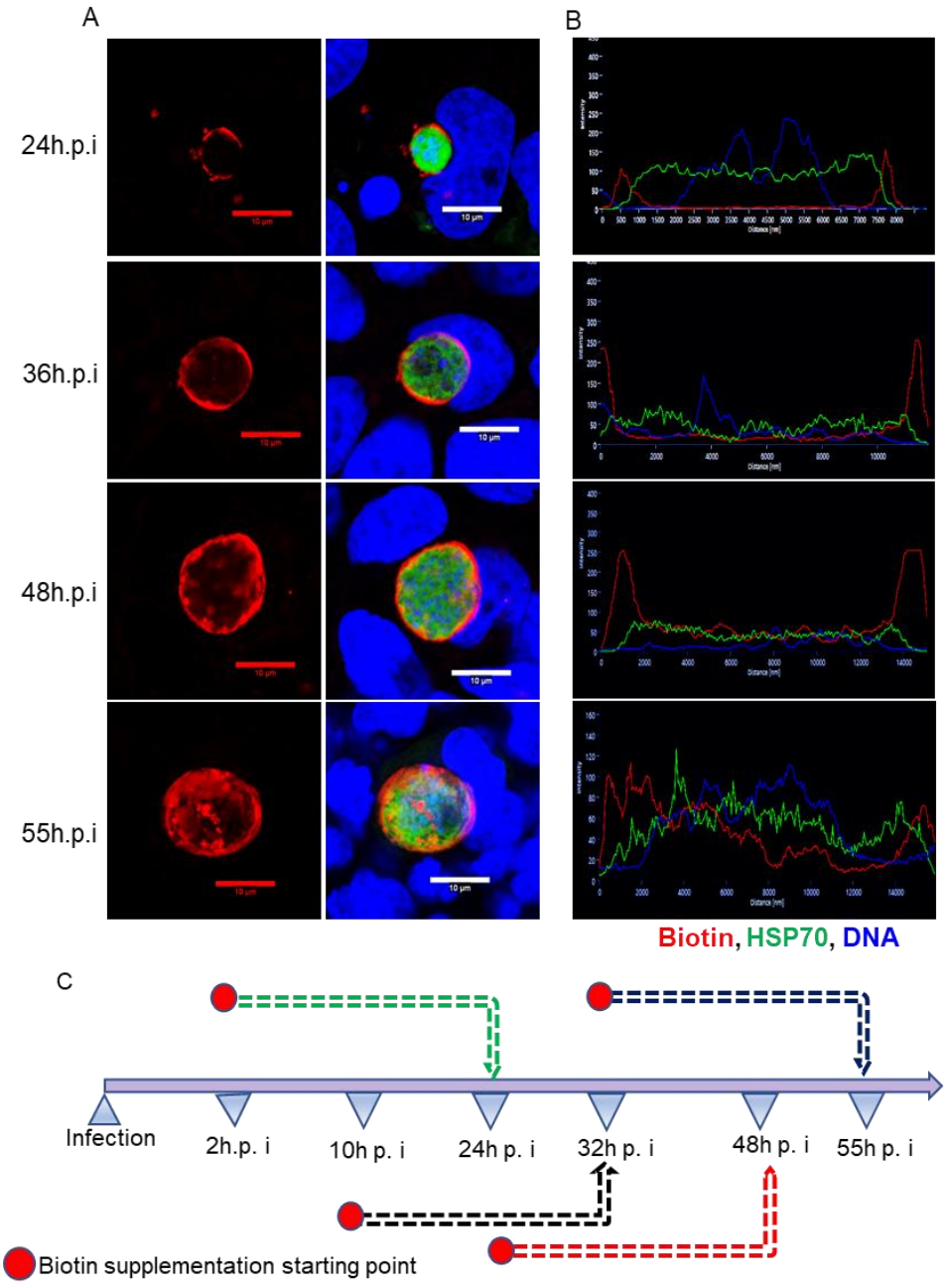


Figure 29. **Spatiotemporal analysis of biotinylation by PbUIS4-BirA*-HA.** A) Huh7 cells were infected with PbUIS4-BirA*-HA and supplemented with 50uM of biotin for 22h, and fixed at different time points. Next, the sample was stained with HPS70 antibody 488, streptavidin 568 and DAPI 405. B) Cross section and quantification of biotin fluorescence intensity was done next. C) Set up of biotin supplementation: Infected cells were supplemented with biotin at 2 h.p.i for the time point at 24 h.p.i and 10 h.p.i for time point taken at 32 h.p.i, for time points of 48 h.p.i and 55 h.p.i, the supplementation was made at 24 h.p.i and 32 h.p.i, respectively.

The pulldown using streptavidin-coated beads was performed against proteins marked with biotin. The Western blot results show that the PbUIS4-BirA*-HA fusion protein is immunoprecipitated with biotin in cells infected with parasites expressing BirA*. That is a good validation for the pull-down because BirA* is self-biotinylated (Figure 30).

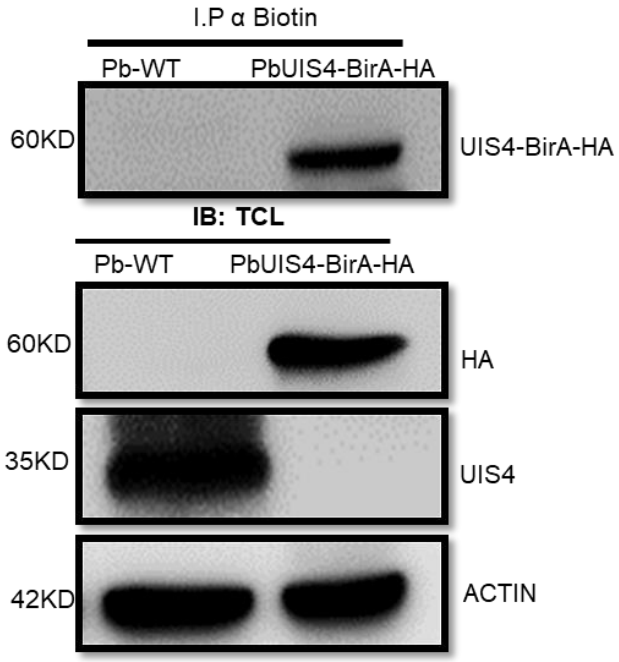


Figure 30. **Western blot analysis of samples obtained by streptavidin pull-down**. Extract from PbUIS4-BirA*-HA as well as Pb-WT infected cells were transferred to a nitrocellulose membrane after separation on SDS-PAGE. The membrane was blocked with 5%BSA, prior probing with anti-HA actin and anti-UIS4 antibodies.

## III.4. Identification of the PbUIS4-BirA*-HA vicinal proteins

The initial PbUIS4-BirA*-HA transgenic parasite line was generated in the P. *berghei* ANKA WT genetic background. All the validation experiments were performed using this cell line. However, a high background was observed when total biotinylated proteins were pulled down and analyzed with Western blot, making it difficult to distinguish between the protein samples obtained with PbUIS4-BirA*-HA and the parental WT line (Figure 31).

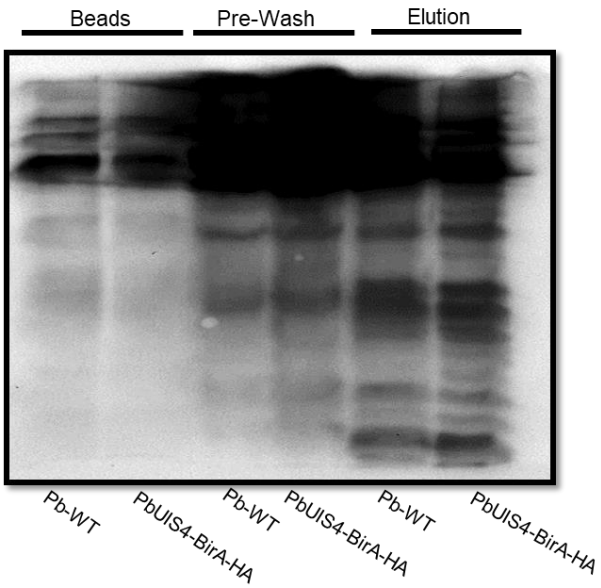


Figure 31. **Biotinylated proteins from PbUIS4-BirA*-HA non-fluorescent background and wild-type parental line**. Infected cells supplemented with 50nM of biotin at 2 h p I for 22-24h and lysed at 24 h.p.i. Following the NP-40 lysis, biotinylated proteins were pulled down with streptavidin-coated beads from the supernatant. The obtained the pulldown, the sample was separated on SDS-PAGE, and after transferring to a nitrocellulose membrane, probed with streptavidin-HRP conjugate

To overcome this issue, new PbUIS4-BirA*-HA transgenic parasite was created from *P. berghei ANKA* constitutively expressing Green Fluorescence Protein (GFP) in the cytosol, hereafter called PbGFP-UIS4-BirA*-HA (Tewari et al., 2010). Due to its fluorescence, this parasite line allows for the infected and non-infected hepatoma cells to be sorted using Fluorescence Activated Cell Sorting (FACS) flow cytometry.

Before performing the large-scale experiment to find the PbUIS4-BirA*-HA neighboring proteins, a small-scale infection with PbUIS4-BirA*-HA plus wild-type parental line was carried out. The pull-down of biotinylated proteins was performed using sorted cell populations, which minimizes the background noise. As expected, while some protein bands were observed in both extracts (since some proteins are endogenously biotinylated), PbFGP-UIS4-BirA*-HA extract showed more bands, suggesting it carries more biotinylated proteins than the control (Figure 32-A).

In contrast to PbUIS4-BirA*-HA non-fluorescent parasite, a clear difference in the amount of biotinylated proteins is observed between PbGFP-UIS4-BirA*-HA and wild-type parasites. The strong signal of 60 KDa is likely the UIS4-BirA*-HA fusion protein. To better visualize proteins under 60 KDa, we doubled the amount of protein loaded (Figure 32-B).

The same experiments previously performed to validate the non-fluorescent PbUIS4-BirA*-HA parasite were then done for the new fluorescent PbGFP-UIS4-BirA*-HA parasite line.

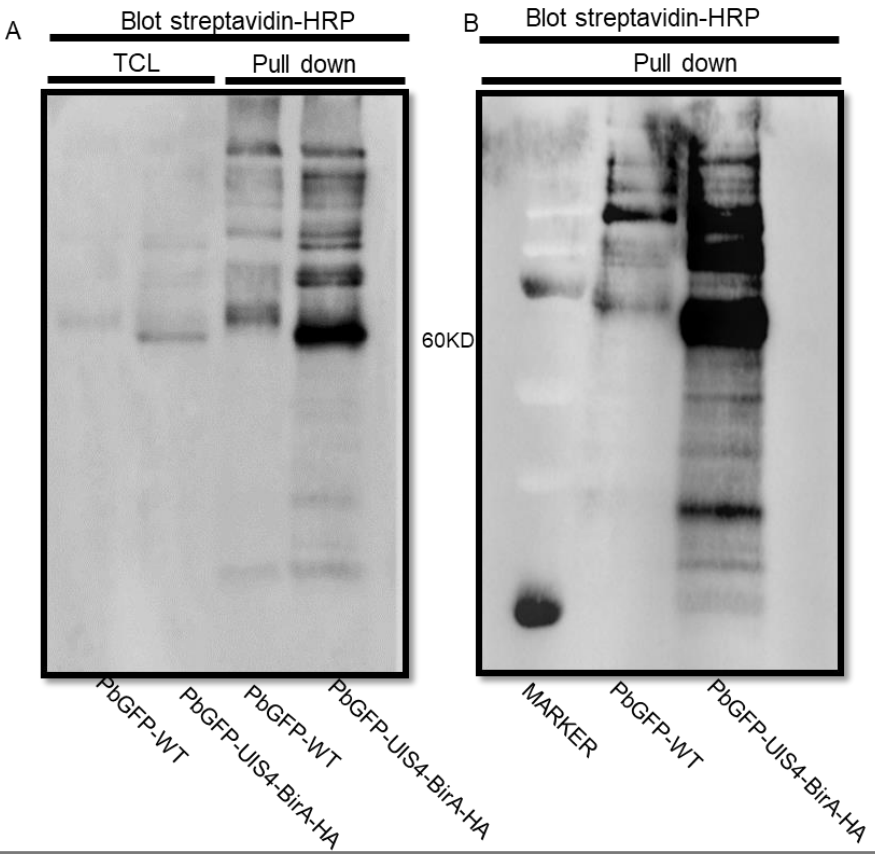


Figure 32. **Immuno-blot of biotinylated proteins from infected cells with PbGFP-UIS4-BirA*-HA or PbGFP-WT.** Cells infected with PbGFP-UIS4-BirA*-HA or PbGFP-WT, were sorted at 6 h.p.i. and reseeded for 16-18 h incubation prior to supplementation with 50nM of biotin for 22-24h long and lysed at 48 h.p.i. Following the NP-40 lysis, biotinylated proteins were pulled down with streptavidin coated beads from the supernatant. 50% of the obtained (32-A) or all (32-B) of the pulldown sample were separated on SDS page gel, and then transferred to a nitrocellulose membrane and probed with streptavidin-HRP conjugate.

Biotinylated proteins were identified through a large-scale infection experiment, with 4.2 million Huh7 hepatoma cells per condition, and infected with the same number of PbGFP-UIS4-BirA*-HA or PbGFP-WT sporozoites. As above, cells were sorted at 6–8 h.p.i. and reseeded. Biotin supplementation was done at 16–18 h.p.i. and kept for 24 hours. The infected cells were then lysed at 48 h.p.i. and used for streptavidin pull-down.

The samples were then separated on SDS-PAGE, and silver staining was performed to visualize the proteins. Unlike the extract from WT parasites, extracts from PbGFP-UIS4-BirA*-HA shows enrichment of several different bands (Figure 33). These protein bands were then excised from the gel and analyzed by mass spectrometry.

Even though there was no visual band in the negative control at the size of 60 KDa, the gel was excised at the corresponding area for additional analysis to confirm the total absence of protein.

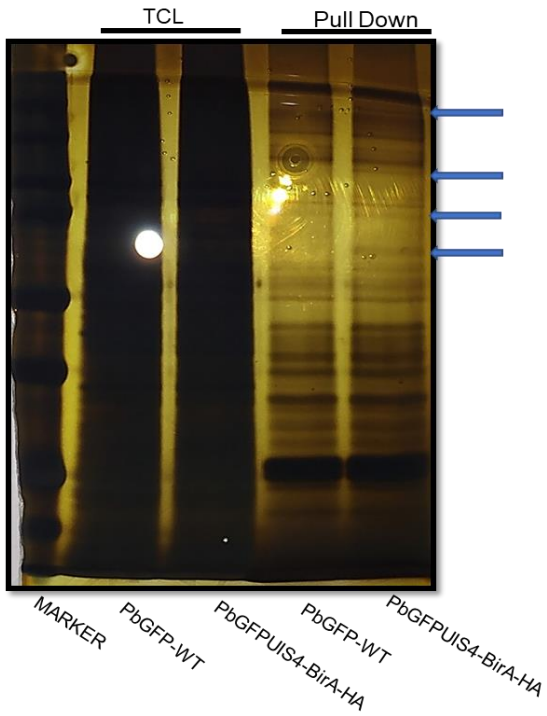


Figure 33. **Silver Stain gel**. Extract from PbGFP-UIS4-BirA*-HA or PbGFP-WT Extract from PbGFP-UIS4-BirA*-HA or PbGFP-WT infected cells were incubated with streptavidin-conjugated beads and incubated overnight followed by several washing procedures and subsequent elution. Silver staining was performed after separation on SDS PAGE. The arrows indicate the bands that are present on PBGFP-UIS4-BirA*-HA and absent in the wild-type parental line

## III.4.a. Mass spectrometry results

The protein excised bands were distained, reduced, alkylated, and digested with trypsin followed by resuspension of the peptides. Peptides were analyzed using Nano-liquid chromatography-tandem mass spectrometry (nanoLC-MS/MS). The 50 most intense precursors were selected for subsequent analysis. A search was performed against the SwissProt protein database with taxonomic restriction, for *Homo sapiens* and *Plasmodium.*

Only those proteins with Protein Score above 1.3 and 95% confidence were considered. All the proteins identified in the PbGFP-WT were considered as background and subtracted from proteins identified in the PbGFP-UIS4-BirA*-HA-expressing parasite (Table 6 and Table 7).

Table 6. *Plasmodium* protein identified from PbGFP-UIS4-BirA*-HA-expressing parasite

| Accession | Name |
|---|---|
| PBANKA_1003000 | Liver specific protein 2 OS=*Plasmodium berghei* |
| W7JIE6_PLAFA | Uncharacterized protein OS=*Plasmodium* falciparum UGT5.1 |
| PBANKA_0700900 | Reticulocyte-binding protein, putative *Plasmodium chabaudi* |
| PBANKA_0903500 | ABC transporter B family member 3, putative |
| Q86QI8_PLABE | REVERSED 31 KDa antigen |

Table 7. Host proteins identified from PbGFP-UIS4-BirA*-HA-expressing parasite

| Accession | Name |
|---|---|
| Q96RQ3\|MCCA | Methylcrotonoyl-CoA carboxylase subunit alpha, mitochondrial OS=Homo sapiens |
| Q96PG2\|M4A10 | Membrane-spanning 4-domains subfamily A member 10 OS=Homo sapiens |
| Q8IZ69\|TRM2A | REVERSED tRNA (uracil-5-)-methyltransferase homolog A OS=Homo sapiens |
| Q9UHX1\|PUF60 | Poly(U)-binding-splicing factor PUF60 OS=Homo sapiens |
| Q9HD23\|MRS2 | Magnesium transporter MRS2 homolog, mitochondrial OS=Homo sapiens |
| Q8IY33\|MILK2 | MICAL-like protein 2 OS=Homo sapiens |
| Q8IWA0\|WDR75 | WD repeat-containing protein 75 OS=Homo sapiens |

After all validations, five Plasmodium proteins were found to be specific to PbGFP-UIS4-BirA*-HA, and one protein was considered specific to PbGFP-WT. However, three Plasmodium proteins were likely to be nonspecific binders, since they were identified in PbGFP-WT and PbGFP-UIS4-BirA*-HA samples (Figure 34-A).

A total of six proteins unique to PbGFP-UIS4-BirA*-HA transgenic parasite, and 12 unique to the wild-type parasite were found. Six nonspecific binders were found (Figure 34-B).

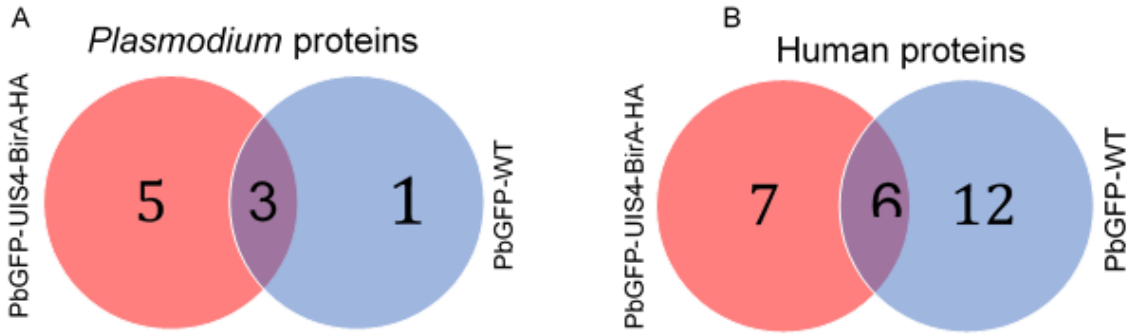


Figure 34. **Identified proteins from PbGFP-WT and PbGFP-UIS4-BirA*-HA**. A) Number of specific *Plasmodium* proteins for each parasite, and the number of shared nonspecific proteins. B) Number of specific and nonspecific human proteins in each parasite.

## In summary:

The generation of Pb-UIS4-BirA*-HA-expressing parasite was successfully performed. Fusion of the BirA* protein with the C-terminus of the UIS4 does not interfere with the function of the latter. Thus, the development of the transgenic parasite during infection was similar to that of the WT, *in vitro*. Although the PbUIS4-BirA*-HA fusion protein is twice the size of the native UIS4, we observed no issues related to folding and exporting of the former, as showed by UIS4 and HA colocalization by IFA. The same was observed *in vivo*, as shown by mice injected either with transgenic or WT parasites. BirA*-HA is correctly expressed and it biotinylates proteins on the PVM at 24h post biotin supplementation. However, exposure to biotin for more than 24h leads to biotinylation of proteins that are not on the PVM, which may result in biotinylation of spurious proteins. Biotin supplementation did not affect parasite growth at the time points analysed.

Identification of proteins biotinylated by UIS4-BirA*-HA was greatly improved by expression of UIS4-BirA*-HA in the fluorescent GFP-expressing *P. berghei* parasites.

Mass spectroscopy analysis identified several *Plasmodium* proteins as well as the host with high protein score. Nonetheless, high keratin contamination was observed, which may be what led to the identification of many proteins with low signal. It is also possible that these proteins are expressed in low abundance.

## III.5. Materials and Methods

### Designing the BioID-expressing transfection vector

### Plasmids

BirA*-HA was amplified from pcDNA3.1 MCS-BirA*(R118G)-HA (Addgene) plasmid using the following primers: AAGGGCCCTTAAGGCCTGTTAACCGGTCGTAC-forward primer and TTGCGGCCGCCTATGCGTAATCCGGTACATCGTAAG-reverse primer. BirA*-HA was fused at the C-terminus of the gene coding for the UIS4 protein by single crossover integration. Approximately 800bp of UIS4 gene sequence was cloned in frame with the BirA*-HA coding sequence, which generated the UIS4-BirA*-HA fusion protein upon integration into the UIS4 locus via a single cross-over recombination and generation of the transgenic parasites. The plasmid linearization was made through the EcorV restriction site introduced by direct mutagenesis with the following primers: GACTAGTGGATCCGAGCTCGGTTCCAAGCTTAAGTTTAAACCG-forward primer and CGGTTTAAACTTAAGCTTGGAACCGAGCTCGGATCCACTAGTC reverse primer.

The transfection plasmid held the DHFR-resistance cassette, providing the transfected parasites resistance to pyrimethamine.

### Generation of a transgenic parasite line expressing stable BioID fusion protein

*P. berghei* transfection was performed using a standard protocol (Janse et al., 2006). First, the mouse was infected with wild-type *P. berghei* ANKA parasites and the infected blood with approximately 1-3% parasitemia was incubated overnight in culture to produce schizonts for transfection. Mature schizonts were collected from the Nycodenz gradient and then electroporated in the presence of the transfection plasmid previously generated using the Amaxa electroporation system. After schizonts transfection, the solution (containing transfected merozoites) was injected into a tail vein of a mouse under anesthesia. The transformed parasites were selected by injecting 100 µg of pyrimethamine 30 h.p.i., which allowed the survival of the transgenic parasites only.

Transformed parasites were then genotyped using the following primers:

CTTTCAGCACATAATTATTACGTCTG-forward primer

CATAAAACAATTTGTTCTCTTTCTGAATTAC- reverse primer, for amplification of the wild-type UIS4 locus.

For integration detection, the following primers were used:

CTTTCAGCACATAATTATTACGTCTG-forward primer

TTGCGGCCGCCTATGCGTAATCCGGTACATCGTAAG- reverse primer.

For PCR control, UIS4-ORF locus was targeted using the following primers:

AAGGTACCCCACATACGTTTCTCTATTTTTTATC-forward primer and

TTGGGCCCTATGTATGGGCCGAATGATTT-reverse primer.

Cloning of transgenic parasites was performed by injecting 1-2 transgenic parasites per mouse, to obtain a genetically homogenous transgenic parasite line.

**Phenotype Validation of the transgenic parasites expressing PbUIS4-BirA*-HA Fusion Protein**

The validation experiments were performed to ensure that the fusion protein had the correct size (Western blot after migration by SDS-PAGE) and localized correctly (immunofluorescence microscopy). Also, transgenic parasites were investigated phenotypically (parasite growth) and compared to the wild-type parasites, to ensure that the BirA*-HA fusion was not interfering with the function of UIS4.

**Cell infection and BioID pull-down**

**Sporozoites purification**

The sporozoites production was achieved through mosquitoes infected by blood feeding on mice infected with blood stage transgenic parasites, more specifically the parasite clone selected as described above. Infected mosquitoes were dissected after 21-35 d.p.i. Sporozoites expressing UIS4-BirA*-HA was collected from the salivary glands of dissected mosquitoes.

**Liver-stage infection**

To set up the liver-stage infection *in vitro*, hepatoma cell lines (Huh7) were infected by direct exposure to the sporozoites collected from the salivary glands of the infected

mosquitoes. Cells were incubated at 37ºC with 5% $CO_2$. The culture medium was replaced after 2 h.p.i. with fresh medium containing fungizone.

**Biotin**

1mM biotin (Sigma B4501) stock solution was prepared in serum-free RPMI culture medium. The Solution was sterilized by passing through a 0.22-µm syringe-driven filter unit and stored at -20°C.

**BioID protein labelling**

To label the proteins in the PbUIS4 proximity, the infected cells were supplemented with 50 µM biotin (final concentration) and incubated for 22-24 h.p.i., before undergoing lysis (for blotting experiments) or fixation (for IFA analysis).

**Immunofluorescence**

Huh7 hepatoma cells were seeded on coverslips one day before infection. At the desired time point, cells were fixed with 4% of paraformaldehyde (paraformaldehyde solution 4% in PBS - Santa Cruz Biotechnology Cat: sc-281692:) and permeabilized with a solution containing 2% BSA (Albumin Bovine, Fraction V, Nzytech Cat: MB 04602) and 0.2% saponin on PBS. To detect the fusion protein, goat anti-UIS4 from SICGEN (Ref: AB0042-500), Alexa Fluor® 488 anti-HA.11 Epitope Tag Antibody for HA detection from: (BioLegend, Cat: 901509). Biotinylated proteins were detected using streptavidin Alexa flour 568 (Streptavidin, Alexa Fluor™ 568 conjugate, Thermo Fisher, Cat: S11226). Samples images were captured using Zeiss LSM710 confocal point-scanning microscope

**Capture of biotinylated proteins**

Hepatoma cell lines were infected either with Pb-GFP-UIS4-BirA*-HA or wild-type parental line with 1:1 infection ratio and sorted at 6-8 h.p.i.

Sorted cells were reseeded in complete media supplemented with fungizone, Pen-strep and gentamycin for 24h p.i. The medium was supplemented with 50 µM biotin for 24h. After 3x PBS washes, cells were lysed at 25°C in 1 ml lysis buffer (50 mM Tris, pH 7.4, 500 mM NaCl, 0.4% SDS; 5 mM EDTA; 1 mM DTT; 1x Complete protease inhibitor, 2%,

Phenylmethylsulfonyl fluoride (PMSF) 1mM and Triton X-100 added prior to lysis) directly on the plate and sonicated after the harvester. All these procedures were performed at 25°C.

Lysing cells were centrifuged at 4°C for 20 minutes at 16,000rpm. The supernatant was incubated with 200µl of Dynabeads (Invitrogen, MyOne Streptavidin C1, for overnight with agitation. Beads were collected with the magnetic rack and washed 2x for 8 min at 25°C in 1 ml wash buffer 1 (**:** 2% SDS (w/v). The same procedure was repeated once with wash buffer 2, (0.1% (w/v) deoxycholic acid**;** 1% (w/v) Triton X-100; 1 mM EDTA; 500 mM NaCl; 50 mM HEPES, pH 7.5) 1x wash buffer 3 ( 0.5% (w/v) deoxycholic acid, 0.5% (w/v) NP-40, 1 mM EDTA, 250 mM LiCl, 10 mM Tris·Cl, pH 8.1) and 2x with wash buffer 4 (50 mM Tris, pH 7.4; 50 mM NaCl ). For mass spectrometry analysis, two additional washes were performed with 50mM ammonium bicarbonate ($NH_4HCO_3$).

Bound proteins were eluted from the beads with 50µl of SDS-sample buffer at 98°C for 10 min.

**Wash procedure**

A total of 500µL of wash buffer were added to beads and mixed with cut tip. The tube was placed on the bar magnet rack and left until the liquid was clear and then removed. This procedure was repeated 2x with wash buffer1, 1x with wash buffer 2, 1x with wash buffer 3 and 4.

**BSA blocking buffer:** 2.5% bovine serum albumin, fraction V**,** 0.2% (w/v) Triton X-100**.**

**Western blot:** Proteins were separated on 5% stacking gel (30% Acrylamide, 1M Tris-HCl, 10% SDS, 10% APS, TEMED) and 10% SDS PAGE resolving gel (30% Acrylamide, 1.5M Tris-HCl, 10% SDS, 10% APS, TEMED), and transferred into Nitrocellulose Membrane. To detect PbUIS4-BirA*-HA, the membrane was blocked with TBS with 5% of BSA and 0.2% Tween20 for 1hour at room temperature, and probe with goat anti-UIS4 1:1000 or with rabbit anti-HA (Sigma REF. P9795) at 4ºC for overnight with rotation and washed three times with PBST 0.2%, subsequently probed with rabbit anti-goat HRP conjugated 1:10000 (Invitrogen REF: 81-1620). The actin detection was performed by probing the membrane with rabbit anti-actin 1:1000 (Sigma, REF: A2066) overnight, following the

incubation with goat anti-rabbit HRP conjugated 1:10000 (Cell Signaling, (C29F4) REF: 3724)) for HA detection.

Biotinylated protein detection was done as described above, however with the following modifications: the membrane was blocked with 5% BSA in 1X PBS with 0.4% Triton X-100 for 1 hour at room temperature subsequently probed with streptavidin-HRP (Cell Signaling P22629, REF:3999S) conjugated diluted 1:40000 into blocking buffer.

**Silver stain**

The Silver Stain was performed, following the protocol from the Thermo Scientific Silver Stain Kit (Prod # 24612), and PROTSIL from Sigma (PROTSIL1-1KT).

After protein separation on SDS-PAGE 10%, the gel was washed 2X for 5 minutes in ultrapure water. Fixation was done for 15 minutes in a solution containing 30% ethanol and 10% acetic acid.

Following the fixation, the gel was washed 10 minutes in 30% ethanol, then 2 × 5 minutes in ultrapure water. The gel was sensitized for 10 minutes, then washed 2X 10 minutes with water.

After sensitization, the gel was stained with silver stain solution gel for 30 minutes.

The gel was developed in a developer solution after washing for 1.5 minutes. Development was ended after reaching the desired band intensity with 5% acetic acid or stopping solution for 10 minutes.

**Mass spectrometry analysis**

Nano-liquid chromatography-tandem mass spectrometry (nanoLC-MS/MS) analysis was performed on an ekspert™ NanoLC 425 cHiPLC® system coupled with a TripleTOF® 6600 with a NanoSpray® III source (Sciex). Peptides were resuspended in 0.1% formic acid in water (Fisher Chemicals, Geel, Belgium) and separated through reversed-phase chromatography (RP-LC) in a trap-and-elute mode. Trapping was performed at 2 µl/min with 100% A (0.1% formic acid in water, Fisher Chemicals, Geel, Belgium), for 10 min, on a Nano cHiPLC Trap column (Sciex 200 µm x 0.5 mm, ChromXP C18-CL, 3 µm, 120

Å). Separation was performed at 300 nl/min (90 min gradient), on a Nano cHiPLC column (Sciex 75 µm x 15 cm, ChromXP C18-CL, 3 µm, 120 Å).

Peptides were sprayed into the MS through an uncoated fused-silica PicoTip™ emitter (360 µm O.D., 20 µm I.D., 10 ± 1.0 µm tip I.D., New Objective, Oullins, France). The source parameters were set as follows: 15 GS1, 0 GS2, 30 CUR, 2.5 keV ISVF and 100 $^{0}$C IHT. An information dependent acquisition (IDA) method was set with a TOF-MS survey scan of 400-2000 m/z. The 50 most intense precursors were selected for subsequent fragmentation, and the MS/MS were acquired in high sensitivity mode. The obtained spectra were processed and analyzed using ProteinPilot™ software, with the Paragon search engine (version 5.0, Sciex). The search was performed against Swissprot protein database (version 2015_05) with taxonomic restriction to Homo sapiens and *Plasmodium*. Trypsin was selected as digestion type; Iodoacetamide was chosen as the source of Cys alkylation, gel-based ID was selected as a special factor (only when analyzing the gel bands) and the TripleTOF 6600 as the Instrument. The ID focus was on biological modifications and amino acid substitutions. The search effort was set as thorough. Only the proteins with Unused Protein Score above 1.3 and 95% confidence were considered.

# CHAPTER IV- GENERAL DISCUSSION

## GENERAL DISCUSSION

Known since remote times, *Plasmodium* has been co-evolving with humans. Its adaptation to the human host strongly supports that the two species have been living very closely and some studies even suggest that malaria has had a critical role in shaping some aspects of the human genome (Kwiatkowski, 2005). Throughout evolution, these two species have been in a tug-of-war in which the parasite develops new strategies for a successful infection and survival during different stages of the disease, while the human species develops ways to protect itself.

Malaria infects around 5% of the global population. Africa is still the most affected continent. Since the launching of the malaria elimination program, deaths due to malaria have decreased significantly (White, 2014). We as a species may feel victorious and believe we are winning the fight against the disease. However, we should be cautious to not celebrate before the battle is really over, as we still may see a turning point in which the parasite develops new strategies or acquires resistance that threatens our efforts, as has happened in the past. Figure 35 shows the number of deaths per hour for malaria in the past 20 years. Note that this number has been decreasing significantly in the last 15 years.

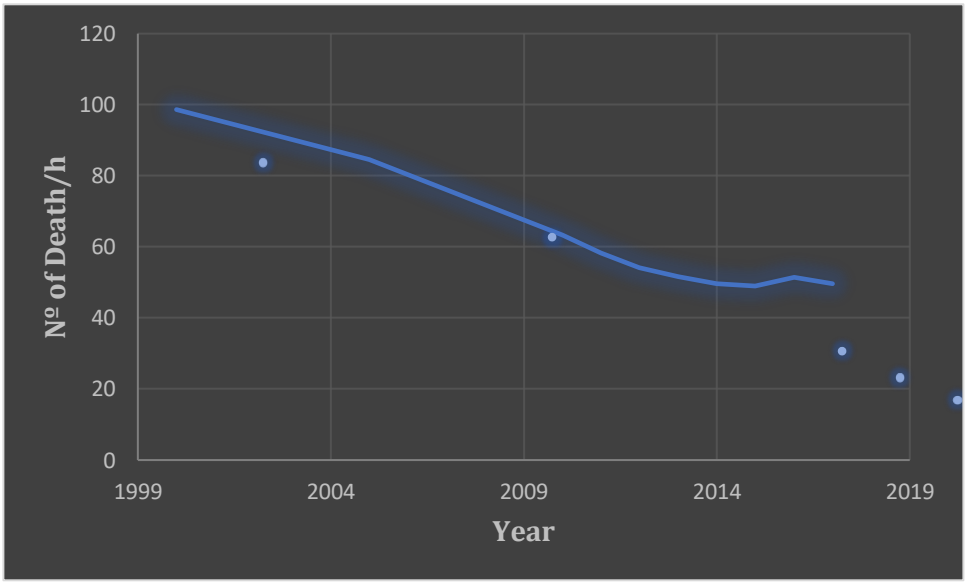


Figure 35. Number of death due to malaria per hour from 1999 to 2018

The two main human-infecting *Plasmodium* species occur in regions that are geographically distinct. While *P. falciparum* is limited to Africa and is characterized by causing cerebral malaria, *P. vivax* is widespread in the Indo-Pacific and South-West Asia and is known for its ability to develop dormant forms of the parasite that are responsible for disease relapses occurring many years after the initial infection took place.

It is known that in Africa many populations have evolved resistance mechanisms against P. *vivax*, but malaria by *P. vivax* still occurs in Ethiopia and Madagascar. How can we explain the occurrence of malaria caused by *P. vivax* in these two countries?

The liver stage of *Plasmodium* infection represents the first obligate step of the malaria parasite life cycle within the vertebrate host. During this stage, tens of sporozoites are injected by mosquitoes during an infective blood meal. However, at the end of the parasite liver-stage development, each sporozoite generates tens of thousands of red blood cell–infectious merozoites, which trigger the disease. Nonetheless, despite being an essential step for the onset of malaria, the liver stage of infection remains the most uncharacterized developmental stage of the *Plasmodium* life cycle in humans.

*Plasmodium* development in hepatocytes occurs inside the parasitophorous vacuole, which is set apart from the host cell cytosol by the PVM, which may offer a hiding spot for the parasite to escape the host immune response. PVM is a specialized compartment with highly selective permeability that allows only molecules of 856 Daltons or lower. That raises a question of how large particles from the host cytosol reach the parasite, and vice versa. Are there specific transporters or vesicles to transport large molecules? Or perhaps large molecules are fused with the membrane of the PV?

Nevertheless, *Plasmodium* parasites must deal with the intracellular anti-pathogen defense machinery, such as the ubiquitin system, autophagy, and other cell defense systems. Given their survival and fast multiplication rate within hepatocytes, we can say that *Plasmodium* parasites have evolved efficient mechanisms to avoid the host's diverse intracellular anti-pathogen defense mechanisms. Nevertheless, little is known about the molecular components of such mechanisms.

Several parasite proteins are exported to the PVM. Among these there are members of a set of 35 proteins named Upregulated in Infectious Sporozoite (UIS). While two of these proteins have been characterized, and their biologic function uncovered – UIS3 is an autophagy inhibitor that acts by binding the host LC3 and thereby promoting parasite survival (Real et al., 2017) whereas UIS2 is a phosphatase (Zhang et al., 2016) – the vast majority of these proteins still have unknown biological function. Among them is UIS4, which is known to be necessary for parasite survival during the liver stage, but whose biological function remains to be established. One of the objectives of the present work was to unveil the role of this protein during the liver stage of *Plasmodium* infection.

Due to its unique structure and lack of structural homology with the proteins known from other species, the prediction of UIS4's role is difficult. Thus, this study sought to investigate the function of UIS4 by finding its potential interactors, using a classical immunoprecipitation approach.

Surprisingly, our findings show that UIS4 interacts with the host actin. This interaction is mediated by the soluble domain of UIS4, including amino acids 121 to 220, which is the domain that faces the host cell cytosol. However, it is still not known which specific amino acid residues are responsible for this interaction.

Interestingly, previous findings have reported high actin reorganization around *P. berghei* during its development inside hepatoma cells (Gomes-Santos et al., 2012). While the authors have made a correlation between significant dynamic actin organization around the parasite and its own disappearance, whether this event relies on a coordinated mechanism or is in fact an isolated event remains unclear. However, it is known that actin is implicated in one of the cell's self-defense mechanisms, autophagy. Thus, the possibility that this event is part of a coordinated process cannot be ruled out.

On the other hand, it has recently been shown that the recruitment of lysosome around the parasite highly depends on UIS4 being at the PVM, but details about the mechanism of this process are not yet known (Petersen et al., 2017). Lysosomes are one of the key players in the autophagy machinery, which is one of the mechanisms used by the host cell

to eliminate the pathogen (Real et al., 2017). However, it should be noted that host cell lysosomes do not fuse with PVM (Lopes da Silva et al., 2012).

Moreover, our most recent and still preliminary data suggest a role for UIS4 in actin polymerization dynamics, as initial results of ongoing experiments show that UIS4 promotes actin polymerization *in vitro*.

Nevertheless, it is not expected for the parasite to promote actin polymerization close to the PVM if this may cause its elimination. Does this elimination involve the host cell autophagy machinery?

How to make sense of all these findings? The accumulation of lysosomes around the parasite can also be considered as related to the host cell's autophagy machinery and actin polymerization around the PVM, as this vesicle needs actin cables to move short distances (Kast and Dominguez, 2017). It should be noted that actin has also been implicated in autophagy (J. Y. Lee et al., 2010). Alternatively, it could be a simple nutrient-scavenging mechanism to feed the parasite through UIS4.

Indeed, *Plasmodium* has been proposed to explore the host late endocytic pathway (Lopes da Silva et al., 2012), possibly scavenging nutrients from host vesicles. It is thus appealing to speculate that the parasite might induce actin polymerization through UIS4 to promote the transport of vesicles that are rich in nutrients such as cholesterol; without UIS4 these vesicles vanish. Indeed, sequestration of cholesterol within the late endocytic compartment has been shown to impact parasite development (Petersen et al., 2017). Thus, it is possible that the *Plasmodium* parasite could be blocking autophagy to protect itself and not risk being eliminated by the host cell, and while doing this it may take up the nutrients of these vesicles.

An ongoing *in vivo* experiment that aims to evaluate actin dynamics by live imaging and uses wild-type and PbANKA-UIS4-KO parasites, has shown so far that there are high frequencies of actin polymerization events around PbUIS4-KO parasites, compared to their wild-type counterparts. At first sight, this result seems to disagree with the results of the *in vitro* actin assay experiment mentioned above.

However, it is known that actin structures are highly dynamic – they assemble, grow, and disassemble in a time scale of a second to a minute ( Blanchoin, L. et al., 2014) – and that treadmilling implies a continuous equilibrium of polymerization/depolymerization events.

Taking this into account, it can be speculated that UIS4 polymerizes and maintains actin in the filamentous form, inhibiting the treadmilling events from taking place. This is an attractive hypothesis in which, by inducing actin polymerization, the parasite creates a barrier that restrains the lysosomes, which then accumulate around the PVM. It is known that lysosome fusion requires transient actin polymerization, while a robust actin polymerization impairs this event (Eitzen, 2003). In consequence, the polymerization events are less pronounced around WT parasites. and this dynamic is recovered in the UIS4-KO parasite.

Thus, even though these findings may seem contradictory at first sight, together they may help us build a fresh view of what occurs during development of the parasite in the liver stage.

However, the possibility that UIS4 is the defense mechanism or nutrient scavenging for the parasite cannot be ruled out.

To have the highest replicative rate among eukaryote organisms while up-taking nutrients from the host cell and successfully escaping elimination, truly requires tactical prowess. For *Plasmodium,* the parasitophorous vacuole seems to be the main player for its success.

The parasitophorous vacuole is a compartment located at the host–parasite interface, which acts as a shield, protecting the parasite while at the same time ensuring that the parasite acquires the nutrients it requires. It is a highly specialized and selective compartment, accomplishing a variety of tasks, from signaling and defense to nutrient uptake. All these roles are achieved through the molecules/proteins expressed on its surface, which may interact with other essential proteins in their vicinity. That justifies the need to uncover the molecular constituents of the PVM, either from the parasite or the host side.

To this end, the biotin proximity identification approach (BioID) was implemented. This approach differs from classical immunoprecipitation strategies since the proteins are labeled in their physiological environment. Proximity biotin identification is emerging as a suitable approach to identify proteins of the *Plasmodium* PVM. This approach has recently been successfully used to identify new *Plasmodium* blood-stage PVM proteins (Khosh-Naucke et al., 2017; Schnider et al., 2018).

In the present work, the promiscuous biotin enzyme BirA* was fused with UIS4, which ensures its expression on the PVM during the entire parasite development in the liver stage.

Although the size of the fusion protein is twice that of the native protein, which could disturb the folding and function of the latter, this problem was not observed. UIS4 is exported to the PVM immediately upon productive invasion by sporozoites.

Due to the low infection rate of hepatoma cells by *Plasmodium* (around 1%), the use of a BioID strategy during the liver stage of the parasite life cycle is a challenge that requires a very high amount of sporozoites (≈24 million per experiment) to obtain enough material for mass spectrometry analysis.

Biotinylation signal restricted to the PVM was observed in the initial 24 hours post biotin supplementation. However, if the supplementation was provided for more than 24h, the biotinylation signal appeared within the parasite cytosol. Whether these biotinylated proteins have been biotinylated at the cytosol or are recycled proteins from the PVM remains to be established.

Mass spectroscopy analysis of the biotinylated proteins (from the 24h supplementation experiment and therefore restricted to the PVM vicinity) led to the identification of three *Plasmodium* proteins with high score. These proteins could be in proximity of UIS4 on the PVM (most likely) or undergo a transient interaction.

(i) Liver-specific protein 2 (LISP2 - Liver-specific protein 2), which is expressed during the liver stage of infection and is critical for merozoite formation (Orito et al., 2013). The identification of these proteins represents a good control of the method. Although no

direct interaction of UIS4 and LISP2 had been reported, this possibility should not be laid aside.

(ii) Reticulocyte-binding protein (P235 - Reticulocyte-binding protein, putative), known to be expressed at the surface of merozoites, might constitute an off-target hit. There are two reasonable explanations for this hit: a) the timing when the cells were lysed could match the time when this protein started to be expressed; and b) the exact diffusion radius of biotinoyl-5'-AMP is unknown, and it could attain up to 20 nm of distance.

(iii) Uncharacterized protein, W7JIE6. It is predicted to belong as an integral component of the membrane, and possibly plays a role on the surface binding receptor of the host cell. Although predicted, the role and localization of W7JIE6 represent a high probability of being expressed on the PVM.

All the *Plasmodium* proteins identified in this study must be confirmed. Two other *Plasmodium* proteins were also identified with a low score. This is the case for putative ABC transporter B family member 3 (ABCB3 - ABC transporter B family member 3, putative), which does not play any known role in the blood stage (Rijpma et al., 2016). Its role during the liver stage has never been studied, and there are no data to confirm that ABCB3 is expressed during the liver stage of infection. ATP Binding Cassettes (ABCs) are membrane proteins that transport molecules across the membrane. This family of transporters are known for their role in drug resistance – they are also known as multidrug resistance (MDR) proteins – and were also identified in *Plasmodium* (Koenderink et al., 2010).

Besides *Plasmodium* proteins, seven human host proteins were also identified in this study. Nonetheless, a considerable amount of proteins was detected with a low signal, which could be due to high keratin contamination. It is also possible that these proteins have low expression.

The duration for biotinylation of BioID applied in this study is considerably lengthy. However, following the same approach of proximity identification, using an engineered enzyme, ascorbate peroxidase (APEX), biotinylation duration could be substantially

reduced (S. Y. Lee et al., 2016). Like BirA*, the APEX enzyme enables biotinylating the neighbor proteins in 1 minute, leading to increasing biotinylation specificity. Biotinylation checked in periods shorter than 24 hours may identify stage-specific proteomes of the parasite.

This is the first study to successfully apply BioID to search for additional proteins participating in the liver stage of *Plasmodium* in cultured hepatoma cell.

## CONCLUSION AND FUTURE PERSPECTIVES

## CONCLUSION AND FUTURE PERSPECTIVES

Vector-borne diseases constitute a set of illnesses that contribute to a high percentage of human morbidity and mortality worldwide, particularly in tropical regions. Significant efforts have been made to control various vector-borne diseases, with an emphasis on malaria. However, this infectious disease still claims nearly half a million lives every year, mostly in Sub-Saharan African countries. Several decades ago, malaria was present in most areas of the globe, except the earth's poles and deserts.

Massive campaigns to fight malaria, with a strong focus on vector control, led to the elimination of this disease from a large part of the world. Since then, the number of malaria-associated deaths has progressively decreased, thanks to the implementation of malaria vector control strategies in Africa and better case management in non-endemic regions. However, the good results obtained over several years in malaria control appear to have stalled, with a small increase in the estimated number of malaria-related deaths recently observed.

Despite the efficacy of other malaria control strategies, such as the use of effective treatments against the pathology-associated blood stage of infection, vector control remains the most effective strategy to combat this disease. Nonetheless, additional approaches are needed to enhance the efficacy of existing tools and develop other anti-malarial strategies.

Moreover, due to recent achievements in the fight against malaria, important challenges emerge such as the increasing resistance either of the *Plasmodium* parasites to anti-malarial drugs or of the insect vector to insecticides. Furthermore, climate change threatens to change vector behavior in areas where the disease was eradicated, potentially leading to the recrudescence of malaria in those areas.

Indeed, malaria elimination is facing challenges from three different levels:

- Technical challenges

A malaria-free world requires innovative tools and research at all stages, from basic to applied research.

- Political

When malaria burden finally reaches low levels, how to keep political and financial support, considering that this last step is decisive for malaria elimination?

- Societal

In a process that can take up to 20 years, how to keep the local community engaged and interested in achieving a common goal?

For all these reasons, new approaches are required to fight malaria, including not only the development of new anti-plasmodial drugs and insecticides but also innovative strategies that may stem from a deeper understanding of the biology of *Plasmodium* infection.

This work unveiled a novel interaction between the parasite UIS4 molecule and the host cell actin. However additional experiments are required to fully uncover the biological role of this interaction, such as the ongoing assessment of actin dynamics in parasite development during liver-stage infection. The available data suggest that UIS4 polymerizes actin on the PVM, leading to an inhibition of lysosome fusion and accumulation of these vesicles at the parasite surface.

The localization of the proteins identified by mass spectrometry requires validation, by IFA, either by employing antibodies, if available, or tagging those proteins with well-established tags such as HA tag (among others) if such antibodies are not available.

There is no doubt that the fight against malaria is a very complicated struggle and many complementary approaches will be needed to design a powerful malaria eradication campaign. Indeed, malaria-free world is more than disease or vector fight approach but rather poverty and lack information.

**Bibliography**

## Bibliography


Al-Nihmi, F. M. A., Kolli, S. K., Reddy, S. R., Mastan, B. S., Togiri, J., Maruthi, M., … Kumar, K. A. (2017). A Novel and Conserved Plasmodium Sporozoite Membrane Protein SPELD is Required for Maturation of Exo-erythrocytic Forms. *Scientific Reports*, *7*(December 2016), 1–14. https://doi.org/10.1038/srep40407

Aly, A. S. I., Vaughan, A. M., & Kappe, S. H. I. (2009). Malaria Parasite Development in the Mosquito and Infection of the Mammalian Host. *Annual Review of Microbiology*, *63*(1), 195–221. https://doi.org/10.1146/annurev.micro.091208.073403

Amaratunga, C., Lopera-Mesa, T. M., Brittain, N. J., Cholera, R., Arie, T., Fujioka, H., … Fairhurst, R. M. (2011). A role for fetal hemoglobin and maternal immune igg in infant resistance to plasmodium falciparum malaria. *PLoS ONE*, *6*(4), 1–9. https://doi.org/10.1371/journal.pone.0014798

Amino, R., Thiberge, S., Martin, B., Celli, S., Shorte, S., Frischknecht, F., & Ménard, R. (2006). Quantitative imaging of Plasmodium transmission from mosquito to mammal. *Nature Medicine*, *12*(2), 220–224. https://doi.org/10.1038/nm1350

Angrisano, F., Riglar, D. T., Sturm, A., Volz, J. C., Delves, M. J., Zuccala, E. S., … Baum, J. (2012). Spatial localisation of actin filaments across developmental stages of the malaria parasite. *PLoS ONE*, *7*(2). https://doi.org/10.1371/journal.pone.0032188

Antinori, S., Galimberti, L., Milazzo, L., & Corbellino, M. (2012). Biology of human malaria plasmodia including Plasmodium knowlesi. *Mediterranean Journal of Hematology and Infectious Diseases*, *4*(1). https://doi.org/10.4084/MJHID.2012.013

Arrow, K. J., Panosian, C., & Gelband, H. (2004). *Saving Lives, Buying Time: Economics of Malaria Drugs in an Age of Resistance*. *Institute of Medicine (US) Committee on the Economics of Antimalarial Drugs*. https://doi.org/ISBN-10: 0-309-09218-3

Auburn, S., Böhme, U., Steinbiss, S., Trimarsanto, H., Hostetler, J., Sanders, M., … Otto, T. D. (2016). A new Plasmodium vivax reference sequence with improved assembly of the subtelomeres reveals an abundance of pir genes. *Wellcome Open Research*, *1*(0), 4. https://doi.org/10.12688/wellcomeopenres.9876.1

Baer, K., Klotz, C., Kappe, S. H. I., Schnieder, T., & Frevert, U. (2007). Release of hepatic Plasmodium yoelii merozoites into the pulmonary microvasculature. *PLoS Pathogens*, *3*(11), 1651–1668. https://doi.org/10.1371/journal.ppat.0030171

Bano, N., Romano, J. D., Jayabalasingham, B., & Coppens, I. (2007). Cellular interactions of Plasmodium liver stage with its host mammalian cell. *International Journal for Parasitology*, *37*, 1329–1341. https://doi.org/10.1016/j.ijpara.2007.04.005

Baum, J., Chen, L., Healer, J., Lopaticki, S., Boyle, M., Triglia, T., … Cowman, A. F. (2009). Reticulocyte-binding protein homologue 5 - An essential adhesin involved in invasion of human erythrocytes by Plasmodium falciparum. *International Journal for Parasitology*, *39*(3), 371–380. https://doi.org/10.1016/j.ijpara.2008.10.006

Blanford, J. I., Blanford, S., Crane, R. G., Mann, M. E., Paaijmans, K. P., Schreiber, K. V., & Thomas, M. B. (2013). Implications of temperature variation for malaria parasite development across Africa. *Scientific Reports*, *3*, 1–11. https://doi.org/10.1038/srep01300

Bullen, H. E., Charnaud, S. C., Kalanon, M., Riglar, D. T., Dekiwadia, C., Kangwanrangsan, N., … Gilsona, P. R. (2012). Biosynthesis, localization, and macromolecular arrangement of the Plasmodium falciparum translocon of exported proteins (PTEX). *Journal of Biological Chemistry*, *287*(11), 7871–7884. https://doi.org/10.1074/jbc.M111.328591

Bunn, H. F. (2013). The triumph of good over evil: Protection by the sickle gene against malaria. *Blood*, *121*(1), 20–25. https://doi.org/10.1182/blood-2012-08-449397

Burda, P.-C., Caldelari, R., & Heussler, V. T. (2017). Manipulation of the Host Cell Membrane during *Plasmodium* Liver Stage Egress. *MBio*, *8*(2), e00139-17. https://doi.org/10.1128/mBio.00139-17

Burda, P. C., Roelli, M. A., Schaffner, M., Khan, S. M., Janse, C. J., & Heussler, V. T. (2015). A Plasmodium phospholipase is involved in disruption of the liver stage parasitophorous vacuole membrane. *PLoS Pathogens*, *11*(3), e1004760. https://doi.org/10.1371/journal.ppat.1004760

Cappellini, M. D., & Fiorelli, G. (2008). Glucose-6-phosphate dehydrogenase deficiency. *Lancet*, *371*(9606), 64–74. https://doi.org/10.1016/S0140-6736(08)60073-2

Carlton, J. M., Adams, J. H., Silva, J. C., Bidwell, S. L., Lorenzi, H., Caler, E., … Fraser-Liggett, C. M. (2008). Comparative genomics of the neglected human malaria parasite Plasmodium vivax. *Nature*, *455*(7214), 757–763. https://doi.org/10.1038/nature07327

Carruthers, V. B., Giddings, O. K., & Sibley, L. D. (1999). Secretion of micronemal proteins is associated with toxoplasma invasion of host cells. *Cellular Microbiology*, *1*(3), 225–235. https://doi.org/10.1046/j.1462-5822.1999.00023.x

Casadevall, A. (2008). Evolution of Intracellular Pathogens. *Annual Review of Microbiology*, *62*(1), 19–33. https://doi.org/10.1146/annurev.micro.61.080706.093305

Chen, C. L., & Perrimon, N. (2017). Proximity-dependent labeling methods for proteomic profiling in living cells. *Wiley Interdisciplinary Reviews: Developmental Biology*, *6*(4), 1–10. https://doi.org/10.1002/wdev.272

Chin W, Contacos P, Collins W E, Jete M Ii, Alpert E. (1968). Experimental mosquito-tranmission of plasmodium knowlesi to man and monkey. *The American Journal of Tropical Medicine and Hygiene*, *17*(3), 355–358. https://doi.org/10.4269/ajtmh.1968.17.355

Clark, M. A., Goheen, M. M., Fulford, A., Prentice, A. M., Elnagheeb, M. A., Patel, J., … Cerami, C. (2014). Host iron status and iron supplementation mediate susceptibility to erythrocytic stage plasmodium falciparum. *Nature Communications*, *5*, 1–11. https://doi.org/10.1038/ncomms5446

Collins, W. E. (2012). *Plasmodium knowlesi* : A Malaria Parasite of Monkeys and Humans. *Annual Review of Entomology*, *57*(1), 107–121. https://doi.org/10.1146/annurev-ento-121510-133540

Collins, W. E., & Jeffery, G. M. (2005). Plasmodium ovale:Parasite and Disease. *Clinical Microbiology Reviews*, *18*(3), 570. https://doi.org/10.1128/CMR.18.3.570

Colonne, P. M., Winchell, C. G., & Voth, D. E. (2016). Hijacking Host Cell Highways: Manipulation of the Host Actin Cytoskeleton by Obligate Intracellular Bacterial Pathogens. *Frontiers in Cellular and Infection Microbiology*, *6*(September), 1–8. https://doi.org/10.3389/fcimb.2016.00107

Cooper GM. The Cell: A Molecular Approach. 2nd edition. Sunderland (MA): Sinauer Associates; 2000. (n.d.). No Title.

Cooper, J. A., Walker, S. B., & Pollard, T. D. (1983). Pyrene actin: documentation of the validity of a sensitive assay for actin polymerization. *Journal of Muscle Research and Cell Motility*, *4*(2), 253–262. https://doi.org/10.1007/BF00712034

Cox, F. (2010). History of the discovery of the malaria parasites and their vectors. Parasites and Vectors. *Parasites and Vectors*, *3*(1), 5. https://doi.org/doi.org/10.1186/1756-3305-3-5

Culleton, R., Ndounga, M., Zeyrek, F. Y., Coban, C., Casimiro, P. N., Takeo, S., … Tanabe, K. (2009). Evidence for the Transmission of *Plasmodium vivax* in the Republic of the Congo, West Central Africa. *The Journal of Infectious Diseases*, *200*(9), 1465–1469. https://doi.org/10.1086/644510

D.M. Wetzel,* S. Håkansson,*‡ K. Hu,† D. Roos, and L. D. S. (2003). Actin Filament Polymerization Regulates Gliding Motility by Apicomplexan Parasites. *Molecular Biology of the Cell*, *14*(February), 396–406. https://doi.org/10.1091/mbc.E02

Das, S., Lemgruber, L., Tay, C. L., Baum, J., & Meissner, M. (2017). Multiple essential functions of Plasmodium falciparum actin-1 during malaria blood-stage development. *BMC Biology*, *15*(1), 1–16. https://doi.org/10.1186/s12915-017-0406-2

De Koning-Ward, T. F., Gilson, P. R., Boddey, J. A., Rug, M., Smith, B. J., Papenfuss, A. T., … Crabb, B. S. (2009). A newly discovered protein export machine in malaria parasites. *Nature*, *459*(7249), 945–949. https://doi.org/10.1038/nature08104

de Souza, W., & Attias, M. (2015). New views of the Toxoplasma gondii parasitophorous vacuole as revealed by Helium Ion Microscopy (HIM). *Journal of Structural Biology*, *191*(1), 76–85. https://doi.org/10.1016/j.jsb.2015.05.003

Deitsch, K. W., & Wellems, T. E. (1996). Membrane modifications in erythrocytes parasitized by Plasmodium falciparum. *Molecular and Biochemical Parasitology*, *76*(1–2), 1–10. https://doi.org/10.1016/0166-6851(95)02575-8

Dellibovi-Ragheb, T. A., Jhun, H., Goodman, C. D., Walters, M. S., Ragheb, D. R. T., Matthews, K. A., … Prigge, S. T. (2018). Host biotin is required for liver stage development in malaria parasites. *Proceedings of the National Academy of Sciences*, *115*(11), E2604–E2613. https://doi.org/10.1073/pnas.1800717115

Dhorda, M., Nyehangane, D., Rénia, L., Piola, P., Guerin, P. J., & Snounou, G. (2011). Transmission of plasmodium vivax in south-western Uganda: Report of three cases in pregnant women. *PLoS ONE*, *6*(5). https://doi.org/10.1371/journal.pone.0019801

Dluzewski, A. R., Mitchell, G. H., Fryer, P. R., Griffiths, S., & Wilson, R. J. M. (1992). Origins of the parasitophorous vacuole membrane of the malaria parasite , Plasmodium falciparum , in human red blood cells, *532*, 527–532.

Dobrowolski, J. M., Niesman, I. R., & Sibley, L. D. (1997). Actin in the parasite toxoplasma gondii is encoded by a single copy gene, act1 and exists primarily in a globular form. *Cell Motility and the Cytoskeleton*, *37*(3), 253–262. https://doi.org/10.1002/(SICI)1097-0169(1997)37:3<253::AID-CM7>3.0.CO;2-7

Doi, Y., Shinzawa, N., Fukumoto, S., Okano, H., & Kanuka, H. (2010). ADF2 is required for transformation of the ookinete and sporozoite in malaria parasite development.

*Biochemical and Biophysical Research Communications*, *397*(4), 668–672. https://doi.org/10.1016/j.bbrc.2010.05.155

Dominguez, R., & Holmes, K. C. (2011). Actin Structure and Function. *Annual Review of Biophysics*, *40*(1), 169–186. https://doi.org/10.1146/annurev-biophys-042910-155359

Don E. Eyles, G. R. C. and M. E. G. (1960). Vivax-Type Malaria Parasite of Macaques Transmissible to Man. *Science*, *131*(3416, pp. 1812–1813), 10. https://doi.org/10.1126/science

Drakeley, C. J., Carneiro, I., Reyburn, H., Malima, R., Lusingu, J. P. A., Cox, J., … Riley, E. M. (2005). Altitude-Dependent and -Independent Variations in *Plasmodium falciparum* Prevalence in Northeastern Tanzania. *The Journal of Infectious Diseases*, *191*(10), 1589–1598. https://doi.org/10.1086/429669

Drazic, A., Aksnes, H., Marie, M., Boczkowska, M., Varland, S., Timmerman, E., … Arnesen, T. (2018). NAA80 is actin's N-terminal acetyltransferase and regulates cytoskeleton assembly and cell motility. *Proceedings of the National Academy of Sciences*, *10*(3), 201718336. https://doi.org/10.1073/pnas.1718336115

Eitzen, G. (2003). Actin remodeling to facilitate membrane fusion. *Biochimica et Biophysica Acta - Molecular Cell Research*, *1641*(2–3), 175–181. https://doi.org/10.1016/S0167-4889(03)00087-9

Elliott, D. A., & Clark, D. P. (2000). Cryptosporidium parvum induces host cell actin accumulation at the host- parasite interface. *Infection and Immunity*, *68*(4), 2315–2322. https://doi.org/10.1128/IAI.68.4.2315-2322.2000

Favretto, F., Assfalg, M., Molinari, H., & D'Onofrio, M. (2013). Evidence from NMR interaction studies challenges the hypothesis of direct lipid transfer from L-FABP to malaria sporozoite protein UIS3. *Protein Science : A Publication of the Protein Society*, *22*(2), 133–138. https://doi.org/10.1002/pro.2194

Firat-Karalar, E. N., Rauniyar, N., Yates, J. R., & Stearns, T. (2014). Proximity interactions among centrosome components identify regulators of centriole duplication. *Current Biology*, *24*(6), 664–670. https://doi.org/10.1016/j.cub.2014.01.067

Fougère, A., Jackson, A. P., Paraskevi Bechtsi, D., Braks, J. A. M., Annoura, T., Fonager, J., … Franke-Fayard, B. (2016). Variant Exported Blood-Stage Proteins Encoded by Plasmodium Multigene Families Are Expressed in Liver Stages Where They Are Exported into the Parasitophorous Vacuole. *PLoS Pathogens*, *12*(11), 1–37. https://doi.org/10.1371/journal.ppat.1005917

Frénal, K., Dubremetz, J. F., Lebrun, M., & Soldati-Favre, D. (2017). Gliding motility powers invasion and egress in Apicomplexa. *Nature Reviews Microbiology*, *15*(11), 645–660. https://doi.org/10.1038/nrmicro.2017.86

Gardner, M. J., Hall, N., Fung, E., White, O., Berriman, M., Hyman, R. W., … Barrell, B. (2002). Genome sequence of the human malaria parasite Plasmodium falciparum. *Nature*, *419*(6906), 498–511. https://doi.org/10.1038/nature01097

Gates, B., & Chambers, R. (2015). From aspiration to action. What will it take to end malaria? https://doi.org/10.1002/ejoc.201200111

Goley, E. D., & Welch, M. D. (2006). The ARP2/3 complex: An actin nucleator comes of age. *Nature Reviews Molecular Cell Biology*, *7*(10), 713–726. https://doi.org/10.1038/nrm2026

Gomes-Santos, C. S. S., Itoe, M. A., Afonso, C., Henriques, R., Gardner, R., Sepúlveda, N., … Mota, M. M. (2012). Highly dynamic host actin reorganization around developing Plasmodium inside hepatocytes. *PLoS ONE*, *7*(1). https://doi.org/10.1371/journal.pone.0029408

Gonzalez, V., Combe, A., David, V., Malmquist, N. A., Delorme, V., Leroy, C., … Tardieux, I. (2009). Host Cell Entry by Apicomplexa Parasites Requires Actin Polymerization in the Host Cell. *Cell Host and Microbe*, *5*(3), 259–272. https://doi.org/10.1016/j.chom.2009.01.011

Gordon, J. L., & Sibley, L. D. (2005). Comparative genome analysis reveals a conserved family of actin-like proteins in apicomplexan parasites. *BMC Genomics*, *6*, 1–13. https://doi.org/10.1186/1471-2164-6-179

Gruszczyk, J., Kanjee, U., Chan, L.-J., Menant, S., Malleret, B., Lim, N. T. Y., … Tham, W.-H. (2018). Transferrin receptor 1 is a reticulocyte-specific receptor for Plasmodium vivax. *Science*, *359*(6371), 48–55. Retrieved from http://science.sciencemag.org/content/359/6371/48.abstract

Grützke, J., Rindte, K., Goosmann, C., Silvie, O., Rauch, C., Heuer, D., … Ingmundson, A. (2014). The spatiotemporal dynamics and membranous features of the Plasmodium liver stage tubovesicular network. *Traffic*, *15*(4), 362–382. https://doi.org/10.1111/tra.12151

Günther, K., Ansorge, I., & Benting, J. (1994). Characterization of Membrane Proteins Exported from Plasmodium Falciparum Into the Host Erythrocyte. *Parasitology*, *109*(1), 1–9. https://doi.org/10.1017/S0031182000077696

Håkansson, S., Morisaki, H., Heuser, J., & Sibley, L. D. (1999). Time-lapse video microscopy of gliding motility in Toxoplasma gondii reveals a novel, biphasic mechanism of cell locomotion. *Molecular Biology of the Cell*, *10*(11), 3539–3547. https://doi.org/10.1091/mbc.10.11.3539

Hale, V. L., Watermeyer, J. M., Hackett, F., Vizcay-Barrena, G., van Ooij, C., Thomas, J. A., … Saibil, H. R. (2017). Parasitophorous vacuole poration precedes its rupture and rapid host erythrocyte cytoskeleton collapse in *Plasmodium falciparum* egress. *Proceedings of the National Academy of Sciences*, *114*(13), 3439–3444. https://doi.org/10.1073/pnas.1619441114

Hall, R., McBride, J., Morgan, G., Tait, A., Zolg, J. W., Walliker, D., & Scaifi, J. (1983). Antigens of the erythrocytic stages of the human malaria parasite Plasmodium falciparum detected by monoclonal antibodies. *Molecular & Biochemical Parasitology*, *7*, 247–265.

Hay, S. I., Okiro, E. A., Gething, P. W., Patil, A. P., Tatem, A. J., Guerra, C. A., & Snow, R. W. (2010). Estimating the global clinical burden of plasmodium falciparum malaria in 2007. *PLoS Medicine*, *7*(6). https://doi.org/10.1371/journal.pmed.1000290

Heidi G. Elmendorf, K. H. (1994). Plasmodium falciparum Exports the Golgi Marker Sphingomyelin Synthase into a Tubovesicular Network in the Cytoplasm of Mature Erythrocytes. *The Journal of Cell Biology*, *124*(4), 449–462. Retrieved from https://www.ncbi.nlm.nih.gov/pmc/articles/PMC2119907/?report=classic

Herwig Schu ¨ ler,*† Ann-Kristin Mueller, ‡ and Kai Matuschewski‡. (2005). A Plasmodium Actin-depolymerizing Factor That Binds Exclusively to Actin Monomers. *Molecular Biology of the Cell*, *16*(3), 413–423. https://doi.org/10.1091/mbc.E05

Hliscs, M., Millet, C., Dixon, M. W., Siden-Kiamos, I., Mcmillan, P., & Tilley, L. (2015). Organization

and function of an actin cytoskeleton in Plasmodium falciparum gametocytes. *Cellular Microbiology*, *17*(2), 207–225. https://doi.org/10.1111/cmi.12359

Hollingdale, M. R., Leland, P., Leef, J. L., Leef, M. F., & Beaudoin, R. L. (1983). Serological reactivity of in vitro cultured exoerythrocytic stages of Plasmodium berghei in indirect immunofluorescent or immunoperoxidase antibody tests. *American Journal of Tropical Medicine and Hygiene*, *32*(1), 24–30. https://doi.org/10.4269/ajtmh.1983.32.24

Ingmundson, A., Nahar, C., Brinkmann, V., Lehmann, M. J., & Matuschewski, K. (2012). The exported Plasmodium berghei protein IBIS1 delineates membranous structures in infected red blood cells. *Molecular Microbiology*, *83*(6), 1229–1243. https://doi.org/10.1111/j.1365-2958.2012.08004.x

Ishino, T., Boisson, B., Orito, B. B., Lacroix, C., Bischoff, E., Loussert, C., … Baldacci, P. (2009). LISP1 is important for the egress of Plasmodium berghei parasites from liver cellsc. *Cellular Microbiology*, *11*(9), 1329–1339. https://doi.org/10.1111/j.1462-5822.2009.01333.x

Ishino, T., Yano, K., Chinzei, Y., & Yuda, M. (2004). Cell-passage activity is required for the malarial parasite to cross the liver sinusoidal cell layer. *PLoS Biology*, *2*(1), E4. https://doi.org/10.1371/journal.pbio.0020004

Itoe, M. A., Sampaio, J. L., Cabal, G. G., Real, E., Zuzarte-Luis, V., March, S., … Mota, M. M. (2014). Host cell phosphatidylcholine is a key mediator of malaria parasite survival during liver stage infection. *Cell Host and Microbe*, *16*(6), 778–786. https://doi.org/10.1016/j.chom.2014.11.006

Janse, C. J., Ramesar, J., & Waters, A. P. (2006). High-efficiency transfection and drug selection of genetically transformed blood stages of the rodent malaria parasite Plasmodium berghei. *Nature Protocols*, *1*(1), 346–356. https://doi.org/10.1038/nprot.2006.53

Jobe, O., Lumsden, J., Mueller, A., Williams, J., Silva-Rivera, H., Kappe, S. H. I., … Krzych, U. (2007). Genetically Attenuated *Plasmodium berghei* Liver Stages Induce Sterile Protracted Protection That Is Mediated by Major Histocompatibility Complex Class I–Dependent Interferon-γ–Producing CD8 + T Cells. *The Journal of Infectious Diseases*, *196*(4), 599–607. https://doi.org/10.1086/519743

Kast, D. J., & Dominguez, R. (2017). The Cytoskeleton–Autophagy Connection. *Current Biology*, *27*(8), R318–R326. https://doi.org/10.1016/j.cub.2017.02.061

Kaushansky, A., Douglass, A. N., Arang, N., Vigdorovich, V., Kain, H. S., Austin, L. S., … Stefan, H. I. (2016). Malaria parasites target the hepatocyte receptor EphA2 for successful host infection. *Science*, *350*(6264), 1089–1092. https://doi.org/10.1126/science.aad3318.Malaria

Kayath, C. A., Hussey, S., El hajjami, N., Nagra, K., Philpott, D., & Allaoui, A. (2010). Escape of intracellular Shigella from autophagy requires binding to cholesterol through the type III effector, IcsB. *Microbes and Infection*, *12*(12–13), 956–966. https://doi.org/10.1016/j.micinf.2010.06.006

Khosh-Naucke, M., Becker, J., Mesén-Ramírez, P., Kiani, P., Birnbaum, J., Fröhlke, U., … Spielmann, T. (2017). Identification of novel parasitophorous vacuole proteins in P. falciparum parasites using BioID. *International Journal of Medical Microbiology*, (July), 1–12. https://doi.org/10.1016/j.ijmm.2017.07.007

Kim, D. I., Jensen, S. C., Noble, K. A., KC, B., Roux, K. H., Motamedchaboki, K., & Roux, K. J. (2016). An improved smaller biotin ligase for BioID proximity labeling. *Molecular Biology of the Cell*, *27*(8), 1188–1196. https://doi.org/10.1091/mbc.E15-12-0844

Kim, Dae In, Kc, B., Zhu, W., Motamedchaboki, K., Doye, V., & Roux, K. J. (2014). Probing nuclear pore complex architecture with proximity-dependent biotinylation. *Proceedings of the National Academy of Sciences of the United States of America*, *111*, E2453-61. https://doi.org/10.1073/pnas.1406459111

Koenderink, J. B., Kavishe, R. A., Rijpma, S. R., & Russel, F. G. M. (2010). The ABCs of multidrug resistance in malaria. *Trends in Parasitology*, *26*(9), 440–446. https://doi.org/10.1016/j.pt.2010.05.002

Kozycki, C. T., Umulisa, N., Rulisa, S., Mwikarago, E. I., Musabyimana, J. P., Habimana, J. P., … Krogstad, D. J. (2017). False-negative malaria rapid diagnostic tests in Rwanda: impact of Plasmodium falciparum isolates lacking hrp2 and declining malaria transmission. *Malaria Journal*, *16*(1), 1–11. https://doi.org/10.1186/s12936-017-1768-1

Kumar, K. A., Baxter, P., Tarun, A. S., Kappe, S. H. I., & Nussenzweig, V. (2009). Conserved protective mechanisms in radiation and genetically attenuated uis3(-) and uis4(-) Plasmodium sporozoites. *PloS One*, *4*(2), e4480. https://doi.org/10.1371/journal.pone.0004480

Kumar, Y., & Valdivia, R. H. (2009). Leading a Sheltered Life: Intracellular Pathogens and Maintenance of Vacuolar Compartments. *Cell Host and Microbe*, *5*(6), 593–601. https://doi.org/10.1016/j.chom.2009.05.014

Kursula, I., Kursula, P., Ganter, M., Panjikar, S., Matuschewski, K., & Schüler, H. (2008). Structural Basis for Parasite-Specific Functions of the Divergent Profilin of Plasmodium falciparum. *Structure*, *16*(11), 1638–1648. https://doi.org/10.1016/j.str.2008.09.008

Kwiatkowski, D. P. (2005). How Malaria Has Affected the Human Genome and What Human Genetics Can Teach Us about Malaria. *The American Journal of Human Genetics*, *77*(2), 171–192. https://doi.org/10.1086/432519

Laurent Blanchoin, Rajaa Boujemaa-Paterski, Cécile Sykes, and J. P. (2014). Actin Dynamics, Archi- tecture, and Mechanics in Cell Motility. *Genetics*, *94*(1), 235–263. https://doi.org/doi:10.1152/physrev.00018.2013

Laveran, A. (1922). Alphonse Laveran (1845–1922): discovery of the causative agent of malaria in 1880. In F. G.C. Cook, MD, DSc, FRCP, FRCPE, FRACP (Ed.), *Tropical Medicine* (pp. 67–79). https://doi.org/https://doi.org/10.1016/B978-012373991-9.50006-0

Lee, J. Y., Koga, H., Kawaguchi, Y., Tang, W., Wong, E., Gao, Y. S., … Yao, T. P. (2010). HDAC6 controls autophagosome maturation essential for ubiquitin-selective quality-control autophagy. *EMBO Journal*, *29*(5), 969–980. https://doi.org/10.1038/emboj.2009.405

Lee, S. Y., Kang, M. G., Park, J. S., Lee, G., Ting, A. Y., & Rhee, H. W. (2016). APEX Fingerprinting Reveals the Subcellular Localization of Proteins of Interest. *Cell Reports*, *15*(8), 1837–1847. https://doi.org/10.1016/j.celrep.2016.04.064

Lin, & Webb. (2010). Actin and Actin-Binding Proteins: Masters of Dendritic Spine Formation, Morphology, and Function. *Open Neurosci J .*, 54–66. https://doi.org/10.2174/1874082000903020054.Actin

Lingelbach, K., & Joiner, K. (1998). The parasitophorous vacuole membrane surrounding Plasmodium and Toxoplasma: an unusual compartment in infected cells. *Journal of Cell Science*, *111 ( Pt 1*, 1467–1475.

Lisewski, A. M., Quiros, J. P., Ng, C. L., Adikesavan, A. K., Miura, K., Putluri, N., … Lichtarge, O. (2014). Supergenomic network compression and the discovery of exp1 as a glutathione transferase inhibited by artesunate. *Cell*, *158*(4), 916–928. https://doi.org/10.1016/j.cell.2014.07.011

Lopes da Silva, M., Thieleke-Matos, C., Cabrita-Santos, L., Ramalho, J. S., Wavre-Shapton, S. T., Futter, C. E., … Seabra, M. C. (2012). The host endocytic pathway is essential for plasmodium berghei late liver stage development. *Traffic*, *13*(10), 1351–1363. https://doi.org/10.1111/j.1600-0854.2012.01398.x

Lopez-Estraño, C., Bhattacharjee, S., Harrison, T., & Haldar, K. (2003). Cooperative domains define a unique host cell-targeting signal in Plasmodium falciparum-infected erythrocytes. *Proceedings of the National Academy of Sciences of the United States of America*, *100*(21), 12402–12407. https://doi.org/10.1073/pnas.2133080100

Louicharoen, C., Patin, E., Paul, R., Nuchprayoon, I., Witoonpanich, B., Peerapittayamongkol, C., … Sakuntabhai, A. (2009). Positively selected G6PD-mahidol mutation reduces Plasmodium vivax density in Southeast Asians. *Science*, *326*(5959), 1546–1549. https://doi.org/10.1126/science.1178849

Mackellar, D. C., Vaughan, A. M., Aly, A. S. I., Deleon, S., & Kappe, S. H. I. (2011). A systematic analysis of the early transcribed membrane protein family throughout the life cycle of Plasmodium yoelii. *Cellular Microbiology*, *13*(11), 1755–1767. https://doi.org/10.1111/j.1462-5822.2011.01656.x

Marsh, K., & Kinyanjui, S. (2006). Immune effector mechanisms in malaria. *Parasite Immunology*, *28*(1–2), 51–60. https://doi.org/10.1111/j.1365-3024.2006.00808.x

Martens, P., & Hall, L. (2000). Malaria on the move: human population movement and malaria transmission. *Emerging Infectious Diseases*, *6*(2), 103–109. https://doi.org/10.3201/eid0602.000202

Marti, M., Good, R. T., Rug, M., Knuepfer, E., & Cowman, A. F. (2004). Targeting malaria virulence and remodeling proteins to the host erythrocyte. *Science*, *306*(5703), 1930–1933. https://doi.org/10.1126/science.1102452

Matuschewski, K., Ross, J., Brown, S. M., Kaiser, K., Nussenzweig, V., & Kappe, S. H. I. (2002a). Infectivity-associated changes in the transcriptional repertoire of the malaria parasite sporozoite stage. *Journal of Biological Chemistry*, *277*(44), 41948–41953. https://doi.org/10.1074/jbc.M207315200

Matuschewski, K., Ross, J., Brown, S. M., Kaiser, K., Nussenzweig, V., & Kappe, S. H. I. (2002b). Infectivity-associated changes in the transcriptional repertoire of the malaria parasite sporozoite stage. *Journal of Biological Chemistry*, *277*(44), 41948–41953. https://doi.org/10.1074/jbc.M207315200

Mbanefo, E. C., Ahmed, A. M., Titouna, A., Elmaraezy, A., Trang, N. T. H., Phuoc Long, N., … Hirayama, K. (2017). Association of glucose-6-phosphate dehydrogenase deficiency and malaria: A systematic review and meta-analysis. *Scientific Reports*, *7*(September 2016), 1–10. https://doi.org/10.1038/srep45963

Meireles, P., Mendes, A. M., Aroeira, R. I., Mounce, B. C., Vignuzzi, M., Staines, H. M., & Prudêncio, M. (2017). Uptake and metabolism of arginine impact Plasmodium development in the liver. *Scientific Reports*, *7*(1), 1–12. https://doi.org/10.1038/s41598-017-04424-y

Meireles, P., Sales-Dias, J., Andrade, C. M., Mello-Vieira, J., Mancio-Silva, L., Simas, J. P., … Prudêncio, M. (2016). GLUT1-mediated glucose uptake plays a crucial role during Plasmodium hepatic infection. *Cellular Microbiology*, *19*(2). https://doi.org/10.1111/cmi.12646

Ménard, R. (2001). Gliding motility and cell invasion by Apicomplexa: Insights from the Plasmodium sporozoite. *Cellular Microbiology*, *3*(2), 63–73. https://doi.org/10.1046/j.1462-5822.2001.00097.x

Mikolajczak, S. A. et al. (2015). Plasmodium vivax liver stage development and hypnozoite persistence in human liver-chimeric mice. *Cell Host Microbe*, *17*(4), 526–535. https://doi.org/10.1016/j.chom.2015.02.011.Plasmodium

Mikolajczak, S. a, Jacobs-Lorena, V., MacKellar, D. C., Camargo, N., & Kappe, S. H. I. (2007). L-FABP is a critical host factor for successful malaria liver stage development. *International Journal for Parasitology*, *37*(5), 483–489. https://doi.org/10.1016/j.ijpara.2007.01.002

Miller, L. H., Mason, S. J., Clyde, D. F., & McGinniss, M. H. (1976). The Resistance Factor to Plasmodium vivax in Blacks. *New England Journal of Medicine*, *295*(6), 302–304. https://doi.org/10.1056/NEJM197608052950602

Millholland, M. G., Chandramohanadas, R., Pizzarro, A., Wehr, A., Shi, H., Darling, C., … Greenbaum, D. C. (2011). The Malaria Parasite Progressively Dismantles the Host Erythrocyte Cytoskeleton for Efficient Egress. *Molecular & Cellular Proteomics*, *10*(12), M111.010678. https://doi.org/10.1074/mcp.M111.010678

Moody, A. (2002). Rapid Diagnostic Tests for Malaria Parasites. *Clinical Microbiology Reviews*, *15*(1), 66–78. https://doi.org/10.1128/CMR.15.1.66

Moore, R. B., Oborník, M., Janouškovec, J., Chrudimský, T., Vancová, M., Green, D. H., … Carter, D. A. (2008). A photosynthetic alveolate closely related to apicomplexan parasites. *Nature*, *451*(7181), 959–963. https://doi.org/10.1038/nature06635

Mordecai, E. A., Paaijmans, K. P., Johnson, L. R., Balzer, C., Ben-Horin, T., de Moor, E., … Lafferty, K. D. (2013). Optimal temperature for malaria transmission is dramatically lower than previously predicted. *Ecology Letters*, *16*(1), 22–30. https://doi.org/10.1111/ele.12015

Moreau, C. A., Bhargav, S. P., Kumar, H., Quadt, K. A., Piirainen, H., Strauss, L., … Frischknecht, F. (2017). A unique profilin-actin interface is important for malaria parasite motility. *PLoS Pathogens*, *13*(5). https://doi.org/10.1371/journal.ppat.1006412

Morrissette, N. S., & Sibley, L. D. (2002). Cytoskeleton of Apicomplexan Parasites Cytoskeleton of Apicomplexan Parasites. *Microbiology and Molecular Biology Reviews*, *66*(1), 21–38. https://doi.org/10.1128/MMBR.66.1.21

Mota, M M, Pradel, G., Vanderberg, J. P., Hafalla, J. C., Frevert, U., Nussenzweig, R. S., … Rodríguez, a. (2001). Migration of Plasmodium sporozoites through cells before infection. *Science (New York, N.Y.)*, *291*(5501), 141–144. https://doi.org/10.1126/science.291.5501.141

Mota, Maria M, Hafalla, J. C. R., & Rodriguez, A. (2002). Migration through host cells activates Plasmodium sporozoites for infection. *Nature Medicine*, *8*(11), 1318–1322.

https://doi.org/10.1038/nm785

Mueller, A.-K., Camargo, N., Kaiser, K., Andorfer, C., Frevert, U., Matuschewski, K., & Kappe, S. H. I. (2005). Plasmodium liver stage developmental arrest by depletion of a protein at the parasite-host interface. *Proceedings of the National Academy of Sciences of the United States of America*, *102*(8), 3022–3027. https://doi.org/10.1073/pnas.0408442102

Mueller, A., Labaied, M., Kappe, S. H. I., & Matuschewski, K. (2005). Genetically modified Plasmodium parasites as a protective experimental malaria vaccine. *Nature*, *433*(7022), 164–167. https://doi.org/10.1038/nature03188

Muschiol, S., Bailey, L., Gylfe, A., Sundin, C., Hultenby, K., Bergström, S., … Henriques-Normark, B. (2006). A small-molecule inhibitor of type III secretion inhibits different stages of the infectious cycle of Chlamydia trachomatis. *Proceedings of the National Academy of Sciences of the United States of America*, *103*(39), 14566–14571. https://doi.org/10.1073/pnas.0606412103

Myung, J. M., Marshall, P., & Sinnis, P. (2004). The Plasmodium circumsporozoite protein is involved in mosquito salivary gland invasion by sporozoites. *Molecular and Biochemical Parasitology*, *133*(1), 53–59. https://doi.org/10.1016/j.molbiopara.2003.09.002

Nichols, B. A., Chiappino, M. L., & O'Connor, G. R. (1983). Secretion from the Rhoptries of Toxoplasma gondii during host-cell invasion. *Journal of Ultrasructure Research*, *83*(1), 85–98. https://doi.org/10.1016/S0022-5320(83)90067-9

Nyboer, B., Heiss, K., Mueller, A. K., & Ingmundson, A. (2017). The Plasmodium liver-stage parasitophorous vacuole: A front-line of communication between parasite and host. *International Journal of Medical Microbiology*, (June), 0–1. https://doi.org/10.1016/j.ijmm.2017.09.008

O'Leary, P. (1928). Treatment of Neurosyphilis By Malaria—Fourth Annual Report. *California and Western Medicine*, *XXIX*(3), 160–163. Retrieved from http://www.ncbi.nlm.nih.gov/pmc/articles/pmc1655978/

Oh, S. S., Chishti, A. H., Palek, J., & Liu, S. C. (1997). Erythrocyte membrane alterations in Plasmodium falciparum malaria sequestration. *Current Opinion in Hematology*. https://doi.org/10.1097/00062752-199704020-00012

Oh, S. S., Voigt, S., Fisher, D., Yi, S. J., LeRoy, P. J., Derick, L. H., … Chishti, A. H. (2000). Plasmodium falciparum erythrocyte membrane protein 1 is anchored to the actin-spectrin junction and knob-associated histidine-rich protein in the erythrocyte skeleton. *Molecular and Biochemical Parasitology*, *108*(2), 237–247. https://doi.org/10.1016/S0166-6851(00)00227-9

Orito, Y., Ishino, T., Iwanaga, S., Kaneko, I., Kato, T., Menard, R., … Yuda, M. (2013). Liver-specific protein 2: A Plasmodium protein exported to the hepatocyte cytoplasm and required for merozoite formation. *Molecular Microbiology*, *87*(1), 66–79. https://doi.org/10.1111/mmi.12083

Pei, X., Guo, X., Coppel, R., Mohandas, N., & An, X. (2007). Plasmodium falciparum erythrocyte membrane protein 3 (PfEMP3) destabilizes erythrocyte membrane skeleton. *The Journal of Biological Chemistry*, *282*(37), 26754–26758. https://doi.org/10.1074/jbc.M701612200

Perrin, B. J., & Ervasti, J. M. (2010). The actin gene family: Function follows isoform. *Cytoskeleton*,

*67*(10), 630–634. https://doi.org/10.1002/cm.20475

Petersen, W., Stenzel, W., Silvie, O., Blanz, J., Saftig, P., Matuschewski, K., & Ingmundson, A. (2017). Sequestration of cholesterol within the host late endocytic pathway restricts liver-stage *Plasmodium* development. *Molecular Biology of the Cell*, *28*(6), 726–735. https://doi.org/10.1091/mbc.E16-07-0531

Portugal, S., Carret, C., Recker, M., Armitage, A. E., Gonçalves, L. A., Epiphanio, S., … Mota, M. M. (2011). Host-mediated regulation of superinfection in malaria. *Nature Medicine*, *17*(6), 732–737. https://doi.org/10.1038/nm.2368

Real, E., Rodrigues, L., Cabal, G. G., Enguita, F. J., Mancio-Silva, L., Mello-Vieira, J., … Mota, M. M. (2017). Plasmodium UIS3 sequesters host LC3 to avoid elimination by autophagy in hepatocytes. *Nature Microbiology*, 1–9. https://doi.org/10.1038/s41564-017-0054-x

Rijpma, S. R., van der Velden, M., Annoura, T., Matz, J. M., Kenthirapalan, S., Kooij, T. W. A., … Koenderink, J. B. (2016). Vital and dispensable roles of Plasmodium multidrug resistance transporters during blood- and mosquito-stage development. *Molecular Microbiology*, *101*(1), 78–91. https://doi.org/10.1111/mmi.13373

Risco-Castillo, V., Topçu, S., Marinach, C., Manzoni, G., Bigorgne, A. E., Briquet, S., … Silvie, O. (2015). Malaria sporozoites traverse host cells within transient vacuoles. *Cell Host and Microbe*, *18*(5), 593–603. https://doi.org/10.1016/j.chom.2015.10.006

Rodrigues, C. D., Hannus, M., Prudêncio, M., Martin, C., Gonçalves, L. A., Portugal, S., … Mota, M. M. (2008). Host Scavenger Receptor SR-BI Plays a Dual Role in the Establishment of Malaria Parasite Liver Infection. *Cell Host and Microbe*, *4*(3), 271–282. https://doi.org/10.1016/j.chom.2008.07.012

Roux, K. J. (2013). Marked by association: techniques for proximity-dependent labeling of proteins in eukaryotic cells. *Cellular and Molecular Life Sciences : CMLS*, *70*(19), 3657–3664. https://doi.org/10.1007/s00018-013-1287-3

Roux, K. J., Kim, D. I., Raida, M., & Burke, B. (2012). A promiscuous biotin ligase fusion protein identifies proximal and interacting proteins in mammalian cells. *The Journal of Cell Biology*, *196*(6), 801–810. https://doi.org/10.1083/jcb.201112098

Ryan, J. R., Stoute, J. A., Amon, J., Dunton, R. F., Mtalib, R., Koros, J., … Rosenberg, R. (2006). Evidence for transmission of Plasmodium vivax among a Duffy antigen negative population in Western Kenya. *American Journal of Tropical Medicine and Hygiene*, *75*(4), 575–581. https://doi.org/75/4/575 [pii]

Sá e Cunha, C., Nyboer, B., Heiss, K., Sanches-Vaz, M., Fontinha, D., Wiedtke, E., … Mueller, A.-K. (2017). *Plasmodium berghei* EXP-1 interacts with host Apolipoprotein H during *Plasmodium* liver-stage development. *Proceedings of the National Academy of Sciences*, *114*(7), E1138–E1147. https://doi.org/10.1073/pnas.1606419114

Sabbatani, S., Fiorino, S., & Manfredi, R. (2012). Plasmodium knowlesi: from Malaysia, a novel health care threat. *Le Infezioni in Medicina : Rivista Periodica Di Eziologia, Epidemiologia, Diagnostica, Clinica e Terapia Delle Patologie Infettive*, *20*(1), 5–11. Retrieved from http://www.ncbi.nlm.nih.gov/pubmed/22475654

Sadasivaiah, S., Tozan, Y., & Breman, J. G. (2007). Dichlorodiphenyltrichloroethane (DDT) for indoor residual spraying in Africa: How can it be used for malaria control? *American Journal*

*of Tropical Medicine and Hygiene*, *77*(SUPPL. 6), 249–263. https://doi.org/77/6_Suppl/249 [pii]

Sanchez, G. I., Rogers, W. O., Mellouk, S., & Hoffman, S. L. (1994). Plasmodium falciparum: exported protein-1, a blood stage antigen, is expressed in liver stage parasites. *Experimental Parasitology*. https://doi.org/10.1006/expr.1994.1060

Schnider, C. B., Bausch-Fluck, D., Brühlmann, F., Heussler, V. T., & Burda, P.-C. (2018). BioID Reveals Novel Proteins of the *Plasmodium* Parasitophorous Vacuole Membrane. *MSphere*, *3*(1), e00522-17. https://doi.org/10.1128/mSphere.00522-17

Schüler, H., Mueller, A. K., & Matuschewski, K. (2005). Unusual properties of Plasmodium falciparum actin: New insights into microfilament dynamics of apicomplexan parasites. *FEBS Letters*, *579*(3), 655–660. https://doi.org/10.1016/j.febslet.2004.12.037

Seakins, M., Gibbs, W. N., Service, M., & Division, H. (1973). Erythrocyte Hb-S Concentration AN IMPORTANT FACTOR IN THE LOW OXYGEN. *The Journal of Clinical INvestigation*, *52*(February).

Siden-Kiamos, I., Schüler, H., Liakopoulos, D., & Louis, C. (2010). Arp1, an actin-related protein, in Plasmodium berghei. *Molecular and Biochemical Parasitology*, *173*(2), 88–96. https://doi.org/10.1016/j.molbiopara.2010.05.008

Silva, P. A., Guerreiro, A., Santos, J. M., Braks, J. A. M., Janse, C. J., & Mair, G. R. (2016). Translational control of UIS4 protein of the host-parasite interface is mediated by the RNA binding protein Puf2 in Plasmodium berghei sporozoites. *PLoS ONE*, *11*(1), 1–12. https://doi.org/10.1371/journal.pone.0147940

Silvie, O., Briquet, S., Müller, K., Manzoni, G., & Matuschewski, K. (2014). Post-transcriptional silencing of UIS4 in Plasmodium berghei sporozoites is important for host switch. *Molecular Microbiology*, *91*(6), 1200–1213. https://doi.org/10.1111/mmi.12528

Singh, A. P., Buscaglia, C. A., Wang, Q., Levay, A., Nussenzweig, D. R., Walker, J. R., … Nussenzweig, V. (2007). Plasmodium Circumsporozoite Protein Promotes the Development of the Liver Stages of the Parasite. *Cell*, *131*(3), 492–504. https://doi.org/10.1016/j.cell.2007.09.013

Singh, B., Sung, L. K., Matusop, A., Radhakrishnan, A., Shamsul, S. S. G., Cox-Singh, J., … Conway, D. J. (2004). A large focus of naturally acquired Plasmodium knowlesi infections in human beings. *The Lancet*, *363*(9414), 1017–1024. https://doi.org/10.1016/S0140-6736(04)15836-4

Skillman, K. M., Diraviyam, K., Khan, A., Tang, K., Sept, D., & Sibley, L. D. (2011). Evolutionarily divergent, unstable filamentous actin is essential for gliding motility in apicomplexan parasites. *PLoS Pathogens*, *7*(10). https://doi.org/10.1371/journal.ppat.1002280

Stephens, J. W. W. (1914). A new malaria parasite of man. *Annals of Tropical Medicine and Parasitology*, *8*(1), 119–128. https://doi.org/10.1080/00034983.1914.11687646

Sturm, A., Amino, R., van de Sand, C., Regen, T., Retzlaff, S., Rennenberg, A., … Heussler, V. T. (2006). Manipulation of host hepatocytes by the malaria parasite for delivery into liver sinusoids. *Science (New York, N.Y.)*, *313*(5791), 1287–1290. https://doi.org/10.1126/science.1129720

Sullivan, D. (2006). Malariology Overview, 1–34.

Suss-Toby, E., Zimmerberg, J., & Ward, G. E. (1996). Toxoplasma invasion: the parasitophorous vacuole is formed from host cell plasma membrane and pinches off via a fission pore. *Proceedings of the National Academy of Sciences of the United States of America*, *93*(16), 8413–8418. https://doi.org/10.1073/pnas.93.16.8413

Tanser, F. C., Sharp, B. L., & le Sueur, D. (2003). Potential effect of climate change on malaria transmission in Africa. *The Lancet*, *362*(9398), 1792–1798. https://doi.org/10.1016/S0140-6736(03)14898-2

Taylor, S. M., Parobek, C. M., & Fairhurst, R. M. (2012). Haemoglobinopathies and the clinical epidemiology of malaria: A systematic review and meta-analysis. *The Lancet Infectious Diseases*, *12*(6), 457–468. https://doi.org/10.1016/S1473-3099(12)70055-5

Tewari, R., Straschil, U., Bateman, A., Böhme, U., Cherevach, I., Gong, P., … Billker, O. (2010). The systematic functional analysis of plasmodium protein kinases identifies essential regulators of mosquito transmission. *Cell Host and Microbe*, *8*(4), 377–387. https://doi.org/10.1016/j.chom.2010.09.006

Tian, B., & Brasier, A. (2003). Identification of a nuclear factor kappa B-dependent gene network. *Recent Progress in Hormone Research*. https://doi.org/10.1210/rp.58.1.95

Tobias Spielmann, David J. P. Fergusen, and H.-P. B. (2003). etramps, a New Plasmodium falciparum Gene Family Coding for Developmentally Regulated and Highly Charged Membrane Proteins Located at the Parasite– Host Cell Interface. *Molecular Biology of the Cell*, *14*(April), 1529–1544. https://doi.org/10.1091/mbc.E02

Van De Sand, C., Horstmann, S., Schmidt, A., Sturm, A., Bolte, S., Krueger, A., … Heussler, V. T. (2005). The liver stage of Plasmodium berghei inhibits host cell apoptosis. *Molecular Microbiology*, *58*(3), 731–742. https://doi.org/10.1111/j.1365-2958.2005.04888.x

Vieira, R. C., A., L., H.V., O., O.M., B. J., D., S. J., & A.L., C. (2001). Anal paracoccidioidomycosis: an unusual presentation of disseminated disease. *Revista Da Sociedade Brasileira de Medicina Tropical*, *34*(6), 583–586. https://doi.org/10.1590/S0037-86822001000600014

Voskou, S., Aslan, M., Fanis, P., Phylactides, M., & Kleanthous, M. (2015). Oxidative stress in β-thalassaemia and sickle cell disease. *Redox Biology*. https://doi.org/10.1016/j.redox.2015.07.018

Wang, Q., Fujioka, H., & Nussenzweig, V. (2005). Exit of plasmodium sporozoites from oocysts is an active process that involves the circumsporozoite protein. *PLoS Pathogens*, *1*(1), 0072–0079. https://doi.org/10.1371/journal.ppat.0010009

Wegner, A., & Isenbergt, G. (1983). 2-Fold difference between the critical monomer concentrations of the two ends of actin filaments in physiological salt conditions. *Biochemistry*, *80*(August), 4922–4925. https://doi.org/10.1073/pnas.80.16.4922

Wesseling, J. G., de Ree, J. M., Ponnudurai, T., Smits, M. A., & Schoenmakers, J. G. G. (1988). Nucleotide sequence and deduced amino acid sequence of a Plasmodium falciparum actin gene. *Molecular and Biochemical Parasitology*, *27*(2–3), 313–320. https://doi.org/10.1016/0166-6851(88)90051-5

Wesseling, J. G., Smits, M. A., & Schoenmakers, J. G. G. (1988). Extremely diverged actin proteins in Plasmodium falciparum. *Molecular and Biochemical Parasitology*, *30*(2), 143–153. https://doi.org/10.1016/0166-6851(88)90107-7

Wesseling, J. G., Snijders, P. J. F., van Someren, P., Jansen, J., Smits, M. A., & Schoenmakers, J. G. G. (1989). Stage-specific expression and genomic organization of the actin genes of the malaria parasite Plasmodium falciparum. *Molecular and Biochemical Parasitology*, *35*(2), 167–176. https://doi.org/10.1016/0166-6851(89)90119-9

White, E. A. A. and N. J. (2014). The duration of Plasmodium falciparum infections. *Malaria Journal*, *13*(1). https://doi.org/10.1186/1475-2875-13-500

White, N. J. (2014). Malaria. *Manson's Tropical Infectious Diseases*, 532-600.e1. https://doi.org/10.1016/B978-0-7020-5101-2.00044-3

Whitrow, M. (1990). Wagner-Jauregg and fever therapy. *Medical History*, *34*(3), 294–310. https://doi.org/10.1017/S0025727300052431

Williams, T. N. (2012). Balancing act: Haemoglobinopathies and malaria. *The Lancet Infectious Diseases*, *12*(6), 427–428. https://doi.org/10.1016/S1473-3099(12)70067-1

World Health Organization. (2017). World Malaria Report, 196.

World Health Organization. (2018). *World {Malaria} {Report}*.

World malaria report 2018. (2018). *World malaria report 2018*. https://doi.org/ISBN 978 92 4 1564403

Wu, X., Lu, Y., Zhou, S., Chen, L., & Xu, B. (2016). Impact of climate change on human infectious diseases: Empirical evidence and human adaptation. *Environment International*, *86*, 14–23. https://doi.org/10.1016/j.envint.2015.09.007

Xu, Y., & Beckett, D. (1996). Evidence for interdomain interaction in the Escherichia coli repressor of biotin biosynthesis from studies of an N-terminal domain deletion mutant. *Biochemistry*, *35*(6), 1783–1792. https://doi.org/10.1021/bi952269e

Yalaoui, S., Huby, T., Franetich, J. F., Gego, A., Rametti, A., Moreau, M., … Froissard, P. (2008). Scavenger Receptor BI Boosts Hepatocyte Permissiveness to Plasmodium Infection. *Cell Host and Microbe*, *4*(3), 283–292. https://doi.org/10.1016/j.chom.2008.07.013

Yamana, T. K., & Eltahir, E. A. (2013). Incorporating the effects of humidity in a mechanistic model of Anopheles gambiae mosquito population dynamics in the Sahel region of Africa. *Parasites & Vectors*, *6*(1), 235. https://doi.org/10.1186/1756-3305-6-235

Yang, A. S. P., O'Neill, M. T., Jennison, C., Lopaticki, S., Allison, C. C., Armistead, J. S., … Boddey, J. A. (2017). Cell Traversal Activity Is Important for Plasmodium falciparum Liver Infection in Humanized Mice. *Cell Reports*, *18*(13), 3105–3116. https://doi.org/10.1016/j.celrep.2017.03.017

Zhang, M., Mishra, S., Sakthivel, R., Fontoura, B. M. A., & Nussenzweig, V. (2016). UIS2: A Unique Phosphatase Required for the Development of Plasmodium Liver Stages. *PLoS Pathogens*, *12*(1), 1–20. https://doi.org/10.1371/journal.ppat.1005370

Zuzarte-Luís, V., Mello-Vieira, J., Marreiros, I. M., Liehl, P., Chora, Â. F., Carret, C. K., … Mota, M. M. (2017). Dietary alterations modulate susceptibility to Plasmodium infection. *Nature Microbiology*, *2*(12), 1600–1607. https://doi.org/10.1038/s41564-017-0025-2

**ANNEXE**

**Table 8**

**List of primers**

| Sequence | sense | organism | Gene |
|---|---|---|---|
| AAGGGCCCATGGAACAAAAACTCATCTCAG | BirA*- Forw. | P. *berghei* | PbUIS4 |
| TTGCGGCCGCTCAGCGGTTTAAACTTAAGCTTG | BirA*- Rever. | P. *berghei* | PbUIS4 |
| AAGGTACCCCACATACGTTTCTCTATTTTTTATC | PbUIS4-f Forw. | P. *berghei* | PbUIS4 |
| TTGGGCCCTATGTATGGGCCGAATGATTT | PbUIS4- Rever. | P. *berghei* | PbUIS4 |
| CTTTCAGCACATAATTATTACGTCTG | UIS4_5'UTR-Forw. | P. *berghei* | PbUIS4 |
| CATAAAACAATTTGTTCTCTTTCTGAATTAC | UIS4_3'UTR- Rever. | P. *berghei* | PbUIS4 |
| GA CTA GTG GAT CCG AGC TCG GTT CCA AGC TTA AGT TTA AAC CG | BirA* SDM- Forw | P. *berghei* | BirA* |
| CGGTTTAAACTTAAGCTTGGAACCGAGCTCGGATCCACTAGTC | BirA* SDM- Rever. | P. *berghei* | BirA* |
| AAGGGCCCTTAAGGCCTGTTAACCGGTCGTAC | BirA*-HA- Forw. | P. *berghei* | BirA* |
| TTGCGGCCGCCTATGCGTAATCCGGTACATCGTAAG | BirA*-HA- Rever. | P. *berghei* | BirA* |
| GATGTAAACACCCCTCAAGATATCTCATTAATAAATCCAGTCGAA | UIS4-SDM-Forw. | P. *berghei* | PbUIS4 |
| TTCGACTGGATTTATTAATGAGATATCTTGAGGGGTGTTTACATC | UIS4-SDM-Revers. | P. *berghei* | PbUIS4 |
| CTGGACGGCGACGTAAACGGCCACAAGTTCAGCGT | UIS4-SDM-EcorV-Forw. | P. *berghei* | plasmid |
| ACGCTGAACTTGTGGCCGTTTACGTCGCCGTCCAG | UIS4-SDM-EcorV-Rever. | P. *berghei* | plasmid |
| atGGTACCTGGATTCATTTTTTGATGCATGC | PbUIS4 5'KO- Forw. | P. *berghei* | UIS4 |
| atGGGCCCTTTATTCAGACGTAATAATTATGTGC | PbUIS4 5'KO-Rever. | P. *berghei* | UIS4 |
| AAGATATCATAATTCATTATGAGTAGTGTAATTCAG | PbUIS4 3'KO- Forw | P. *berghei* | UIS4 |
| atGCGGCCGCAAGTTTGCATATACGGCTGCTTCC | PbUIS4 3'KO- Rever. | P. *berghei* | UIS4 |

## Proteomic data

### Mass Spectrometry results, from PbANKA-WT and PbUIS4-KO

Table 9

| **PbANKA-WT fraction 1** | |
|---|---|
| **Accession** | **Description** |
| CH60_HUMAN | 60 KDa heat shock protein, mitochondrial OS=Homo sapiens GN=HSPD1 PE=1 SV=2 |
| KIF28_HUMAN | Kinesin-like protein KIF28P OS=Homo sapiens GN=KIF28P PE=3 SV=2 |

Table 10

| **PbUIS4-KO fraction 1** | |
|---|---|
| **Accession** | **Description** |
| RIPK1_HUMAN | Receptor-interacting serine/threonine-protein kinase 1 OS=Homo sapiens GN=RIPK1 PE=1 SV=3 |

Table 11

| **PbANKA-WT fraction 2** | |
|---|---|
| **Accession** | **Description** |
| ACTG_HUMAN | Actin, cytoplasmic 2 OS=Homo sapiens GN=ACTG1 PE=1 SV=1 |
| ACTB_HUMAN | Actin, cytoplasmic 1 OS=Homo sapiens GN=ACTB PE=1 SV=1 |
| K1C18_HUMAN | Keratin, type I cytoskeletal 18 OS=Homo sapiens GN=KRT18 PE=1 SV=2 |
| POTEE_HUMAN | POTE ankyrin domain family member E OS=Homo sapiens GN=POTEE PE=2 SV=3 |
| ACTBL_HUMAN | Beta-actin-like protein 2 OS=Homo sapiens GN=ACTBL2 PE=1 SV=2 |
| ACTC_HUMAN | Actin, alpha cardiac muscle 1 OS=Homo sapiens GN=ACTC1 PE=1 SV=1 |
| ACTS_HUMAN | Actin, alpha skeletal muscle OS=Homo sapiens GN=ACTA1 PE=1 SV=1 |
| ACTA_HUMAN | Actin, aortic smooth muscle OS=Homo sapiens GN=ACTA2 PE=1 SV=1 |

| | |
|---|---|
| ACTH_HUMAN | Actin, gamma-enteric smooth muscle OS=Homo sapiens GN=ACTG2 PE=1 SV=1 |
| POTEF_HUMAN | POTE ankyrin domain family member F OS=Homo sapiens GN=POTEF PE=1 SV=2 |
| ACTBM_HUMAN | Putative beta-actin-like protein 3 OS=Homo sapiens GN=POTEKP PE=5 SV=1 |
| POTEI_HUMAN | POTE ankyrin domain family member I OS=Homo sapiens GN=POTEI PE=3 SV=1 |

**Table 12**

**PbUIS4-KO fraction 2**

| **Accession** | **Description** |
|---|---|
| SEMG1_HUMAN | Semenogelin-1 OS=Homo sapiens GN=SEMG1 PE=1 SV=2 |

Table 13

| **PbANKA-WT fraction 3** | |
|---|---|
| **Accession** | **Description** |
| ROA1_HUMAN | Heterogeneous nuclear ribonucleoprotein A1 OS=Homo sapiens GN=HNRNPA1 PE=1 SV=5 |
| GBB1_HUMAN | Guanine nucleotide-binding protein G(I)/G(S)/G(T) subunit beta-1 OS=Homo sapiens GN=GNB1 |

Table 14

| **PbUIS4-KO fraction 3** | |
|---|---|
| Accession | **Description** |
| CC151_HUMAN | Coiled-coil domain-containing protein 151 OS=Homo sapiens GN=CCDC151 PE=1 SV=1 |

**Mass Spectrometry results, from PbGFP-WT and PbGPUIS4-BirA*-HA**

**Table 15**

**PbGFP-UIS4-BirA*-Host proteins**

| | | Speciess |
|---|---|---|
| sp\|P07305\|H10_HUMAN | Histone H1.0 OS=Homo sapiens | HUMAN |
| sp\|P02768\|ALBU_HUMAN | Serum albumin OS=Homo sapiens | HUMAN |
| sp\|P81605\|DCD_HUMAN | Dermcidin OS=Homo sapiens | HUMAN |
| sp\|Q9BYE4\|SPR2G_HUMAN | Small proline-rich protein 2G OS=Homo sapiens | HUMAN |
| sp\|Q96RQ3\|MCCA_HUMAN | Methylcrotonoyl-CoA carboxylase subunit alpha, mitochondrial OS=Homo sapiens | HUMAN |
| sp\|P25311\|ZA2G_HUMAN | Zinc-alpha-2-glycoprotein OS=Homo sapiens | HUMAN |
| sp\| G21Q96PG2\|M4A10_HUMAN | Membrane-spanning 4-domains subfamily A member 10 OS=Homo sapiens | HUMAN |
| sp\|Q9BYE4\|SPR2G_HUMAN | Small proline-rich protein 2G OS=Homo sapiens | HUMAN |
| sp\|P02768\|ALBU_HUMAN | Serum albumin OS=Homo sapiens | HUMAN |
| sp\|P81605\|DCD_HUMAN | Dermcidin OS=Homo sapiens | HUMAN |
| RRRRRsp\|Q8IZ69\|TRM2A_HUMAN | REVERSED tRNA (uracil-5-) -methyltransferase homolog A OS=Homo sapiens | HUMAN |
| sp\|P02768\|ALBU_HUMAN | Serum albumin OS=Homo sapiens | HUMAN |
| sp\|P81605\|DCD_HUMAN | Dermcidin OS=Homo sapiens | HUMAN |
| sp\|P39060\|COIA1_HUMAN | Collagen alpha-1(XVIII) chain OS=Homo sapiens | HUMAN |
| sp\|P02768\|ALBU_HUMAN | Serum albumin OS=Homo sapiens | HUMAN |
| sp\|Q9UHX1\|PUF60_HUMAN | Poly(U)-binding-splicing factor PUF60 OS=Homo sapiens | HUMAN |
| sp\|Q9HD23\|MRS2_HUMAN | Magnesium transporter MRS2 homolog, mitochondrial OS=Homo sapiens | HUMAN |
| sp\|Q8IY33\|MILK2_HUMAN | MICAL-like protein 2 OS=Homo sapiens | HUMAN |
| sp\|P54253\|ATX1_HUMAN | Ataxin-1 OS=Homo sapiens | HUMAN |
| sp\|Q8IWA0\|WDR75_HUMAN | WD repeat-containing protein 75 OS=Homo sapiens | HUMAN |

**Table 16**

**PbGFP-WT-Host proteins**

| | | |
|---|---|---|
| sp\|P02452\|CO1A1_HUMAN | Collagen alpha-1(I) chain OS=Homo sapiens | HUMAN |
| sp\|P15924\|DESP_HUMAN | Desmoplakin OS=Homo sapiens | HUMAN |
| sp\|P02768\|ALBU_HUMAN | Serum albumin OS=Homo sapiens | HUMAN |
| sp\|P08123\|CO1A2_HUMAN | Collagen alpha-2(I) chain OS=Homo sapiens | HUMAN |
| sp\|P05090\|APOD_HUMAN | Apolipoprotein D OS=Homo sapiens | HUMAN |
| sp\|Q02413\|DSG1_HUMAN | Desmoglein-1 OS=Homo sapiens | HUMAN |
| sp\|P07305\|H10_HUMAN | Histone H1.0 OS=Homo sapiens | HUMAN |
| sp\|Q13085\|ACACA_HUMAN | Acetyl-CoA carboxylase 1 OS=Homo sapiens | HUMAN |
| sp\|P0DOX5\|IGG1_HUMAN | Immunoglobulin gamma-1 heavy chain OS=Homo sapiens | HUMAN |
| sp\|P02461\|CO3A1_HUMAN | Collagen alpha-1(III) chain OS=Homo sapiens | HUMAN |
| sp\|P81605\|DCD_HUMAN | Dermcidin OS=Homo sapiens | HUMAN |
| sp\|Q8TF72\|SHRM3_HUMAN | Protein Shroom3 OS=Homo sapiens | HUMAN |
| sp\|Q08188\|TGM3_HUMAN | Protein-glutamine gamma-glutamyltransferase E OS=Homo sapiens | HUMAN |
| sp\|P28347\|TEAD1_HUMAN | Transcriptional enhancer factor TEF-1 OS=Homo sapiens | HUMAN |
| sp\|Q9Y586\|MB212_HUMAN | Protein mab-21-like 2 OS=Homo sapiens | HUMAN |
| sp\|Q9BYE4\|SPR2G_HUMAN | Small proline-rich protein 2G OS=Homo sapiens | HUMAN |
| sp\|Q86YZ3\|HORN_HUMAN | Hornerin OS=Homo sapiens OX=9606 | HUMAN |
| sp\|P84098\|RL19_HUMAN | 60S ribosomal protein L19 OS=Homo sapiens | HUMAN |
| sp\|P61964\|WDR5_HUMAN | WD repeat-containing protein 5 OS=Homo sapiens | HUMAN |
| sp\|P49207\|RL34_HUMAN | 60S ribosomal protein L34 OS=Homo sapiens | HUMAN |
| sp\|P35321\|SPR1A_HUMAN | Cornifin-A OS=Homo sapiens | HUMAN |
| sp\|P25311\|ZA2G_HUMAN | Zinc-alpha-2-glycoprotein OS=Homo sapiens | HUMAN |
| sp\|P0DOY3\|IGLC3_HUMAN | Immunoglobulin lambda constant 3 OS=Homo sapiens | HUMAN |
| sp\|P20700\|LMNB1_HUMAN | Lamin-B1 OS=Homo sapiens | HUMAN |
| sp\|P16402\|H13_HUMAN | Histone H1.3 OS=Homo sapiens | HUMAN |
| sp\|Q9Y586\|MB212_HUMAN | Protein mab-21-like 2 OS=Homo sapiens | HUMAN |

| | | |
|---|---|---|
| sp\|Q9NYQ8\|FAT2_HUMAN | Protocadherin Fat 2 OS=Homo sapiens | HUMAN |
| sp\|Q9BYE4\|SPR2G_HUMAN | Small proline-rich protein 2G OS=Homo sapiens | HUMAN |
| sp\|P25311\|ZA2G_HUMAN | Zinc-alpha-2-glycoprotein OS=Homo sapiens | HUMAN |
| RRRRRsp\|P29353\|SHC1_HUMAN | REVERSED SHC-transforming protein 1 OS=Homo sapiens | HUMAN |
| sp\|Q8N1G1\|REXO1_HUMAN | RNA exonuclease 1 homolog OS=Homo sapiens | HUMAN |
| sp\|Q9UBC9\|SPRR3_HUMAN | Small proline-rich protein 3 OS=Homo sapiens | HUMAN |
| sp\|P81605\|DCD_HUMAN | Dermcidin OS=Homo sapiens | HUMAN |
| sp\|P54253\|ATX1_HUMAN | Ataxin-1 OS=Homo sapiens | HUMAN |
| sp\|P31629\|ZEP2_HUMAN | Transcription factor HIVEP2 OS=Homo sapiens | HUMAN |
| sp\|P07305\|H10_HUMAN | Histone H1.0 OS=Homo sapiens | HUMAN |
| RRRRRsp\|Q96FN5\|KIF12_HUMAN | REVERSED Kinesin-like protein KIF12 | HUMAN |
| sp\|P02768\|ALBU_HUMAN | Serum albumin OS=Homo sapiens | HUMAN |
| sp\|Q02413\|DSG1_HUMAN | Desmoglein-1 OS=Homo sapiens | HUMAN |
| sp\|P81605\|DCD_HUMAN | Dermcidin OS=Homo sapiens | HUMAN |
| sp\|P25311\|ZA2G_HUMAN | Zinc-alpha-2-glycoprotein OS=Homo sapiens | HUMAN |
| sp\|P07305\|H10_HUMAN | Histone H1.0 OS=Homo sapiens | HUMAN |
| sp\|P11498\|PYC_HUMAN | Pyruvate carboxylase, mitochondrial OS=Homo sapiens | HUMAN |
| sp\|P15924\|DESP_HUMAN | Desmoplakin OS=Homo sapiens | HUMAN |
| sp\|P81605\|DCD_HUMAN | Dermcidin OS=Homo sapiens | HUMAN |
| sp\|Q9UKX2\|MYH2_HUMAN | Myosin-2 OS=Homo sapiens | HUMAN |

**Table 17**

**PbGFP-UIS4-BirA*-*Plasmodium* proteins**

| | | |
|---|---|---|
| A0A1D3LVA4_PLABE | Liver specific protein 2 OS=*Plasmodium berghei* | PLABE |
| A0A1A8VYS5_9APIC | Uncharacterized protein OS=*Plasmodium* ovale curtisi | 9APIC |
| A0A1C3KYH9_PLAMA | Cdc2-related protein kinase 4, putative OS=*Plasmodium* malariae | PLAMA |
| W7JIE6_PLAFA | Uncharacterized protein OS=*Plasmodium* falciparum UGT5.1 | PLAFA |
| A0A1D3RXD8_PLACH | Reticulocyte binding protein, putative OS=*Plasmodium* chabaudi SV=1 | PLACH |
| A0A1B1DX03_9APIC | Uncharacterized protein OS=*Plasmodium* coatneyi | 9APIC |
| A0A122I7L5_PLABE | ABC transporter B family member 3, putative OS=*Plasmodium berghei* | PLABE |
| Q86QI8_PLABE | REVERSED 31 KDa antigen OS=*Plasmodium berghei* | PLABE |

**Table 18**

**PbGFP-WT-*plasmodium* proteins**

| | | |
|---|---|---|
| A0A1C3KQU5_9APIC | Uncharacterized protein OS=*Plasmodium* ovale | 9APIC |
| A0A1D3JKV3_PLAMA | Uncharacterized protein OS=*Plasmodium* malariae | PLAMA |
| A0A1A8VYS5_9APIC | Uncharacterized protein OS=*Plasmodium* ovale curtisi | 9APIC |
| A0A1C3KYH9_PLAMA | Cdc2-related protein kinase 4, putative OS=*Plasmodium* malariae | PLAMA |

**Table 19**

**Extra peptide identified on PbGFP-UIS4-Bir**

| Accession | Description |
|---|---|
| 06709\|BirA_*E. coli* | Bifunctional ligase/repressor BirA OS=*Escherichia coli* (strain K12) |